A STUDY OF
THE FORMATION AND DECAY
OF METEOR TRAILS

A Thesis

Submitted to the Faculty of Graduate Studies

in Partial Fulfilment of the Requirements

for the Degree of

Master of Science

in the Department of Physics

University of Saskatchewan

by

Delbert Walter Rice

Written under the Supervision of

P.A. Forsyth

Saskatoon, Saskatchewan

September, 1961

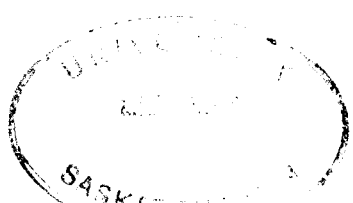

A B S T R A C T

Combinations of VHF forward-scatter and backscatter circuits, one also involving the Prince Albert Radar Laboratory, were examined in order to assess their utility in measurements of the ambipolar diffusion coefficient by means of meteor signal decay rates. While observations using the Prince Albert Radar were not possible, experimental work using the other circuit combinations indicates that the most useful arrangement is a forward-scatter circuit used in conjunction with a UHF radar. Observations of the decay rates of forward-scattered signals indicate the presence of the same large dispersion that has been reported for backscatter measurements. A qualitative mechanism, based upon an irregularly ionized meteor trail, appears adequate to account for the dispersion.

F O R E W A R D

During the course of this research, the author has received assistance from many members of the Department of Physics. He is especially grateful to Dr. P.A. Forsyth, who supervised the work and provided stimulating guidance and unceasing encouragement. Many of the technicians provided their special skills when they were needed. Mr. D.R. McCracken ably assisted with the analysis of records, and performed most of the calculations required for Chapter VII.

As originally planned, much of this work was to have made use of the facilities of the Prince Albert Radar Laboratory. To this end, the author constructed the photographic read-out for the radar, described in Appendix B. While this read-out was not yet in use at the time of the fire in early 1961 which destroyed the main building of the radar, preliminary observations had already been made on one occasion just previous to the fire. The assistance of the staff of the Radar Laboratory in this preliminary work is gratefully acknowledged.

A part of the funds for this research has been provided by the United States Air Force Command and Control Development Division, under contract #AF19(604)-7329.

The author has received financial assistance provided by a National Research Council Bursary, from June, 1960 to September, 1961.

T A B L E O F C O N T E N T S

L I S T O F I L L U S T R A T I O N S

L I S T O F I L L U S T R A T I O N S (Continued)

LIST OF TABLES

CHAPTER I - INTRODUCTION

Much useful information has been gained about the ionosphere in the 80 to 100 km. region by radio studies of the ionized trails formed in that region by meteors. Such atmospheric parameters as scale height, density, diffusion coefficient, and recombination coefficient have been the subjects of various studies. As well, upper atmospheric winds have been studied by means of the movements they produce in the positions of long-enduring meteor trails.

While a good understanding of meteoric processes has developed, several problems remain. One of these involves the measurement of the diffusion coefficient from the decay rate of signals reflected from meteor trails. In this thesis, methods of measuring the diffusion coefficient, utilizing combinations of forward-scatter and backscatter systems in order to reduce the uncertainty in the measurements, will be evaluated.

1 HISTORICAL

Historical records show that meteors have been observed by the unaided eye for many centuries. By the eighteenth century observers realized that meteors originated from outer space, and that they were caused by particles entering the earth's atmosphere with velocities of many kilometers per second to appear at heights of 80 to 100 km.

The earliest radio work which can be identified as linked with meteoric phenomena was reported by workers studying radio reflections from the normal ionosphere. They noticed abnormal effects which indicated sudden increases in the ionization of the E region. During the

Leonid meteor shower of 1932, Skellett (1935) was able to correlate sudden increases in E region ionization with visual observations of meteors. Mention was also made about this time by various workers of abnormal effects whereby high-frequency radio signals were received at great distances from the transmitting station. In 1938 Pierce suggested that such bursts of signal could be transmitted by way of ionized meteor trails. During the Second World War, workers investigated such forward-scattered signal bursts in more detail, and obtained correlations with visual occurrences of meteors.

The technological development during the war of radar equipment operating in the VHF region provided workers in the following years with an important tool with which to study meteoric phenomena. Since that time a great wealth of both observational and theoretical evidence has accumulated.

2 DEFINITIONS, VISUAL BRIGHTNESS, PHYSICAL PROCESSES

A definition of terms is useful: strictly, meteor refers to the optical phenomena, but it is often used in a more general sense to refer to all bodies entering the earth's atmosphere from interplanetary space. Meteoroid refers to the particle itself, while a meteorite is a meteoroid which has sufficient size to survive the passage through the atmosphere and strike the surface of the earth.

The visual brightness of meteors is measured on the same logarithmic brightness scale as are the stars. The brightest star is assigned a magnitude of +1, while the faintest star visible to the naked eye has a brightness of magnitude +6. Five magnitudes represent a ratio of 100:1 in luminous flux. For a very bright meteor of magnitude -5, the meteoroid

radius is about .8 cm., while for a meteor of magnitude +10, the radius is about .008 cm. This latter size is about the minimum detectable by radar. The total number of particles incident upon the earth per unit time increases with decreasing particle size. This results in a radar meteor rate which may be orders of magnitude greater than the visual rate. Watson (1941) has suggested the empirical relation

$$N \propto \frac{1}{m} \qquad \text{- - - - - - - - - - - - - - - (1)}$$

where N is the total number of meteors with mass greater than m.

Opik (1958) has described the physical process of ablation of a meteroid in the upper atmosphere. For the majority of meteoric particles, and for all of interest in radio studies, the particle radius is much less than the mean free path of atmospheric atoms in the appropriate height range. Also, the particle velocity is much greater than the thermal velocity of the atoms. Inelastic collisions occur between the particle and individual atoms, with most of the resultant energy being expended in heating the meteoric particle. As a result of the heating, individual meteor atoms are split off. These are removed with very high velocities, and are slowed down through collisions with atmospheric constituents. The energy given up in the slowing down process appears as heat and as excitation and ionization energy. A consideration of ionization potentials indicates that meteoric rather than atmospheric atoms contribute the major portion of ionization. Observed recombination rates for meteoric ionization also support this conclusion. The velocity of the meteroid, as the meteoroid is reduced in size, remains relatively constant.

3 THEORY OF RADIO SCATTERING FROM METEOR TRAILS

At low radio frequencies, the power reflected from a meteor trail

may be calculated by assuming the trail to be formed instantaneously as a line charge at time t=0. Solution of the diffusion equation for diffusion from an initial line source, shows that the ionization density assumes a Gaussian distribution about the trail axis, so that

$$N = \frac{q}{4\pi Dt} \exp\left\{-\frac{r^2}{4Dt}\right\} \quad \text{- - - - - - - - - - - (2)}$$

where N is electron density, q is the line charge density, D is the diffusion coefficient, and r is the radial distance from the trail axis.

For line charge densities less than 10^{14} electrons per meter, each electron in the trail scatters independently. Such low density trails are termed "underdense". For this case, Lovell and Clegg (1948) have shown that the signal amplitude scattered back to the vicinity of the transmitter is given by

$$A = A_o \exp\left\{-\frac{16\pi^2 Dt}{\lambda^2}\right\}, t>0 \quad \text{- - - - - - - - - - (3)}$$

where A_o is the amplitude at time t = 0, A is the amplitude at time t, D is the diffusion coefficient, and λ is the radio wavelength. Thus the time constant

$$\tau = \frac{\lambda^2}{16\pi^2 D} \quad \text{- - - - - - - - - -(4a)}$$

is the time required for the amplitude to decay to $\frac{1}{e}$ of its initial value. It is often taken as a measure of the duration of underdense trails. The expression for A_o will not be given here, except to note that it is proportional to q, the line charge density. In the forward-scatter case, where the scattered signal is received at some distance from the transmitter, the time constant τ of equation (4a) is increased by a factor $\sec^2\phi$, where 2ϕ is the angle subtended at the reflection point by the transmitter-receiver axis (Eshleman and Manning 1954).

Equation (4a) then becomes

$$\tau = \frac{\lambda^2 \sec^2\phi}{16\pi^2 D} \qquad \text{- - - - - - - - - - - - - - - (4b).}$$

Values of $\sec^2\phi$ are about 10 for a transmitter-receiver path of 1000 km., but may be as large as 25 for very long paths. In much of the early literature, signal duration was measured as the total time a signal exceeded a fixed level, usually the noise level of the receiver. Occasionally durations were measured at a level which was $\frac{1}{e}$ of the maximum amplitude. However, it should be pointed out that durations measured in either of these ways have no simple theoretical background. In what follows, duration, for underdense trails, will be taken to mean the time for the signal amplitude to decay by a ratio of $\frac{1}{e}$, that is, the value of τ given by equation (4a) or (4b).

In calculating the value of A_o, the initial amplitude returned from the trail, Lovell and Clegg (1948) have shown that Fresnel diffraction theory applies, so that the amplitude is expressible in terms of Fresnel integrals. Provided the trail extends a distance sufficient to include the principal Fresnel zone about the specular reflection point, the length of trail scattering coherently is just the half-length of the principal Fresnel zone

$$F_B = \sqrt{\frac{R\lambda}{2}} \qquad \text{- - - - - - - - - - - - - - (5)}$$

where R is the range to the specular reflection point, and λ is the radio wavelength. The subscript B refers to backscatter.

In the forward-scatter case, the Fresnel zone length is given by

$$F_F = \left\{ \frac{\lambda R_T R_R}{(R_T R_R)(1-\sin^2\phi\cos^2\beta)} \right\}^{\frac{1}{2}} \qquad \text{- - - - - - - - - - -(6)}$$

where R_T and R_R are the distances of the reflection point from the transmitter and the receiver, 2ϕ is the angle subtended at the reflection point by the transmitter-receiver axis, and β is the angle between the trail axis and the plane of propagation (see Figure 1b). For $\beta = 90^\circ$, and $R_T = R_R$, $F_B = F_F$ for the same range R. For $\beta = 0$, $F_F = F_B \sec\phi$, so that in general, the Fresnel zone length is increased by a factor of from one to five, for the forward-scatter case. The increased Fresnel zone length causes an increase in the amplitude of the forward-scattered signal over the backscattered signal.

The theory outlined thus far has assumed free penetration of the trail by the radio wave, independent scattering by individual electrons, an initially zero trail radius, and instantaneous formation of the trail. When these assumptions do not hold, the theory must be modified. The last two assumptions depend upon the radio wavelength involved. Since the signal decay has a time constant proportional to wavelength squared, the duration of a signal decreases as the wavelength is decreased. When the time of formation of the principal Fresnel zone becomes comparable to one decay time, the signal from the initially formed part of the trail has already decayed significantly by the time the remainder of the trail is formed. The result is a peak amplitude which is less than that predicted for an instantaneously formed trail. The time taken to form one half the principal Fresnel zone is

$$t = \frac{1}{v} \sqrt{\frac{R\lambda}{2}} \qquad \text{- - - - - - - - - - - - - - - - (7)}$$

for backscatter, where v is the meteor velocity. Equating (7) and (4a), and using values v = 40 km/sec, D = 5 m^2/sec, R = 200 km., then the wavelength is about 3 meters. Hence the effect becomes important above about

100 Mc, for this case.

The effects of a finite initial trail radius have been investigated by Manning (1958). He has shown that an initial trail radius of 14 ionic mean free paths is reached almost instantaneously, from which normal diffusion ensues. The effect of the initial radius is to reduce the amplitude of the reflected signal at very high frequencies.

When the line density of ionization exceeds about 10^{14} electrons/m, the electrons do not scatter independently. The trail assumes a core with a negative dielectric constant, and free penetration by the radio wave is prevented. Meteor trails which behave in this way are known as "overdense". The approach then is to regard the reflection as taking place from a metallic cylinder, of radius equal to the radius of zero dielectric constant in the meteor trail. The duration of signals from overdense trails is of interest, it is given for backscatter by (Kaiser and Closs 1952)

$$\tau' = \frac{\mu_0 e^2}{4m} \frac{q \lambda^2}{4\pi^2 D} \qquad \text{- - - - - - - - - - - - - - (8)}$$

where $\mu_0 = 4\pi \times 10^{-7}$ henry/meter

e = electronic charge

m = electronic mass

q = electronic line density

λ = radio wavelength

D = diffusion coefficient

The time of maximum signal is given by

$$T = \frac{\tau'}{\epsilon} \qquad \text{- - - - - - - - - - - - - - (9)}$$

where $\epsilon = 2.71 \ldots\ldots$ τ' is the time taken for the meteor trail to lose its negative dielectric constant core. After time τ' the signal

decays exponentially as from an underdense trail, however the time for this decay is usually much less than τ', and may be neglected in calculating the signal duration. The maximum signal amplitude is proportional to $q^{\frac{1}{2}}$.

An extension to forward-scattering from overdense trails has been made by Hines and Forsyth (1957). One result of interest at the present is that the duration τ' is increased, as in the underdense case, by $\sec^2\phi$:

$$\tau' = \frac{\mu_0 e^2}{4m} \frac{q\lambda^2 \sec^2\theta}{4\pi^3 D} \qquad \text{- - - - - - - - - - - (10)}$$

Also, they show that the peak amplitude still varies as $q^{\frac{1}{4}}$, as for the backscatter case.

Forsyth (1958) has confirmed the theory developed by Hines and Forsyth, in the case of a detailed analysis of two forward-scattered signals from a single meteor trail. However, the approach of Hines and Forsyth has been criticized by Manning (1959), on the grounds that their neglect of the effects of electrons in the trail outside of the zero refractive index surface introduces serious error. Manning computes ray paths for waves refracted from meteor trails, and shows that the $\sec^2\phi$ law of equation (10) should be replaced by $\sec^m\phi$, where m may range from 0.3 to 2, depending upon the orientation of the trail axis. The work of McKinley and McNamara (1956), in which they found a mean value for m of 1.13 for an overdense group of meteor trails, lends support to the work of Manning.

Obviously, meteor trails exist with line densities $q \sim 10^{14}$ electrons/meter, in which neither the overdense nor the underdense theory applies. The two models apply only to limiting cases, and therefore it has been suggested that the resulting expressions should be expected to have only a statistical validity, describing the average behavior of large numbers of

signals.

4 SECONDARY EFFECTS

The effect of wind shear and turbulence is important for longer duration echoes. These often exhibit fading which is caused by the formation of more than one reflection or "glint" point, so that interference occurs between the waves reflected from different parts of the distorted trail (Manning 1959). Short duration echoes (from underdense trails) do not persist long enough to suffer from such fading.

It has been assumed that the electron density in a trail is reduced by diffusion alone, and that recombination of electrons with positive ions, and attachment of electrons to neutral atoms, may be neglected. In the case of recombination, the procedure is reversed; i.e., the maximum echo durations observed have been used to set an upper limit for the recombination coefficient. McKinley and Millman (1953) have observed echo durations of up to 30 minutes, using 33Mc. equipment. The resultant recombination coefficient is about four orders of magnitude smaller than that observed in the E region. Bates (1950) explains the discrepancy on the assumption that the E region ionization is predominantly O_2^+, with a dissociative recombination coefficient of the order of $10^{-8} cm^3/sec.$, while the recombination coefficient operative in the meteor case is the radiative recombination coefficient of ions of meteoric origin, which is much smaller.

Kaiser (1953) has made estimates of the effect of attachment upon echo duration. The conclusion is that, for decay type echoes from underdense trails, the effect would be negligible except where the reflection point is below 90 km. and the radio wavelength involved is about 100 meters or more. The effect of attachment, where observed, would be to

reduce the exponent of the wavelength dependence of echo duration (equations 4) to below 2. For echoes from overdense trails, as for underdense, attachment could affect only the longest duration trails. The only observable affect upon signals from overdense trails would be to decrease the numbers of echoes with very long durations.

Kaiser also shows that the heating of the trail by the incoming meteoroid is negligibly small, except perhaps for the highest line density trails. He also gives experimental evidence which support this conclusion. The effect of heating, if present, would be to modify the electron distribution about the trail axis from its theoretical Gaussian shape. This would introduce a phase interference effect so that the scattered signal would not decay exponentially.

When the electric vector of the incident radio wave is normal to the trail, resonant scattering may occur. It is most predominant in trails in which the electron line density is 10^{12} electrons/m. or less, the enhancement being a factor of 2 over the amplitude A_0 of equation (3) (Kaiser and Closs 1952). The enhancement factor falls to unity for trails of line density near 10^{14} electrons /m. In practical cases where resonance does occur, the resonant phase of the scattering is terminated quickly and the echo then decays according to equation (3).

5 ADVANTAGES OF FORWARD-SCATTER MEASUREMENTS

All of the work described in the literature on diffusion coefficient measurement involves the use of backscatter equipment. On the other hand, much of the Canadian work in meteoric studies has involved the use of forward-scatter radio systems. These have two main advantages. The first is that it is possible to use continuous wave transmissions. This allows

more precise control of transmitted frequencies and power, with a consequent increase in receiver sensitivity and precision of measurement. The second advantage arises from the fact that forward-scattered signals persist for a longer time than do the corresponding back-scattered signals. This permits more accurate measurement of the decay rate, especially of the particularly short duration signals which arise from reflection points above 100 km.

Unfortunately, the reflection point height is not as easily determined for a forward-scatter system. As well, the factor $\sec^2\phi$ appearing in the expression for the forward-scatter time constant must be evaluated. The use of a UHF radar in conjunction with a forward scatter system would overcome these difficulties, and this will be further explored in a later chapter.

CHAPTER II - AMBIPOLAR DIFFUSION AND MAGNETIC FIELD EFFECTS

When an initial concentration of ionization, containing approximately equal numbers of positive ions and negative electrons, diffuses, the more mobile electrons tend to diffuse more rapidly than the positive heavy ions. Any appreciable charge separation is prevented, however, by space charge effects. The result is that the electrons and ions diffuse together, with a diffusion rate given by the ambipolar diffusion coefficient. The theory of ambipolar diffusion as applied to meteor trails is given by Huxley (1952), while Kaiser discusses the effect upon diffusion of an impressed magnetic field. The ambipolar diffusion coefficient D is given by

$$D = \frac{\alpha_i D_e + \alpha_e D_i}{\alpha_i + \alpha_e} \qquad \text{- - - - - - - - - - (11)}$$

where D_e and D_i and α_e and α_i, are the diffusion coefficients and mobilities of the electrons and of the positive ions. Since $\alpha_i << \alpha_e$,

$$D \approx D_i + \frac{\alpha_i}{\alpha_e} D_e \qquad \text{- - - - - - - - - - - (12)}$$

From kinetic theory, the mobilities are related by

$$\frac{\alpha_i}{\alpha_e} = \frac{\lambda_i}{\lambda_e} \left\{ \frac{T_e m_e}{T_i m_i} \right\}^{\frac{1}{2}} \qquad \text{- - - - - - - - - - - (13)}$$

where λ is the mean free path, m the mass, and T the temperature.

Also the ratio of the diffusion coefficients is

$$\frac{D_e}{D_i} = \frac{\lambda_e}{\lambda_i} \left\{ \frac{T_e m_i}{T_i m_e} \right\}^{\frac{1}{2}} \qquad \text{- - - - - - - - - - -(14).}$$

Putting (13) and (14) into (12), then

$$D = D_i \left\{ 1 + \frac{T_e}{T_i} \right\} \quad \text{or } D = 2\, D_i \qquad \text{- - - - - - (15)}$$

for $T_e = T_i$.

The effect of the earth's magnetic field will be to reduce D_e in directions perpendicular to the field. The diffusion of the much heavier positive ions will be relatively unaffected. Thus at some height, $D_e = D_i$, that is, the diffusion coefficient for electrons in a direction perpendicular to the field will be equal to the diffusion coefficient for the positive ions. Then at this height, $D = D_i$, so that the ambipolar diffusion coefficient is reduced by a factor of two. The ratio of the electron diffusion coefficients parallel and perpendicular to the field is given by

$$\frac{D_{e\perp}}{D_{e\,//}} = \frac{f_c^2}{f_c^2 + \omega_h^2} \qquad \text{- - - - - - - - - - - - - - - - (16)}$$

where f_c is the collision frequency and ω_h is the gyro angular frequency. When $D_{e\perp} = D_i$,

$$\frac{D_i}{D_{e\,//}} = \frac{f_c^2}{f_c^2 + \omega_h^2} = \frac{\lambda_i}{\lambda_e}\left\{\frac{T_i m_e}{T_e m_i}\right\} \qquad \text{- - - - - - - - - - - - - - - (17)}$$

Putting in appropriate values, it is found that $f_c \sim 3 \times 10^5$. This collision frequency will be obtained for a neutral particle density of 2×10^{13}, which corresponds to a height of about 100 km. Thus, above about 100 km., the effect of the earth's magnetic field will be to reduce the diffusion coefficient in directions perpendicular to the field. The observable effect should be an increase in the durations of decay type signals reflected from trails which are parallel to the earth's magnetic field.

Weiss (1955) has also made an estimate of the height at which the effect of the earth's magnetic field becomes important. He gives a height of approximately 92 km for which the ambipolar diffusion coefficient D is reduced by a factor of two in directions perpendicular to the field. He further states that D could not be reduced much more than this, even at greater heights, since it appears unlikely that the electrons would be

able to restrain the motion of the more rapidly diffusing positive ions.

The first experimental evidence of the effect of the earth's magnetic field upon diffusion was reported by Lovell (1947). He measured the durations of back-scattered echoes from the 1946 Orionids, Leonids, and Geminids, and the 1947 Piscids showers, as a function of azimth of the aerial in a northerly direction. In each case he found a marked peak in the average duration for azimuths between 0^{o} and 20^{o} E. The relatively simple experiment and the rather direct interpretation of the result are interesting if not somewhat surprising, however in view of the poor knowledge of meteoric processes at that time, it seems unlikely that all other factors controlling the echo duration were properly accounted for. Changing the azimuth of a radar beam does not, of course, change the direction of a meteor trail with respect to the magnetic field. It seems more likely that the change in azimuth would have produced a change in the average height of reflection, and hence the observed variation in echo duration.

In more recent work, Forsyth and Vogan (1956) have found differences in the intrinsic durations of forward-scattered signals over north-south and east-west paths in Western Canada, the signals over the east-west path having a characteristically longer duration. One possible explanation given was that many of the meteor trails observed on the east-west path would be nearly parallel to the earth's magnetic field, while the majority of meteors observed on the north-south path would be inclined to the magnetic field direction, at angles greater than 37^{o}. However, other factors, such as the heights of the reflection points, and the actual direction and position of each trail in space, must be known before conclusive results can be obtained.

Greenhow and Neufeld (1955), Weiss (1955) *, Murray (1959), and

* Some of the numerical results of Weiss' paper are in error, as noted by Murray.

Greenhow and Hall (1961), have reported measurements of the variation of diffusion coefficient with height. All have indicated a very large scatter in the results obtained, the extreme values of D measured for a given height differing by as much as a factor of ten. There is some disagreement as to the method of analysis appropriate in view of the large spread in experimental values. The results have been most usefully presented graphically, showing the variation of log D with height, or vice versa, depending upon which was selected as the independent variable.

Since from kinetic theory D varies as the square root of temperature and inversely as pressure, it is usual to assume that D varies exponentially with height, the effect of the small temperature change in the meteor region being neglected. Under this assumption D varies with a scale height H equal to that of the atmosphere and the slope of a height-log D graph yields a value for the atmospheric scale height H. The values of H obtained by the different workers range from 6 to over 20, the differences being attributable mainly to the differing treatments of the results, rather than to a real difference in the observed data. Basically the variations arise through differing assumptions as to the relative errors in the values of D and h. If the errors in D are negligible it is appropriate to average the experimental values of h for suitable intervals of log D, while if the errors in h are negligible it is more appropriate to average the values of log D. The two approaches lead to values of H which are too low in the former case, and too high in the latter. Greenhow and Hall have analyzed their data on the assumption that errors in both quantities are significant, and this leads to an intermediate value for H of 7.8. They also present analyses of their data for the cases of error in only one of the two parameters; these are useful for comparison. Greenhow and Hall also

present the results of some two station measurements, in which the h-log D gradient was obtained from comparison of echo durations from two points on the same meteor trail. These indicate a slightly higher value of H, 8.9 km. However, the value does support their method of analysis of the single station h-log D measurements. From the two measurements, they adopt a mean value for H of 8.0 km., and as they point out, this is about 20% greater than the generally accepted value of the atmospheric scale height in the meteor region. Assuming this difference to be real, then there is a real difference between the scale height measured over New Mexico in summer (Rocket Panel 1952), and that measured over Jodrell Bank in winter.

The possible sources of error in the measurements of the diffusion coefficient may be summarized: (1) distortion of the exponential decay by resonance effects, (2) effects due to the finite meteor velocity, (3) the inclusion of signals from trails with line densities near 10^{14} electrons/m., (4) effects due to distortion of the trails by upper atmospheric winds (5) effects due to the earth's magnetic field, (6) actual variations in atmospheric density and temperature, and (7) effects due to imperfections in the individual meteor trail which prevent it from behaving as a true line scatterer for the radio waves.

By careful selection of echoes, many of these sources of error may be eliminated. By measuring decay times from a plot or direct recording of the logarithm of the signal amplitude (in which case the exponential decay appears as a straight line), greater accuracy can be achieved than in the case of the measurement from an amplitude-time display. Also, departures from an exponential decay are much more easily recognized, so that unsatisfactory echoes may be eliminated. Murray has observed no reduction in

scatter from meteor trails with the same radiant and in the same position in the sky, so that magnetic effects are eliminated. Observations of meteor trails in the same part of the sky, within a minute or so of each other, likewise show no reduction in scatter, so that fluctuations in temperature and density are not operative, unless on an almost unbelievably fine scale.

Weiss and Murray both found a significant diurnal variation in the value of D at a given height, but Murray considers this insufficient to explain all of the scatter. Greenhow and Neufeld give a true spread of 1.5:1 in decay times of echoes at a given height, and they suggest effects of resonance and of the magnetic field as possible causes. Greenhow and Hall attribute the entire scatter to errors in measurement, however in order to do this they have estimated errors which are considerably larger than those suggested by the other workers. The only alternative seems to be that there is not yet any satisfactory explanation of the scatter which is observed in measurements of diffusion coefficient.

CHAPTER III - GEOMETRICAL CONSIDERATIONS

In the geometry of low and medium frequency radio reflections from meteor trails, it is assumed that specular reflection occurs, i.e. the angles with which the incident and reflected waves intersect the trail axis, are equal. This is generally true for radio frequencies in the range 3 to 100 Mc. Above this, in the UHF region, specular reflection does not occur, but instead the echo is of the "moving head" type, in which the echo appears to be reflected from a very short length of trail moving with the velocity of the meteoric particle (Flood, 1957).

In the backscatter or radar case, specular reflection implies that the radar beam must intersect the trail axis at right angles. This is shown in Figure 1a, which is drawn in the plane defined by the radar beam and the trail axis. In the forward scatter case, where the transmitter and receiver are separated by a distance of up to 2200 km., the trail, to produce a reflection, must be tangent to one of a family of prolate ellipsoids about the transmitter-receiver (TR) axis, the transmitter and receiver being at the foci of the ellipsoid. Figure 1b is a diagram of the forward scatter case. T and R are the transmitter and receiver locations. The co-ordinate system is so defined that the xy plane passes through T and R, while the z axis is in the direction of the zenith over O the midpoint of TR. TRBA forms the plane of propagation, in which the forward-scattering angle 2ϕ is measured. CDEF is a plane perpendicular to the plane of propagation. The meteor trail lies in the plane CDEF, and makes angle β with the plane of propagation TRBA. The reflection point S on the meteor trail is at a distance h above the xy plane. R_T and R_R are the respective distances of the reflection point S from the transmitter and

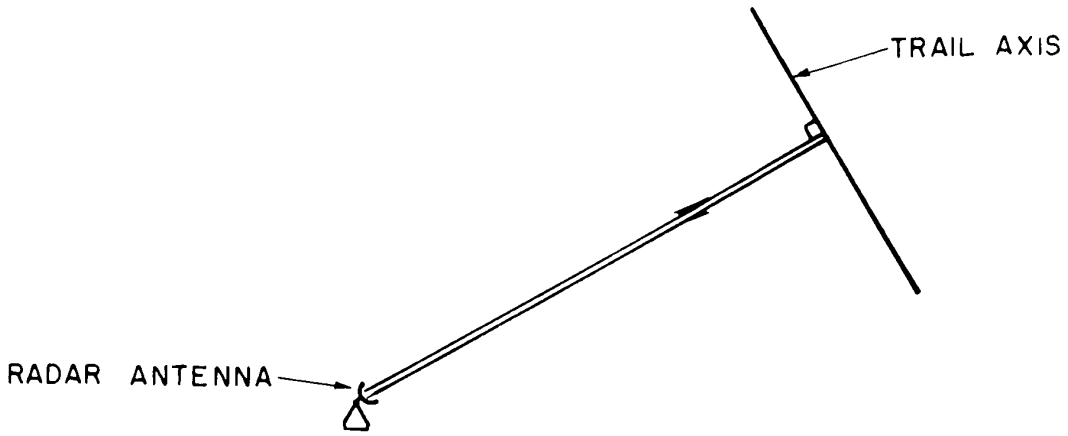

(a) BACKSCATTER FROM A METEOR TRAIL

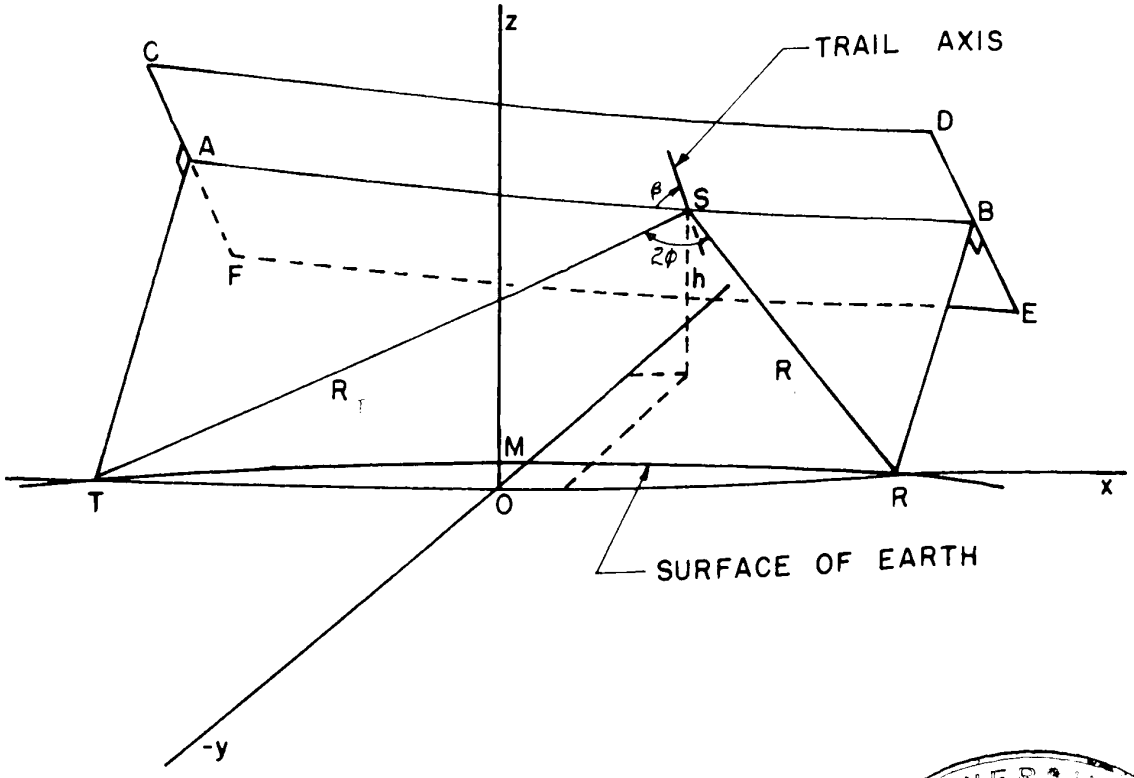

(b) FORWARD-SCATTER FROM A METEOR TRAIL

FIGURE 1

the receiver.

It has been shown (Hines 1955) that the majority of echoes received over a forward-scatter path, originate from meteor trails which have their reflection points concentrated in two regions or "hot spots" on either side of the TR axis, and near the mid-plane bisecting the TR axis. The occurrence of reflection points directly over the TR axis is excluded because this would require meteors travelling in a direction tangent to the earth's surface. For meteors travelling nearly vertically, the off-axis distance becomes so great that the potential reflection point occurs below the horizon.

In the course of this work, the possibility of obtaining coincident reflections from the same meteor trail, on combinations of different radar and forward-scatter equipments, was investigated. Figure 2 is a map of Western Canada, showing the locations of the two forward scatter paths and of the Prince Albert Radar Laboratory.

1 COMBINED UHF RADAR AND FORWARD-SCATTER

It was planned to use the facilities of the Prince Albert Radar Laboratory to locate in space meteor trails which were simultaneously observed over the Saskatoon-Churchill forward scatter path. The radar could observe one of the two hot spots of the forward-scatter path, and thus record the passage of any meteors through the region. Due to the small angular beam-width of the radar ($2\frac{1}{2}^{o}$), only a very small region could be observed, and only very few of the meteors detected in forward scatter would also be observed by the radar. The area observed by the radar, at a given height, increases with range, and the area is elliptical in cross-section. This is shown in Figure 3. Figure 4 shows the dimensions of the area observed,

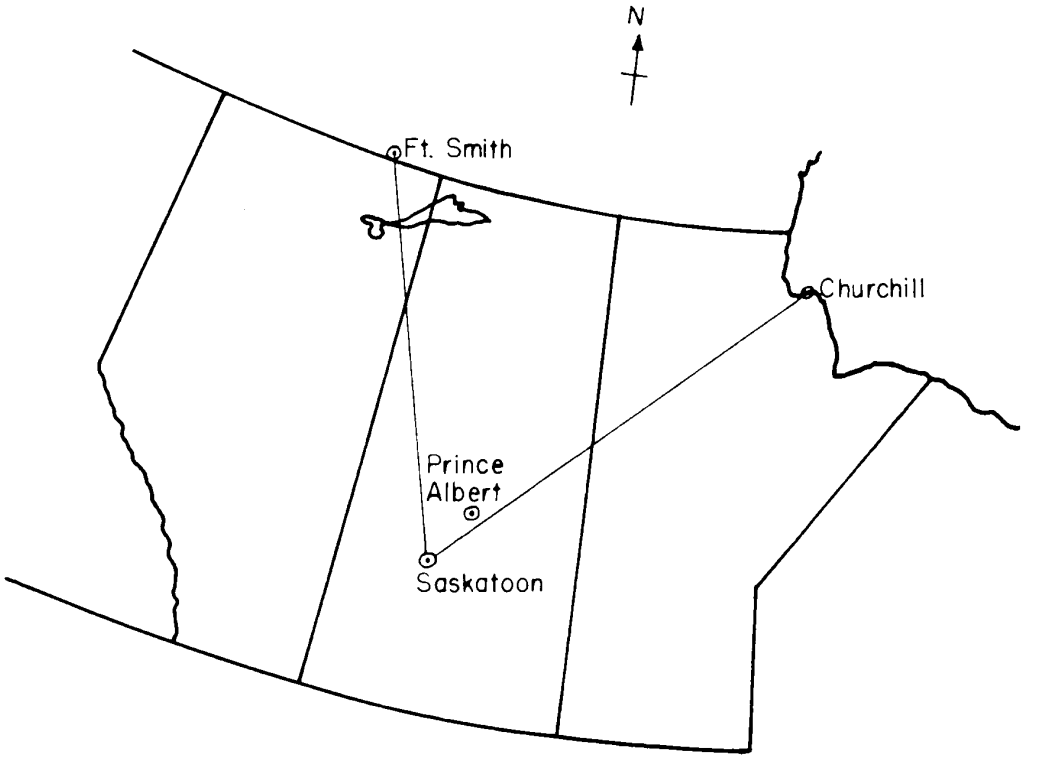

GEOGRAPHIC LOCATION
OF FORWARD-SCATTER PATHS AND RADAR

FIGURE 2

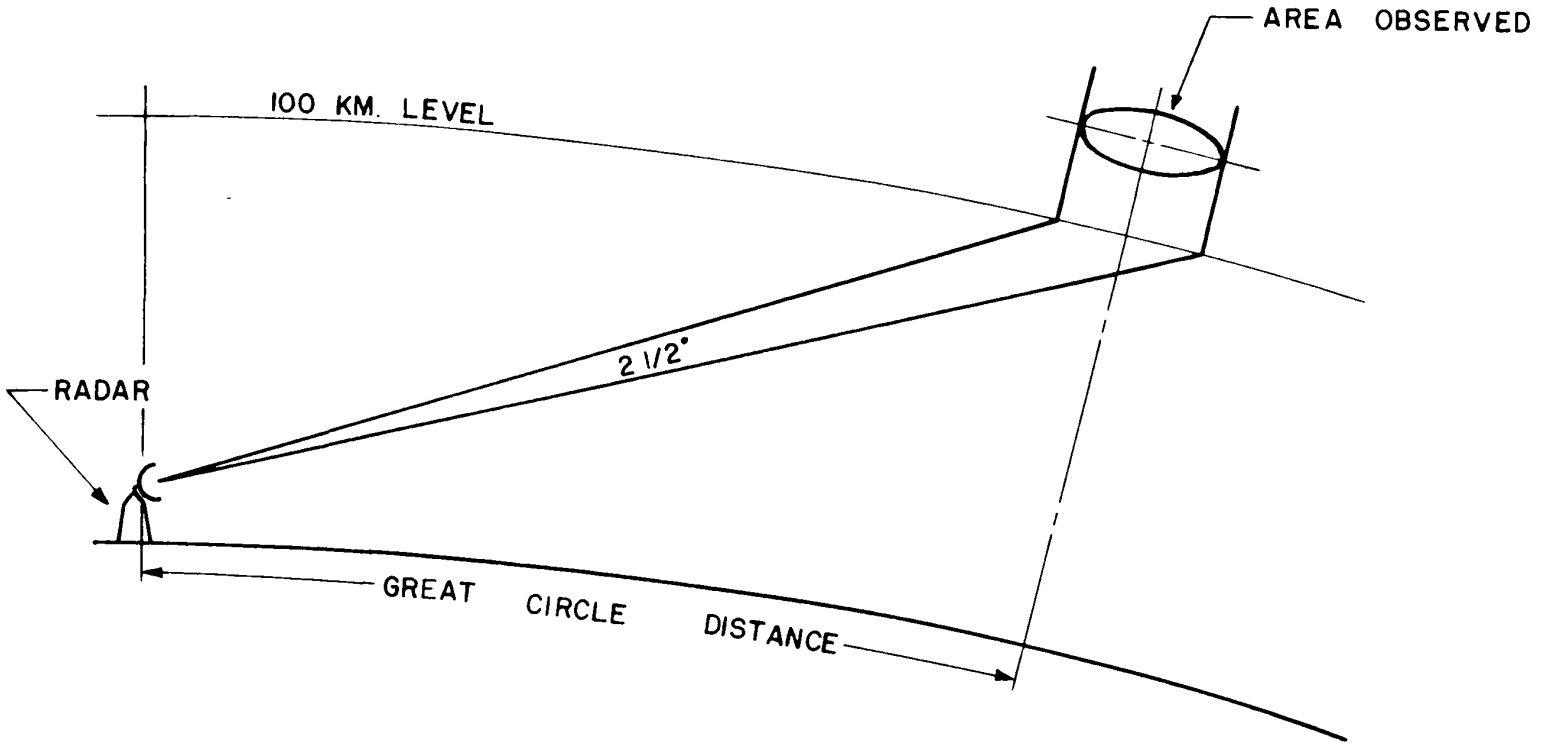

AREA ALONG A CONSTANT HEIGHT LEVEL OBSERVED BY A RADAR

FIGURE 3

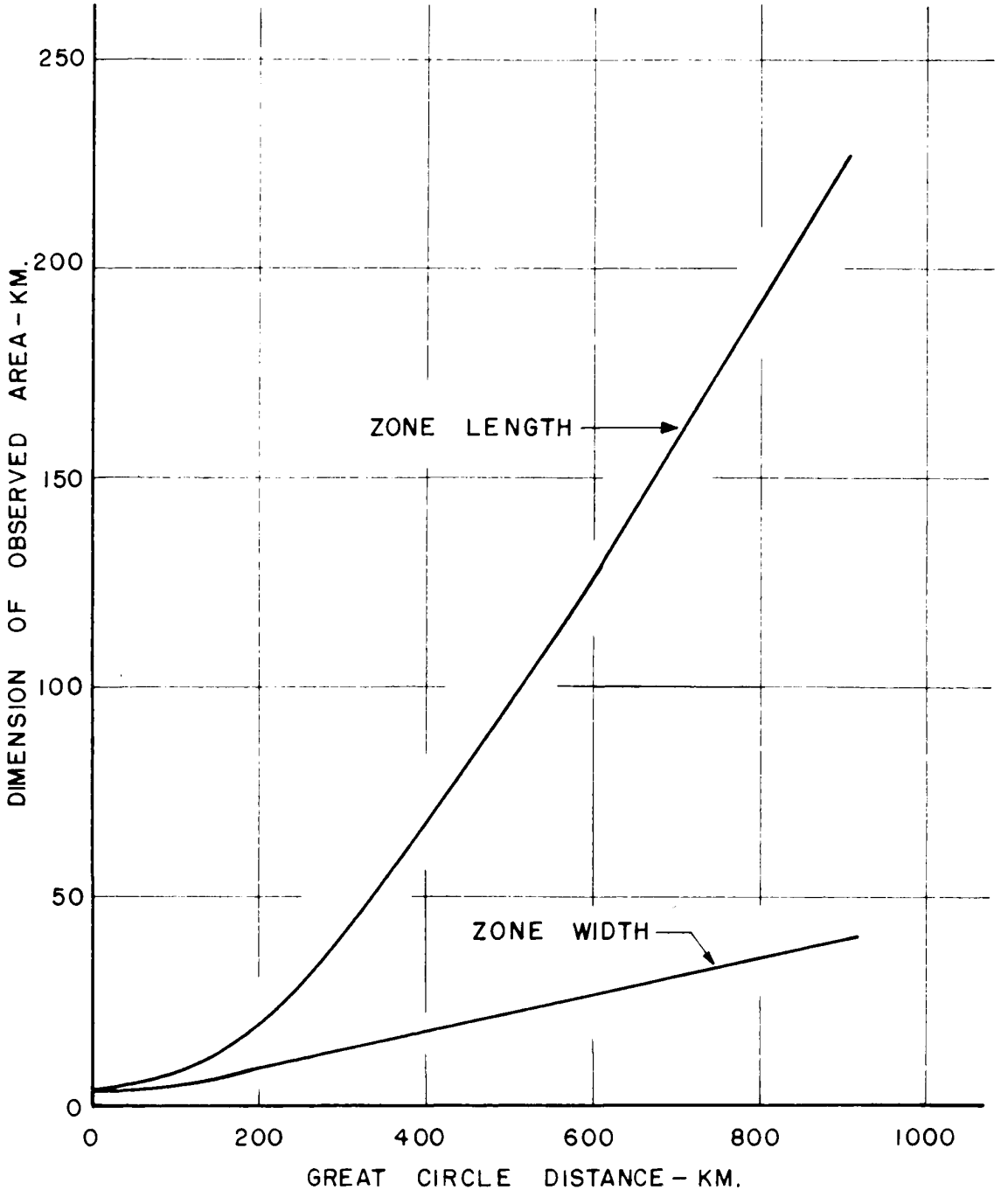

DIMENSIONS OF AREA OBSERVED AT 100KM. LEVEL BY A 2 1/2° RADAR BEAM

FIGURE 4

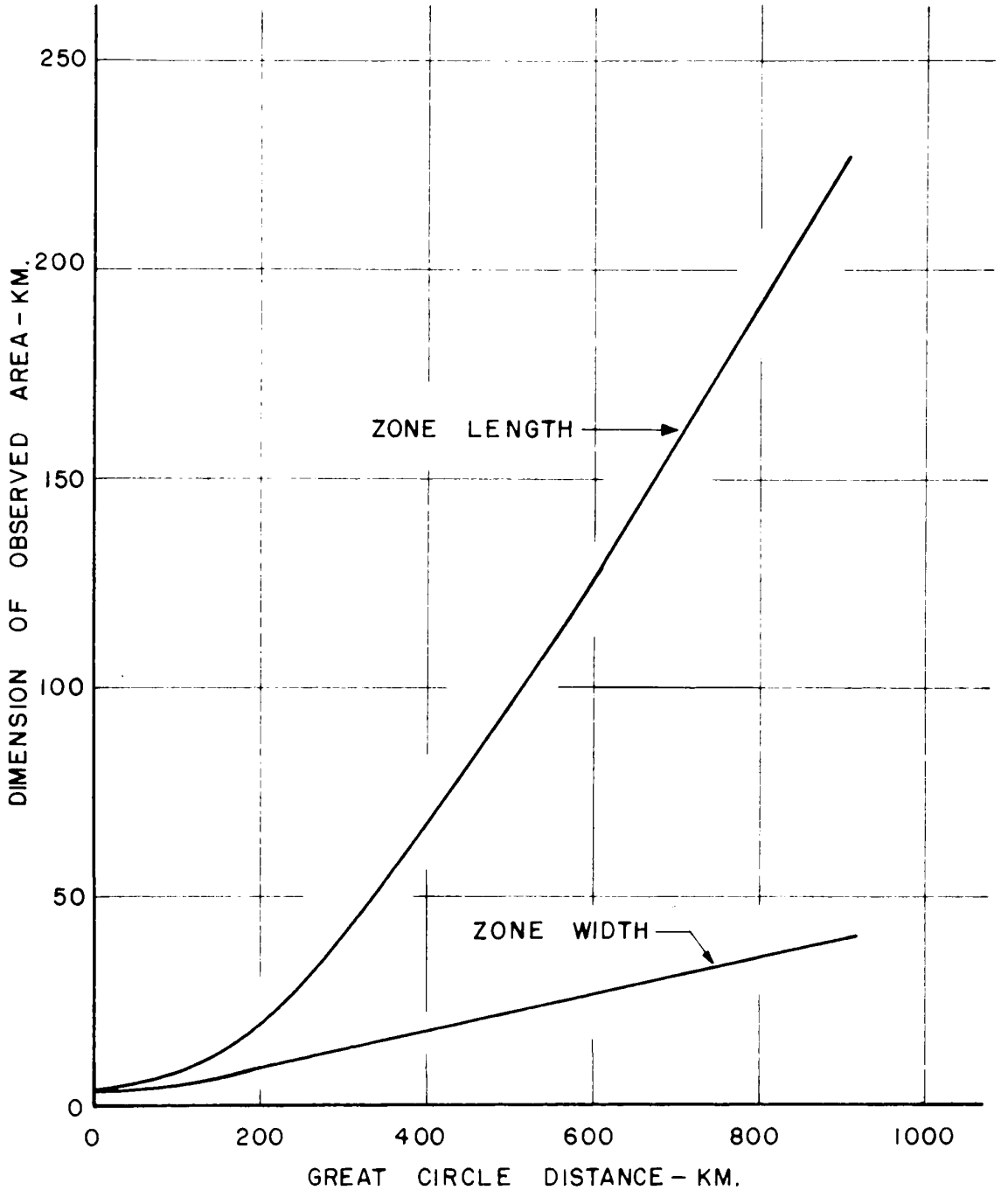

DIMENSIONS OF AREA OBSERVED AT 100KM. LEVEL BY A 2 1/2° RADAR BEAM

FIGURE 4

as a function of great circle distance from the radar station.

The azimuth and elevation of the radar beam, the range to the target, and the Doppler shift of the reflected signal, were available from the radar equipment. In operation the radar antenna was pointed in a suitable direction (azimuth and elevation) with the range and Doppler of meteors crossing the beam being recorded. Although the radar antenna could track such objects as satellites, it could not move rapidly enough to follow a meteor.

Figure 5 is a plan view of the 100 km. level, over the Saskatoon-Churchill forward scatter path. On each side of this path are shown the intersections, with the 100 km. level, of a $2\frac{1}{2}^{o}$ radar beam. Figure 6 is a projection into the vertical plane bisecting the TR axis at the axis mid-point. The area intersected by the radar beam in the plane is shown as the circular cross-hatched area; actually it is slightly elliptical, but the circular approximation is adequate for illustration. The assumed meteor trails are the limiting cases for trails both passing through the radar beam and satisfying the requirements of the forward-scatter geometry.

Two components of the meteor velocity are measurable. The UHF radar measures the Doppler shift and hence the component of velocity in a radial direction from the radar station, while the time delay between the radar and forward-scattered signals is a measure of the velocity in the plane of Figure 6. Thus the direction in space of the meteor trail is fairly well defined. Another parameter which is important is the value of $\sec^2\phi$. The range of values for the two limiting cases shown in Figure 6, at an off-axis distance of 160 km., is from 8.5 to 11.

Another case occurs, Figure 7, when the radar is situated near the midpoint of the forward-scatter TR axis. The radar information fixes

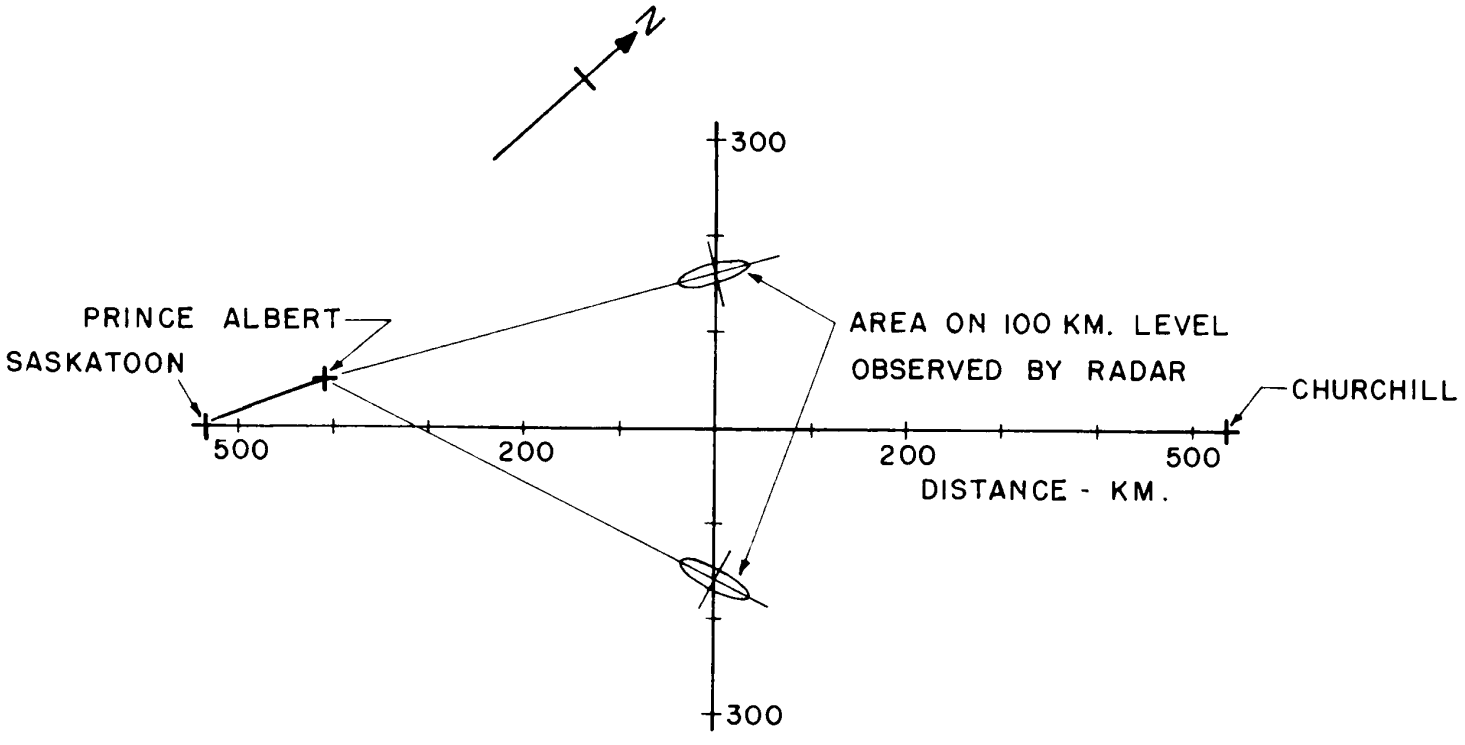

PLAN VIEW OF SASKATOON-CHURCHILL FORWARD-SCATTER PATH AND PRINCE ALBERT RADAR

FIGURE 5

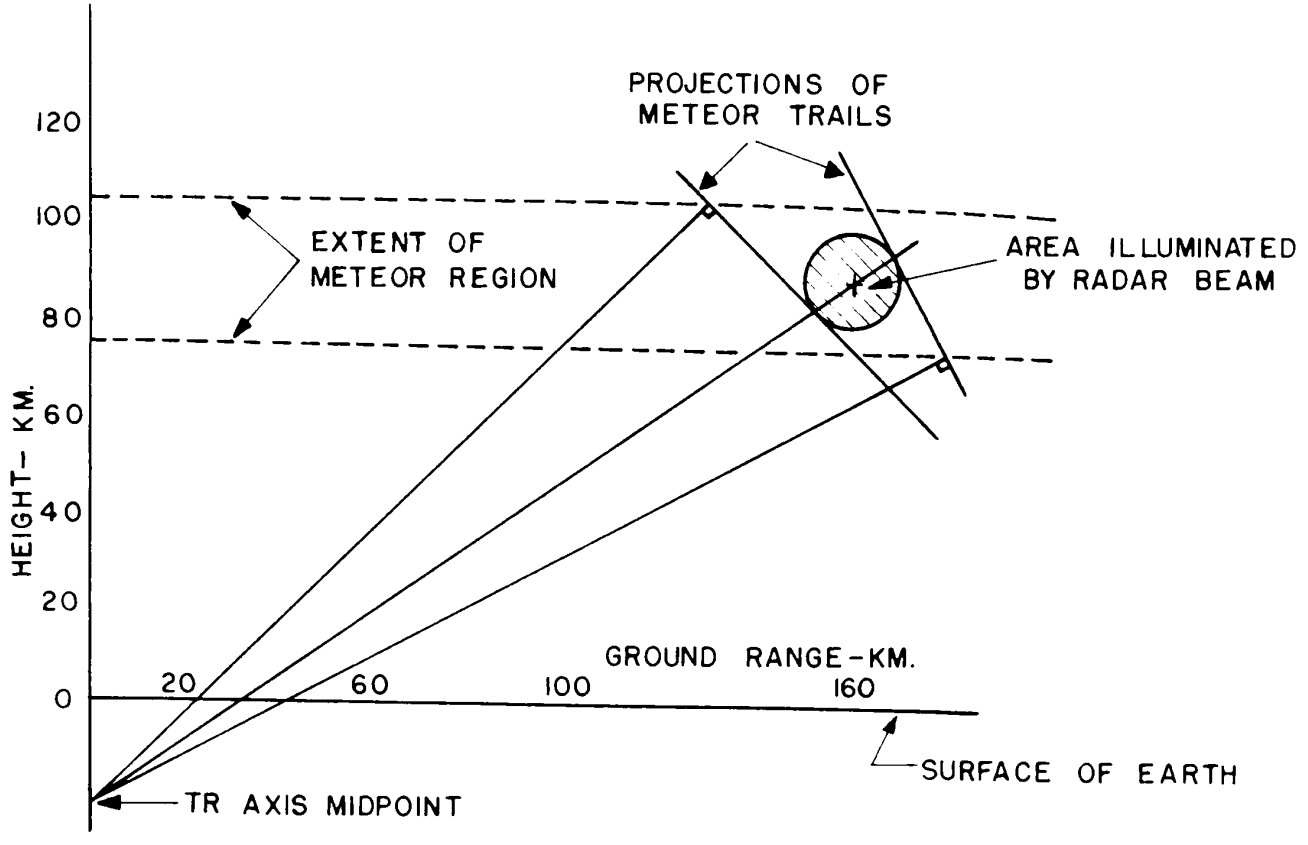

GEOMETRY FOR RADAR SITUATED NEAR ONE END OF FORWARD-SCATTER PATH

FIGURE 6

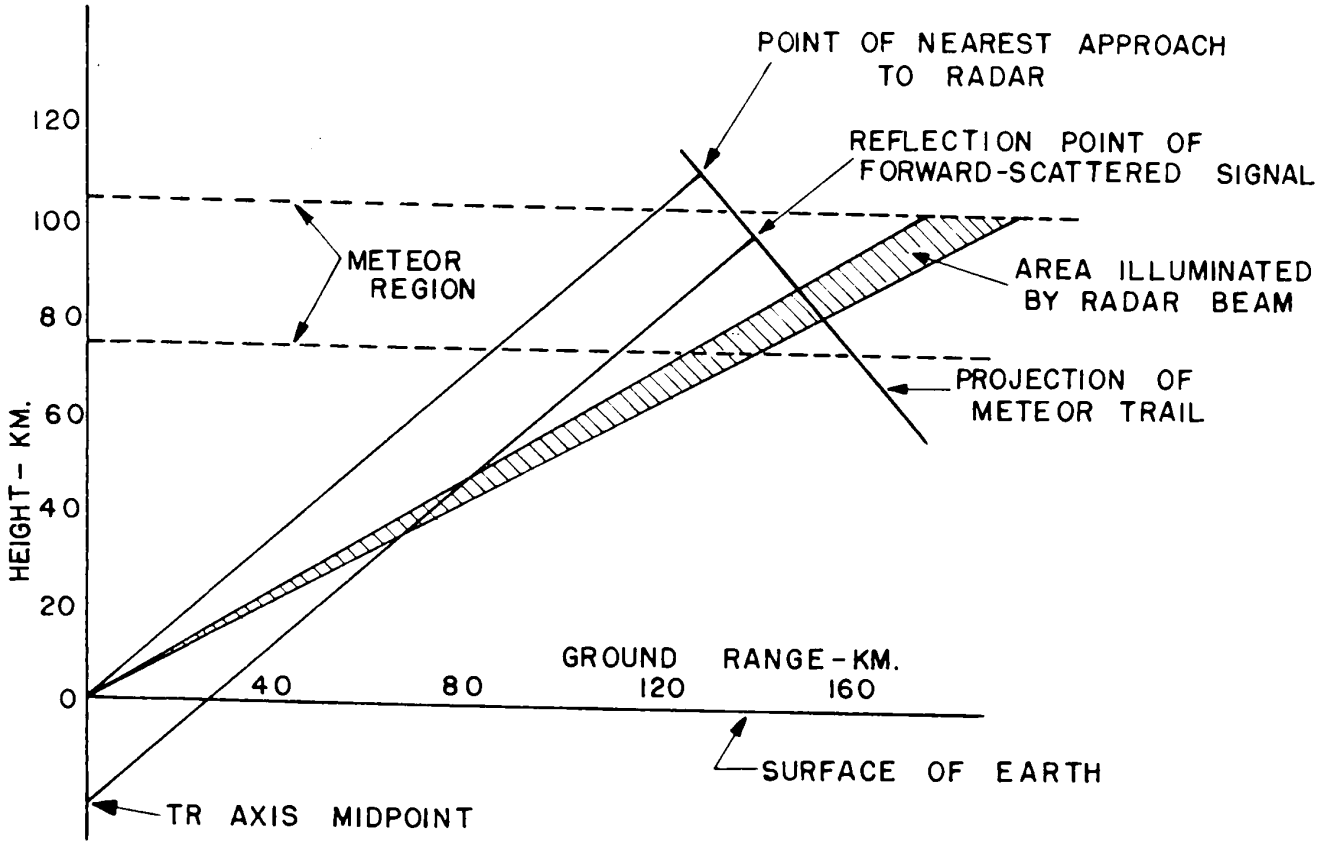

GEOMETRY FOR RADAR SITUATED AT MIDPOINT OF FORWARD-SCATTER PATH

FIGURE 7

completely the position of the projection of the meteor trail into the mid-plane; however the angle which the trail makes with the plane of propagation (the angle β of Figure (1b)) is not determined. This situation is capable of measuring the height of the reflection point of the forward-scattered signal from the radar information alone; however it does not completely specify the direction of the trail.

It would still be possible to measure the height of the reflection point of the forward-scattered signal in Figure 6, if the amplitude of the forward-scattered signal were compared after reception over antennas with differing lobe patterns. This is similar to the backscatter technique used by the Jodrell Bank group (Greenhow 1954). Greater accuracy of measurement in the forward-scatter case would be possible however, because the restricted range of elevation angles from which the signal could be received, would permit narrower antenna lobes than those of the Jodrell Bank height finding equipment, without introducing ambiguities.

The situation in which a UHF radar located near one end of a forward-scatter path is used to locate meteor trails which also provide forward-scattered signals, thus appears to be potentially useful in studying the upper atmosphere through meteors as probes. In particular, it would be useful in studying the effects of the earth's magnetic field upon diffusion, since it provides a reasonable estimate of the angle between the trail and the magnetic field. The inability to measure the absolute direction of meteor trails in space has been a major difficulty in the past. A UHF radar near the forward-scatter path mid-point is less useful, since some auxiliary method would be necessary to measure another component of the meteor velocity. Perhaps a better arrangement would be to use a VHF ($\sim$40 Mc) radar near the mid-point, with two spaced receivers to measure

the component of meteor velocity in the TR axis direction.

2 COINCIDENT REFLECTIONS OVER TWO FORWARD-SCATTER PATHS

Figure 2 shows the geographic location of the Churchill-Saskatoon and Ft. Smith-Saskatoon forward scatter paths. Obviously, the possibility exists that a meteor trail, suitably oriented in the region between the two paths, could reflect forward-scattered signals from both transmitters simultaneously, to Saskatoon. The region to the south of Saskatoon is also a possible one for the location of a meteor trail which would provide such coincident signals. However, each transmitting antenna lobe maximum was such that it intersected the 100 km. level near the mid-point of its respective TR path, so that the transmitted power in the meteor height region to the south of Saskatoon was negligibly small. For this reason it seems very unlikely that any substantial signals would be received from meteors in this region.

The direction in space, of a meteor trail located at a height of 100 km., over the line bisecting the two TR paths, was calculated as a function of the distance from the receiver location at Saskatoon. A right-handed co-ordinate system, Figure 8, was employed such that the xy plane passed through the three points Saskatoon, Churchill and Ft. Smith, with the y axis along the Saskatoon-Ft. Smith line, and Saskatoon the origin. The z axis then had the direction of the zenith over the point which is the centroid of the triangle ABC. On a scale drawing, Figure 9, contours of the distance between the plane passing through the two TR axes, and the surface of the earth, were plotted. From this, the distance z of a meteor trail reflection point at a constant height of 100 km. above the earth's surface, was obtained as a function of position along the bisector of the two TR

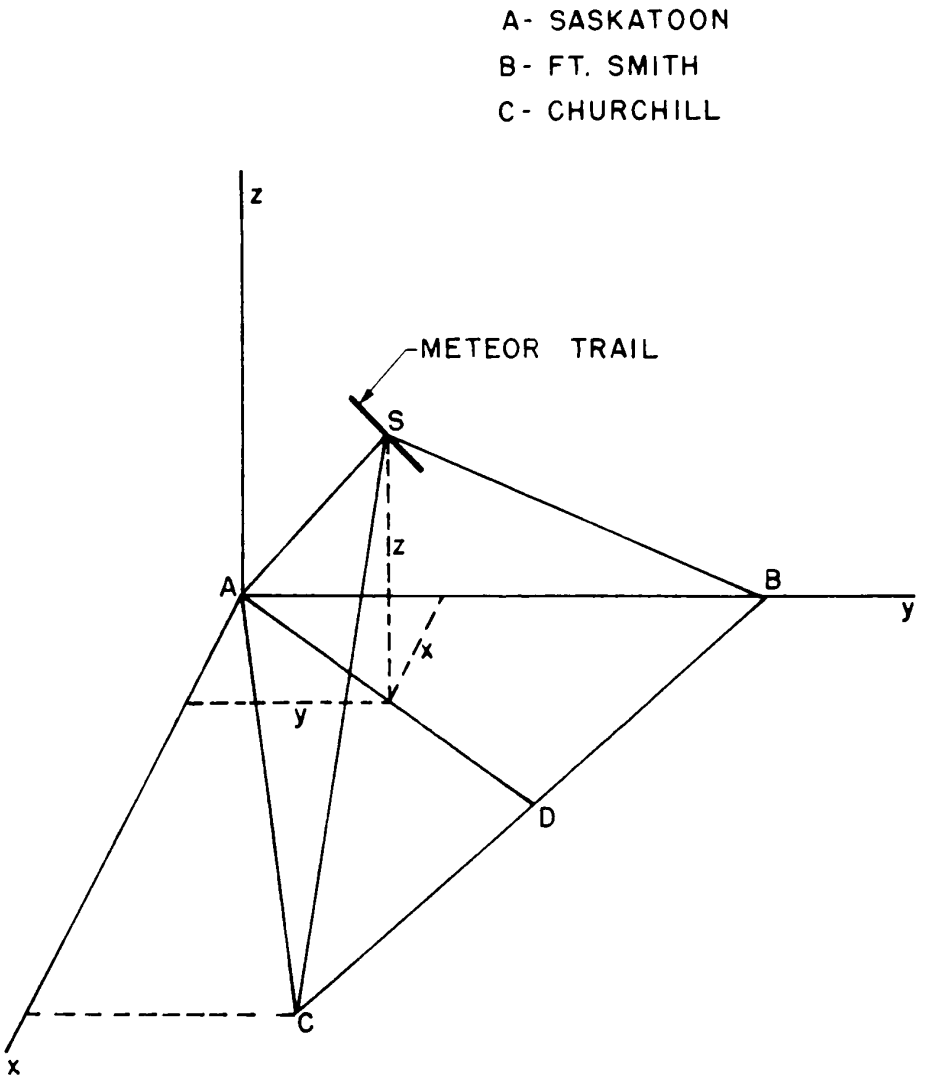

FORWARD-SCATTER COINCIDENCE GEOMETRY

FIGURE 8

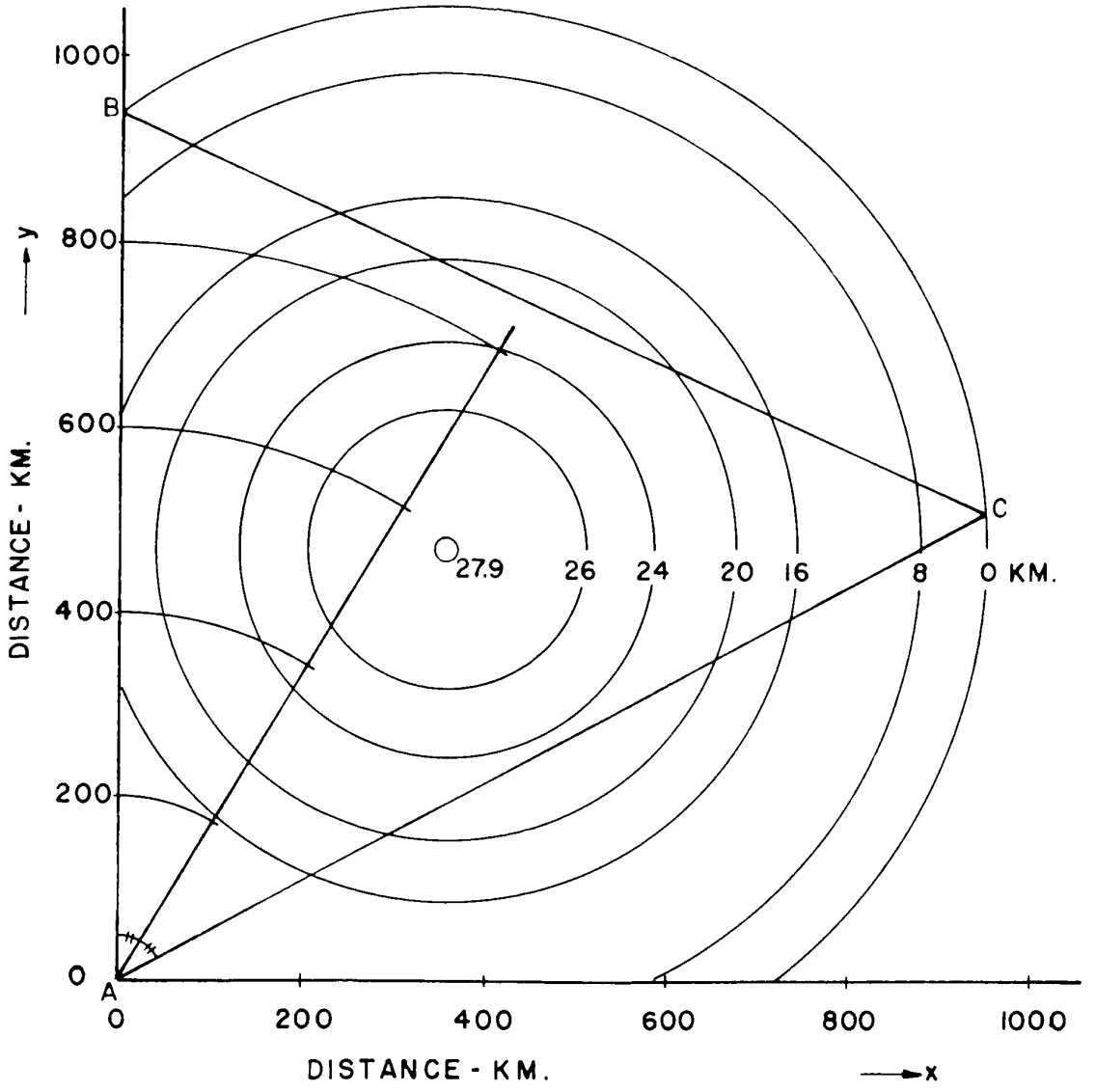

CONTOURS GIVE THE DISTANCE IN KM. BETWEEN THE PLANE THROUGH A,B,C AND THE SURFACE OF THE EARTH

A - SASKATOON B - FT. SMITH C - CHURCHILL

PLAN VIEW OF THE TRIANGLE FORMED BY SASKATOON, FT. SMITH AND CHURCHILL

FIGURE 9

axes. Thus the three co-ordinates of the reflection point, in the co-ordinate system already defined, were obtained. The condition for reflection is that the meteor trail must be tangent to a prolate ellipsoid which has the transmitter and receiver as foci. Then for a reflection over both forward scatter paths, the trail must be tangent to two ellipsoids, one about each TR axis, such that the ellipsoids intersect at the given reflection point. The tangent to the line of intersection is the direction of the meteor trail.

A definition of a conic is: the locus of a point which moves in a plane, so that the ratio of its distance from a given point and a given fixed line is a constant e, the eccentricity. For an ellipse $e < 1$. Then

$$\frac{\sqrt{x^2 + y^2}}{p + y} = e$$

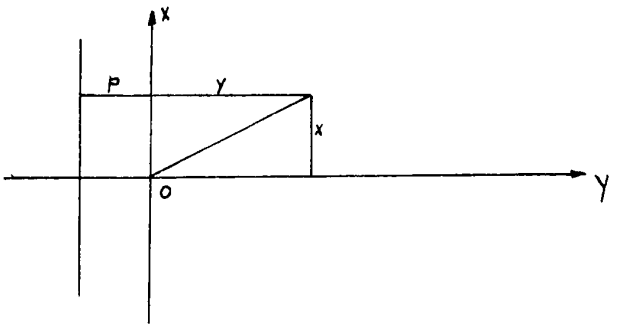

or $y^2 (1-e^2) - 2e^2py + x^2 - e^2 p^2 = 0$ - - - - - - - - - (18),

where p is the distance of the fixed line from the origin O.

In three dimensions, where Oy is an axis of symmetry, x^2 is replaced by $x^2 + z^2$, so that the equation of an ellipsoid is

$$x^2 + z^2 + y^2 (1-e^2) - 2 e^2py - e^2 p^2 = 0 \quad - - - - - - - - -(19)$$

Equation (19) may be put in the form

$$\left\{y - \frac{e^2p}{1-e^2}\right\}^2 + \frac{x^2+z^2}{1 - e^2} = \frac{e^2p^2}{(1-e^2)^2} \quad - - - - - - - - - - - - -(20)$$

Let $\frac{e^2p}{1-e^2} = m$, and $\frac{e^2p^2}{(1-e^2)^2} = a^2$ - - - - - - - - - - - (21)

2m is the distance between the foci of the ellipsoid, while a is the semi-major axis. There are two independent constants of the ellipse to be evaluated. Since the distance 2m is known, it is desirable to substitute m into equation (20), eliminating p. Substituting $e^2p = m(1-e^2)$ and $e^2p^2 = \frac{m^2}{e^2}(1-e^2)^2$ from (21), into equation (19), then

$$e^4(2ym - y^2 - m^2) + e^2(x^2 + y^2 + z^2 - 2ym + 2m^2) - m^2 = 0 \quad - - -(22)$$

Solving the quadratic in e^2:

$$e^2 = \frac{-\{x^2+y^2+z^2-2ym+2m^2\} \pm \{(x^2+y^2+z^2-2ym+2m^2)^2 + 4m^2(2ym-y^2-m^2)\}^{\frac{1}{2}}}{2(2ym-y^2-m^2)} \quad - - - - - - (23a)$$

Thus, given (x,y,z), the co-ordinates of a point on the ellipsoid, and the distance 2m between the foci, the constants of the ellipsoid are determined.

In order to determine the constants of the ellipsoid about AC, it was necessary to transform the co-ordinates of the (xyz) system into a new system (x'y'z') such that the y' axis fell along AC. This was accomplished by a rotation about the z axis, so that

$$x' = x\cos\eta - y\sin\eta$$
$$y' = y\cos\eta + x\sin\eta$$
$$z' = z \qquad - - - - - - - - - - - - - - - (24)$$

where η is the angle of rotation. For the simple case where x and y fall along the bisector of the y and y' axes,

$$x' = -x$$
$$y' = y \qquad - - - - - - - - - - - - - - - (25)$$
$$z' = z$$

The distance $2m_2$ between the foci being a known constant, the

eccentricity e_2 was then determined from an equation like (23a), but written for the co-ordinate system x'y'z', i.e.,

$$e_2^2 = \frac{-\{x'^2+y'^2+z'^2+2m_2^2\} \pm \{(x'^2+y'^2+z'^2+2m_2^2)^2+4m_2^2(2y'm_2-y'^2-m_2^2)\}^{\frac{1}{2}}}{2(2y'm_2-y'^2-m_2^2)} \quad - - - \quad (23b)$$

The subscript 2 refers to the ellipsoid about AC.

If $f = f(x,y,z)$ is the equation of a surface, then the normal to the surface is given by

$$\nabla f = i\frac{\partial f}{\partial x} + j\frac{\partial f}{\partial y} + k\frac{\partial f}{\partial z} \qquad - - - - - - - - - - - - - \quad (26)$$

where i,j,k are unit vectors in the directions x,y,z.

Using the subscript 1 to refer to the ellipsoid about AB, and the subscript 2 to refer to the ellipsoid about AC, then from equation (19),

$$\nabla f_1 = i\,2x + j\left\{2y\,(1-e_1^2) - 2e_1^2p_1\right\} + k\,2z \quad - - - - - - - - - \quad (27)$$

or, eliminating p,

$$\tfrac{1}{2}\nabla f_1 = i\,x + j\,(y-m)(1-e_1^2) + kz \quad - - - - - - - - - - - - \quad (28)$$

The equation of the ellipsoid about AC, in x',y',z' co-ordinates, is

$$f_2 = x'^2 + z'^2 + y'^2\,(1-e_2^2) - 2e_2^2\,p_2y' - e_2^2p_2^2 = 0 \quad - - - \quad (29)$$

Transforming to x y z co-ordinates by equations (24), and forming ∇f_2, then

$$\tfrac{1}{2}\nabla f_2 = i\left\{x(1-e_2^2\sin^2\eta) - ye_2^2\sin\eta\cos\eta - m_2(1-e_2^2)\sin\eta\right\}$$
$$+j\left\{y\,(1-e_2^2\cos^2\eta) - xe_2^2\sin\eta\cos\eta - m_2(1-e_2^2)\cos\eta\right\}$$
$$+kz \qquad - - - - - - \quad (30)$$

Finally, the direction of the meteor trail is given by the cross product

$$\nabla f_1 \times \nabla f_2 = ai + bj + ck \qquad - - - - - - - - - - - - - \quad (31)$$

where a,b,c are the direction numbers of the trail axis. The angle which the trail makes with the zenith over the centroid of the triangle ABC, is given by

$$\cos\chi = \frac{c}{\sqrt{a^2+b^2+c^2}} \qquad \text{- - - - - - - - - - - - - - - - (32)}$$

Figure 10 shows the results of this calculation. Figure 10a shows the zenith angle χ as a function of the distance from Saskatoon along the bisector of the two TR paths. Figure 10b is a plot of the locus of the direction numbers a and b. This latter figure merely confirms that the direction of the meteor trail, in the horizontal plane, is approximately along the direction of the bisector of the two paths.

From an inspection of Figures 9 and 10a, it seems likely that meteors with radiants about 60° from the zenith, in a southerly direction, would potentially be capable of producing simultaneous forward-scattered signals over the two paths. It would therefore seem profitable to record meteor showers which have declinations near -10°. Suitable showers are listed in Table I.

3 COINCIDENT REFLECTIONS OVER ONE FORWARD-SCATTER PATH AND A VHF BACK-SCATTER SYSTEM

In early 1961 a 42 Mc. continuous wave backscatter system was set up to study reflections from radio aurora. This consisted of a 50 watt transmitter, located at Prince Albert, transmitting from a five element Yagi antenna towards magnetic north, together with a receiver, located at Saskatoon, which was similar to the receivers used for the forward scatter circuits. The receiving antenna was also a five element Yagi, beamed towards magnetic north.

Since the region of sensitivity for this system was to the northwest

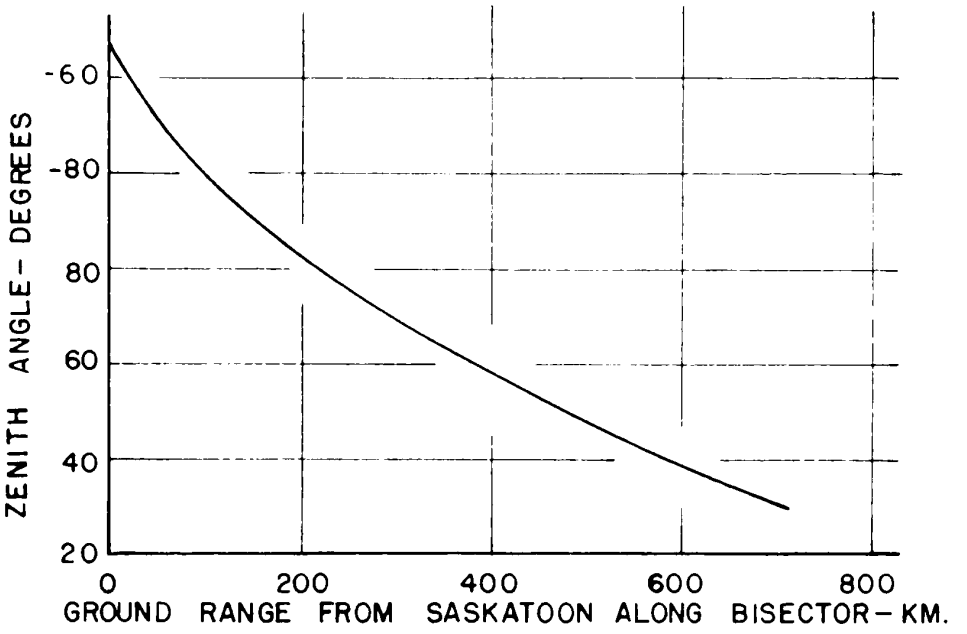

(a) ZENITH ANGLE OF METEOR RADIANT

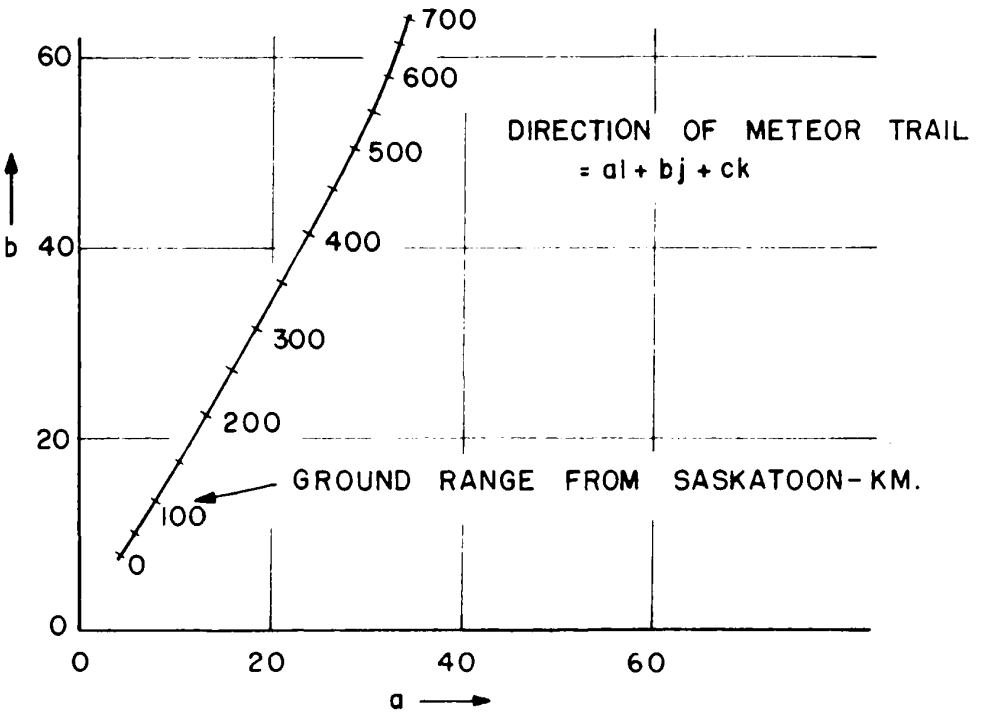

(b) LOCUS OF DIRECTION NUMBERS a AND b

FIGURE 10

TABLE I - METEOR SHOWERS WITH DECLINATIONS NEAR - 10°

Shower	Date of Maximum	Limits	Declination
η Aquarids	May 4	May 2-6	0°
Southern δ Aquarids	July 30	July 21-August 15	-17°
Northern δ Aquarids		July 14-August 19	- 5°
Southern ι Aquarids		July 16-August 25	-14°
Northern ι Aquarids		July 16-August 25	- 5°
α Capricornids	August 1	July 17-August 21	-10°

of the midpoint of the Saskatoon-Churchill forward scatter path, it was decided to investigate the possibilities of utilizing the geometry of these two systems in order to obtain coincident reflections from meteor trails.

The condition of specular reflection in the backscatter or radar case implies that for reflection the meteor trail axis must be tangent to one of a family of spheres about the radar station as a centre. Here the transmitter and receiver were actually separated about 130 km., however the situation will be treated as though the transmitter and receiver were located together at the midpoint of the two locations.

Since the geometry of forward-scatter and back-scatter in coincidence is not unique but has several degrees of freedom, it was desirable to look for shower meteors with well defined radiants. In what follows, therefore, the radiant is assumed to be known.

The geometry for the backscatter case may be represented on a celestial sphere, as in Figure 11. Angles are measured as lengths of arc, e.g. angle θ is measured by the arc WS. Oz is the direction of the zenith over the radar station. P is the north pole, and OS points toward the south. C is the position of a meteor radiant, which moves about P with constant arc length PC. OC is contained in a plane through GDCE, so that FO, a line perpendicular to GDCE, is the direction of a radar which obtains an echo from the meteor trail with radiant position C. The angle WS is the azimuth angle, of the radar. The relation between the elevation angle WF, the angle DZC, and the zenith distance of the radiant, CZ, is simply

$$\cos \text{DZC} = \tan \text{WF} \cot \text{CZ} \qquad \text{- - - - - - - - - - - - - - - - - (33)}$$

Since meteor trails occur in a narrow height region around 100 km., the elevation angle WF fixes the approximate range from which echoes will

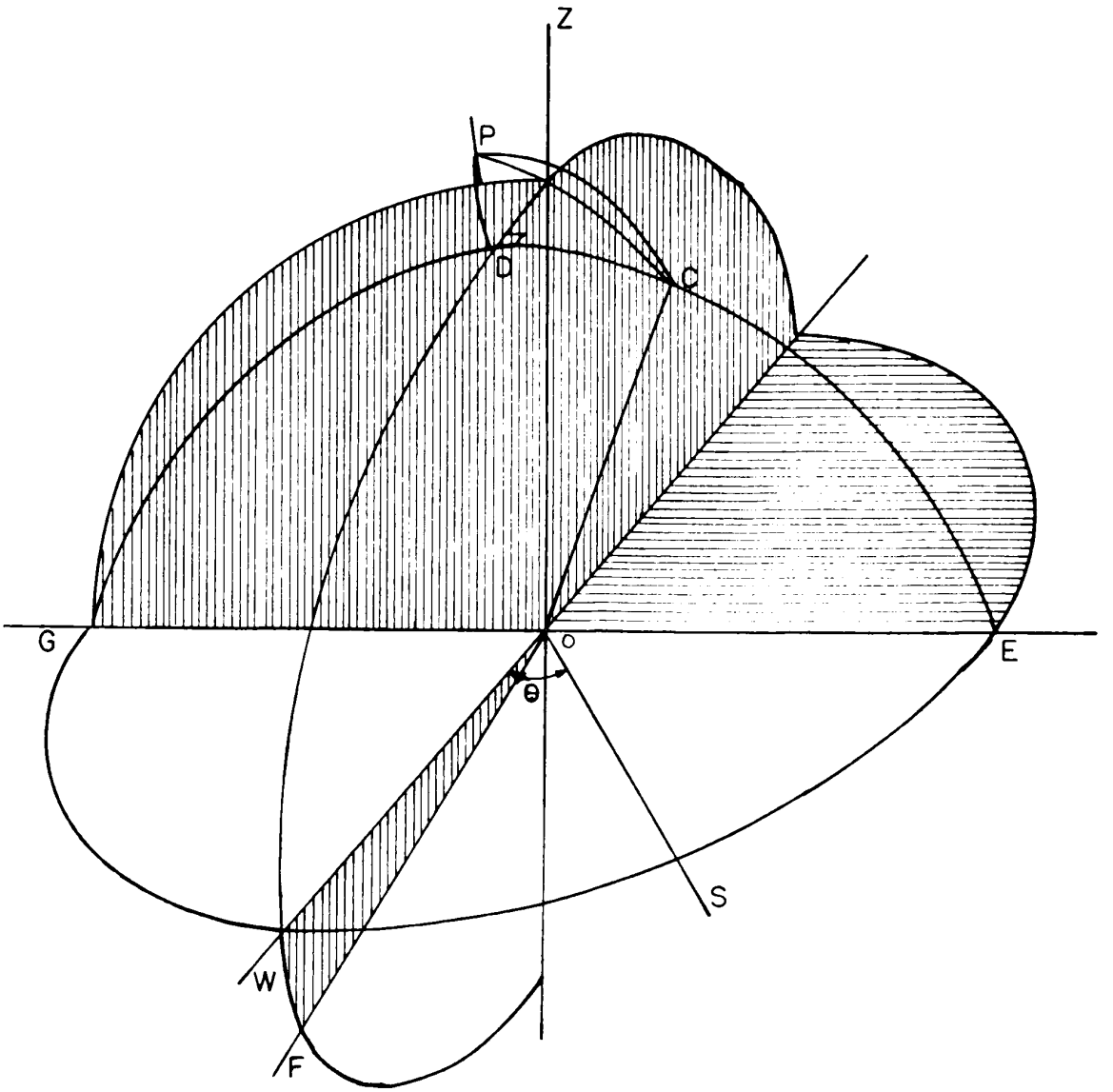

BACKSCATTER GEOMETRY ON THE CELESTIAL SPHERE

FIGURE 11

be obtained, or vice versa. The angle DZC is related to the radar bearing, WS. Thus the radar bearing can be plotted for suitable ranges, as a function of time, for a given meteor radiant. Such a diagram is shown in Figure 12, for the β Taurids shower of June 30 (right ascension 86°, declination $+19^{\circ}$). This diagram is a plan view of the Saskatoon-Churchill forward scatter path, together with a hypothetical radar at the mid-point of the Saskatoon-Prince Albert line. Constant ranges of 400, 500, and 600 km. are plotted about this mid-point. Upon the range contours are plotted other contours which give, as a function of time, the azimuth and range of possible meteor reflection points. The solid contours are for a height of 100 km., while the dotted ones are for 80 km. Also shown, plotted along the bisector of the forward scatter axis, are the locations along this axis, at the 90 km. level, of the reflection points for forward-scattered signals from β Taurid meteors. It may be seen that this is a more slowly varying function of time than the positions of reflection points in backscatter. There is, however, a short time, about fifteen minutes, when reflections over both circuits must take place in the same region, so that coincidences would be possible.

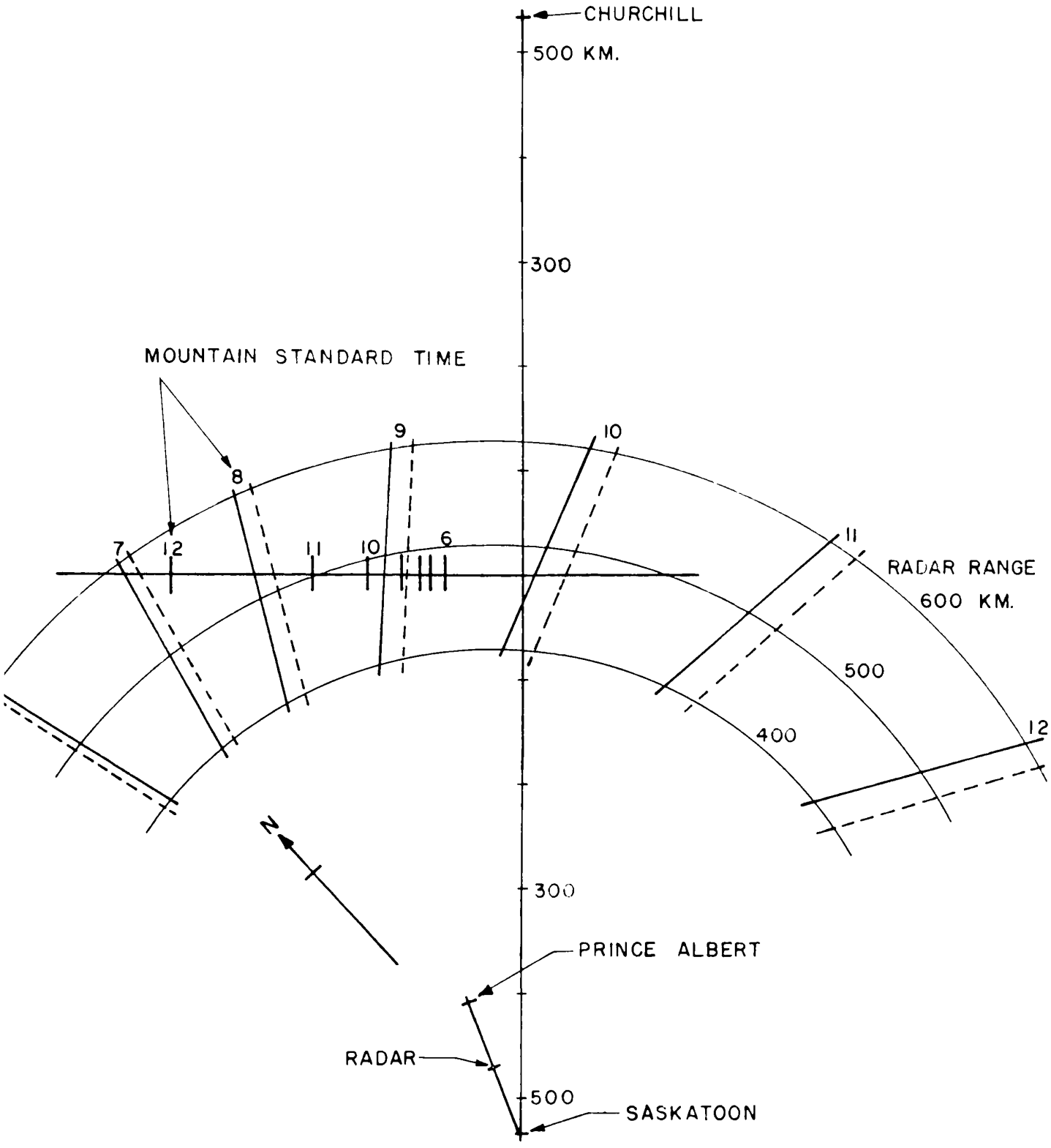

RANGE-AZIMUTH DIAGRAM FOR VHF RADAR LOCATED BETWEEN SASKATOON AND PRINCE ALBERT, β TAURIDS METEOR SHOWER

FIGURE 12

CHAPTER IV - OBSERVATIONS OF SIGNAL COINCIDENCES

1 FORWARD-SCATTER COINCIDENCES

As suggested by the analysis of Section 2 of Chapter III, recordings were made at Saskatoon of the forward-scattered meteor signals from both Ft. Smith and Churchill, during the occasions when the radiants of the showers listed in Table I were in favorable positions.

The equipment used to make these recordings is fully described in Appendix A, but a brief description will be given here. The outputs of the two radio receivers were fed to a magnetic tape delay system, so that all received signals were temporarily stored on magnetic tape. Each time the signal amplitude from one of the receivers exceeded a preset level, a chart recorder was automatically turned on to record the signal as it was played back from the output of the tape delay system. The modulation and demodulation equipment associated with the tape recorder were built by the author as an undergraduate thesis project, however, since some modifications have been made, complete circuit diagrams are included in the appendix. The other major piece of equipment built for this work was the Sanborn Controller, Figure 12 of Appendix A.

Recordings were made for about two hours on May 6, and for approximately six hour periods on fourteen different days between July 18 and August 4, when the radiants of the showers listed in Table I were known to be in favorable positions for coincidences over the two circuits. While there were a few coincidences, the coincidence rate was so low that there was a statistical possibility that for most of the coincidences, the two signals did not arise from the same meteor trail. This was emphasized by the fact that there were several signals from the two paths

which occurred one to two seconds apart in time. Considering probable meteor velocities and the finite length of a trail, this time interval appears too great for the two signals to have originated from separate parts of the same meteor trail. Another difficulty was that, of the signal pairs recorded, often only one exhibited an exponential decay.

The analysis of one of the best signal pairs recorded will be given here, in order to illustrate the type of information which can be gained from such work. Figure 13 shows a signal pair which was recorded at 0508 MST on August 2, 1961. The vertical arrows represent a signal range of 10 db. A straight line representing the mean slope of the decay has been drawn for each signal. There is some uncertainty in the case of Ft. Smith signal, due to the fluctuations in the decay.

Designating the Churchill signal by the subscript 1, and the Ft. Smith signal by 2, then the measured decay times are

$$\tau_1 = 0.089 \text{ sec.}$$

$$\tau_2 = 0.24 \text{ sec.} \qquad \text{- - - - - - - - - - - - - - - - (34)}$$

Assuming the values of $\sec^2\phi$ to be approximately equal for both, then

$$\frac{D_1}{D_2} = 2.7 \qquad \text{- - - - - - - - - - - - - - - - (35)}$$

Using a scale height of 7.8 km. (Greenhow and Hall 1961), this ratio corresponds to a height difference of 3.4 km. The time delay between the start of the two signals is 0.18 sec. Hence the vertical component of velocity is 19 km/sec.

The measured decay times, through their relation to the diffusion coefficient, provide an estimate of the reflection point height. Using

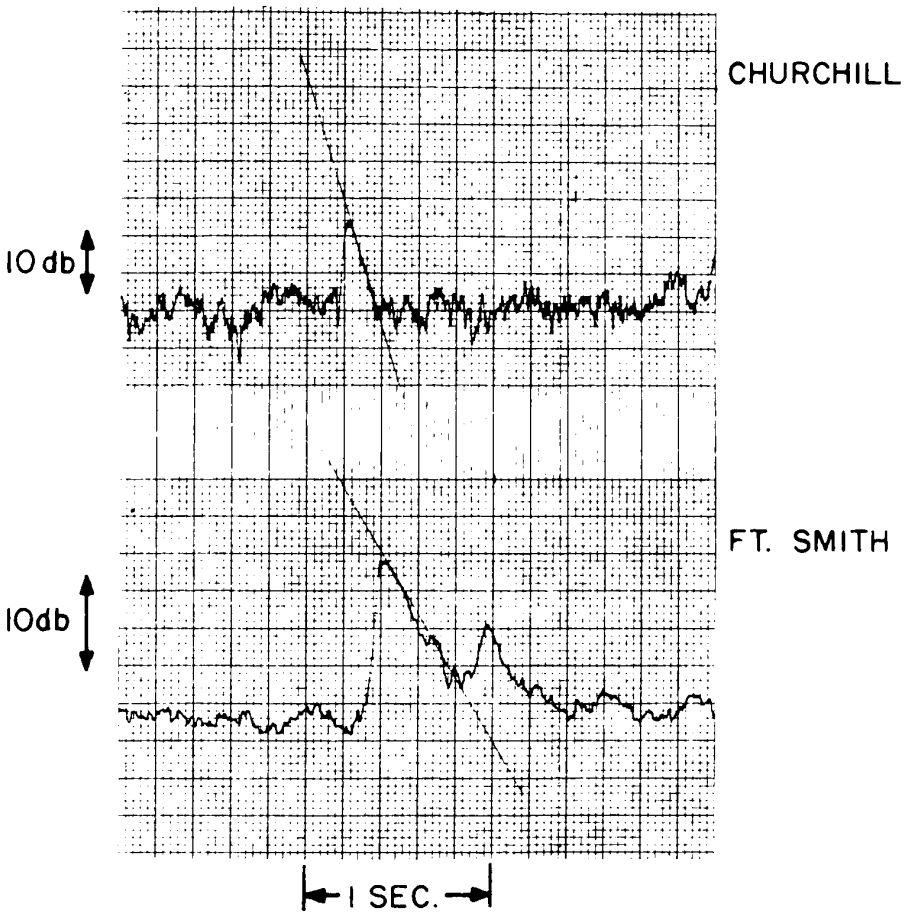

FORWARD-SCATTER COINCIDENT SIGNALS

RECORDED 0508 MST AUGUST 2, 1961

FIGURE 13

a value for $\sec^2\phi$ of 5.5, then

$$D_2 = 8 \qquad \text{- - - - - - - - - - - - - - - - - (36)}$$

This corresponds to a height of 97 km. (Greenhow and Hall 1961). Hence the first reflection point is at a height of about 100 km., while the second is 3.4 km. lower. The value chosen for $\sec^2\phi$ will be justified later.

The velocity of a meteor has been given in terms of the height of maximum ionization by Kaiser (1953). Since signal 2 has the larger peak power, it may be assumed that the peak ionization density occurred near the reflection point for this signal. Kaiser gives a particle velocity of 47 km./sec. for a height of maximum ionization of 97 km. Since the peak received amplitude is proportional to the line density q, the ratio of the peak powers is a measure of the ratio of the line densities at the two points. The ratio of the peak amplitudes for the signal pair of Figure 13 is 2.5, therefore

$$\frac{q_2}{q_1} \sim 2.5 \qquad \text{- - - - - - - - - - - - - - - - - (37)}$$

This value is approximate only, because the geometrical factors which enter into the expression for the peak received amplitude have been assumed to be equal. This assumption is reasonable since the two paths are approximately equal in length (14% difference), and it has already been assumed that the reflection points occurred near the bisector of the two paths, so that the geometrical factors would be similar for each. It is probably impractical to attempt the numerical solution of the expression for the peak received amplitude, since many of the factors in it are not known accurately; for example, the antennae gains in the direction to the reflection point.

Despite the uncertainty in the expression (37), it is worthwhile to compare this result with that of Greenhow and Neufeld (1957). They have measured the mean variation of electron line density along a group of underdense meteor trails. They found the mean ionization curve to rise to maximum more rapidly than had been predicted by theory. The relation (37) states that there was an increase of 2.5 in electron line density in a height of 3.4 km. This rapid increase appears to be in agreement with the experimental work of Greenhow and Neufeld.

From the velocity and the vertical component of velocity which have been deduced, the zenith angle of the meteor radiant is

$$\chi = 66^\circ \qquad \text{- (38)}$$

Referring to Figure 10, this corresponds to a reflection-point distance from Saskatoon of 330 km. Since this now fixes the position of the reflection point in space, reference to Figure 21 shows that $\sec^2\phi = 5.5$, the value which was used earlier. The value of $\sec^2\phi$ is relatively slowly varying with distance from Saskatoon near this point, so the value can be used with some confidence.

Since the direction in space of the meteor trail has been fixed, the angle between the meteor trail and the apex of the earth's way may be calculated. Assuming the meteoric velocity to be the parabolic limit, then the velocity with respect to the earth is 69 km./second. A lower limit may be calculated by assuming the meteor to be in a circular orbit about the sun; then the velocity with respect to the earth would be 57 km./second. Thus, a meteoric particle with the radiant position deduced would have a velocity with respect to the earth of nearly 69 km./second, with a lower limit of 57 km/second.

The foregoing analysis of a pair of coincident forward-scattered signals

has led to a meteor velocity which is too low to be acceptable. The velocity of meteoric particles entering the earth's atmosphere depends principally upon the angle with which the meteor orbit intersects the direction of the apex of the earth's way. Since velocities derived in this way are based upon the well accepted laws of planetary motion, they need not be questioned. The discrepancy may lie in the deduced height separation of the two reflection points, and perhaps the actual height of the reflection points. The measurements do not really contain enough information that checks through the internal consistency of the derived information are possible. Also, only one isolated signal pair has been investigated, while statistical procedures are often necessary when dealing with meteoric phenomena. This has been especially true of measurements relating height and the diffusion coefficient. It seems quite reasonable, therefore, that information for a single meteor trail, derived from such measurements, might be considerably in error.

While it has been found possible to obtain coincident signals from a single meteor trail, over two different forward-scatter paths, the possibilities of utilizing such measurements appear limited. This is especially true where a statistical approach is necessary, as is the case in many meteor measurements. The extremely low coincidence rate would immediately preclude any measurements involving a diurnal variation, for instance.

2 FORWARD-SCATTER-BACKSCATTER COINCIDENCES

A limited observational program was carried out utilizing the geometry outlined in Section 3 of Chapter III. Observations were made as shown in Table II.

TABLE II - METEOR SHOWERS OBSERVED WITH FORWARD-SCATTER-BACKSCATTER GEOMETRY

Shower	Date of Maximum	Limits	Radiant R.A.	Radiant Dec.	Days Observed
Daytime Arietids	June 8	May 29-June 18	44	+23	4
Perseids	June 9	June 1-June 16	62	+23	
Taurids	June 30	June 24-July 6	86	+19	3

During these observations, no signals were received which were believed to be genuine coincidences. However, the probability of observing such a coincidence for a shower meteor is small, since the potential reflection points occur in the same region of space for only about fifteen minutes (see Figure 12). It therefore seems unlikely that more extensive observations of this nature would produce a coincidence rate sufficient to allow significant measurements to be made.

CHAPTER V - THE PERSEIDS

Records of the forward-scattered meteor signals from both Ft. Smith and Churchill were made at Saskatoon on August 10, 1961 from 1248 to 1437 MST, and continuously from 0802 August 11 to 1804 MST August 12. It is well known that the Perseids meteor shower is active on these dates. Although the radiant of the shower was not favorable to coincident signals over the two forward-scatter paths, it was hoped that the enhanced signal rate due to the shower would be sufficient to allow useful information to be extracted. In particular, the angles with which the trails intersect the magnetic field direction, on the Ft. Smith path, are considerably different for trails occurring before and after upper transit (about 0600 MST). This should have an effect upon the diffusion coefficients measured before and after upper transit.

The Perseids meteor shower is one of the most consistent and best documented showers. The velocity with which Perseid meteors enter the earth's atmosphere has been measured to be 60.3 km./second. For this velocity, Kaiser (1953) gives a height of maximum ionization of the trail, of 102 km. Then, assuming all of this ionization to be distributed within one scale height of the maximum (Greenhow and Neufeld 1957), the height of all reflection points must lie within a height region of about two scale heights. The average height of reflection will be the same as the maximum height of ionization, or perhaps 2.5 km. less (Rao and Armstrong 1958). Due to the higher than average height of trail formation, signals from Perseid meteor trails may be expected to have shorter durations than those from meteors of the sporadic background.

Since the number of signals received over the Ft. Smith path considerably

exceeded those over the Churchill path, the Ft. Smith data has been analyzed in some detail. From several hundred recognizable meteor signals, 156 were selected which exhibited exponential decays, and which were felt to be free from effects due to resonance, the finite meteor velocity, or distortion of the originally straight trail. A few short-duration trails were included which appeared to be slightly overdense, however, these all exhibited exponential decays over at least two amplitude decay times, and their inclusion should not adversely affect the analysis. Figure 14 shows a few examples of the recorded signals.

The individual points of Figure 15 are the common logarithms of the durations of the 156 signals which were selected. It is immediately obvious that there is a considerable scatter in these durations, and that a statistical approach is required. However, from several lines of evidence it may be shown that many of the signals measured were indeed those from Perseid meteor trails. Figure 16 is a plot on a probability graph of the cumulative or ogive distribution of the logarithm of the durations observed, the straight line representing a Gaussian distribution with a mean of -0.86 and a standard deviation of 0.32. It may be seen that the distribution is fairly well represented by a Gaussian function; however the departures from this distribution near $\text{Log}\tau = -1.1$ are significant.

The results obtained during the Perseids may be compared with a group of meteor signals which were similarly recorded, in the period 2200 MST August 1 to 0600 MST August 2, 1961. Several weak showers were known to be active at this time, however their radiants all lie near -10° in declination, and their rates over these forward-scatter paths may be expected to be low. A total of 66 signals were selected from this group. Figure 17

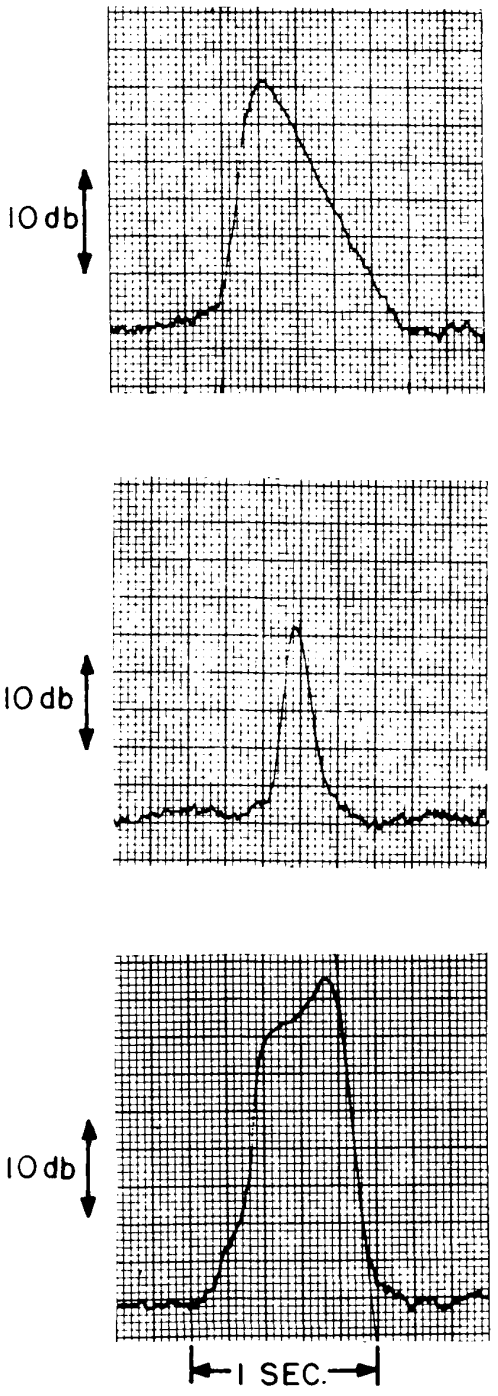

EXAMPLES OF SIGNALS RECORDED DURING TIME OF 1961 PERSEID SHOWER

FIGURE 14

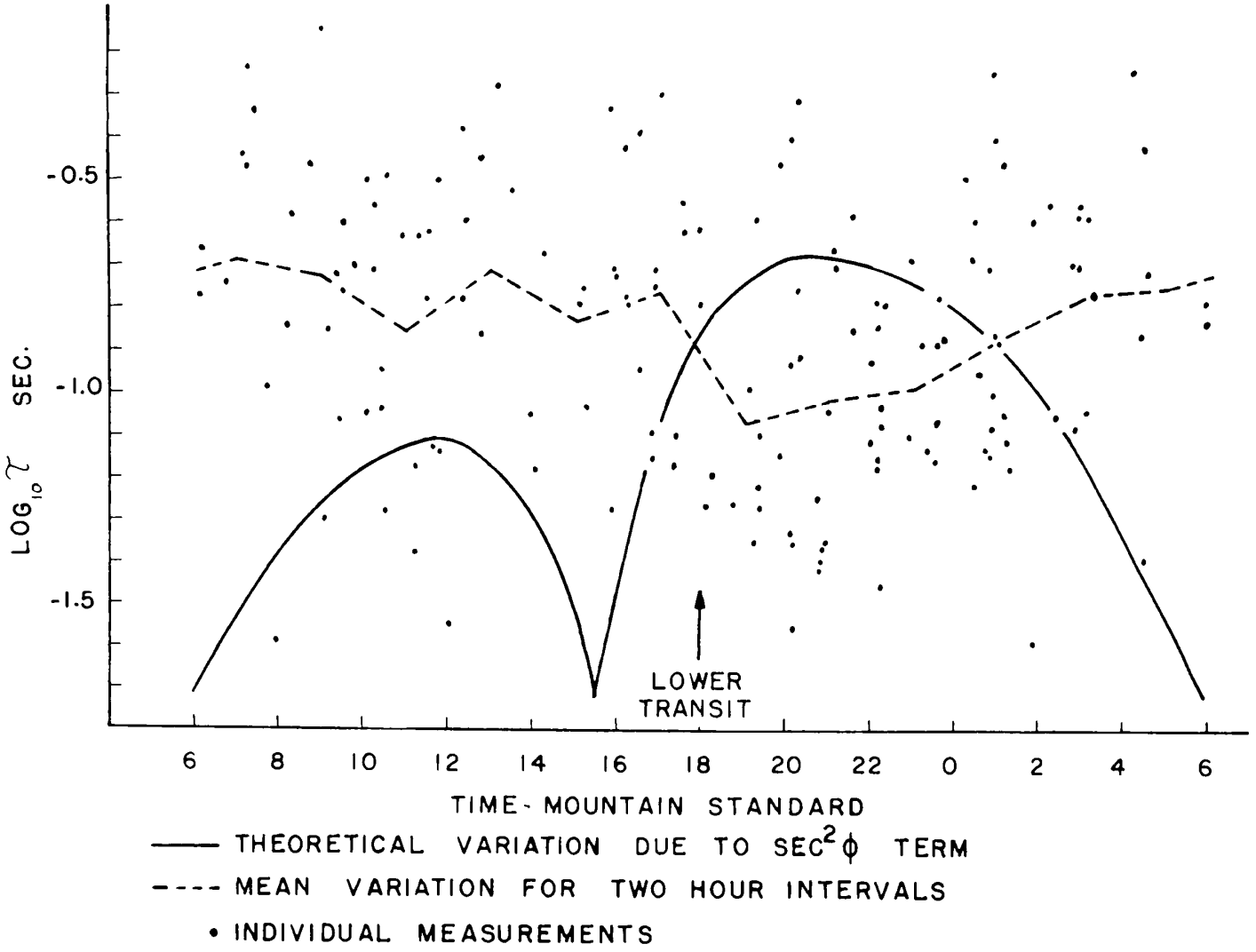

DURATIONS OF METEOR SIGNALS RECORDED DURING TIME OF PERSEID SHOWER

FIGURE 15

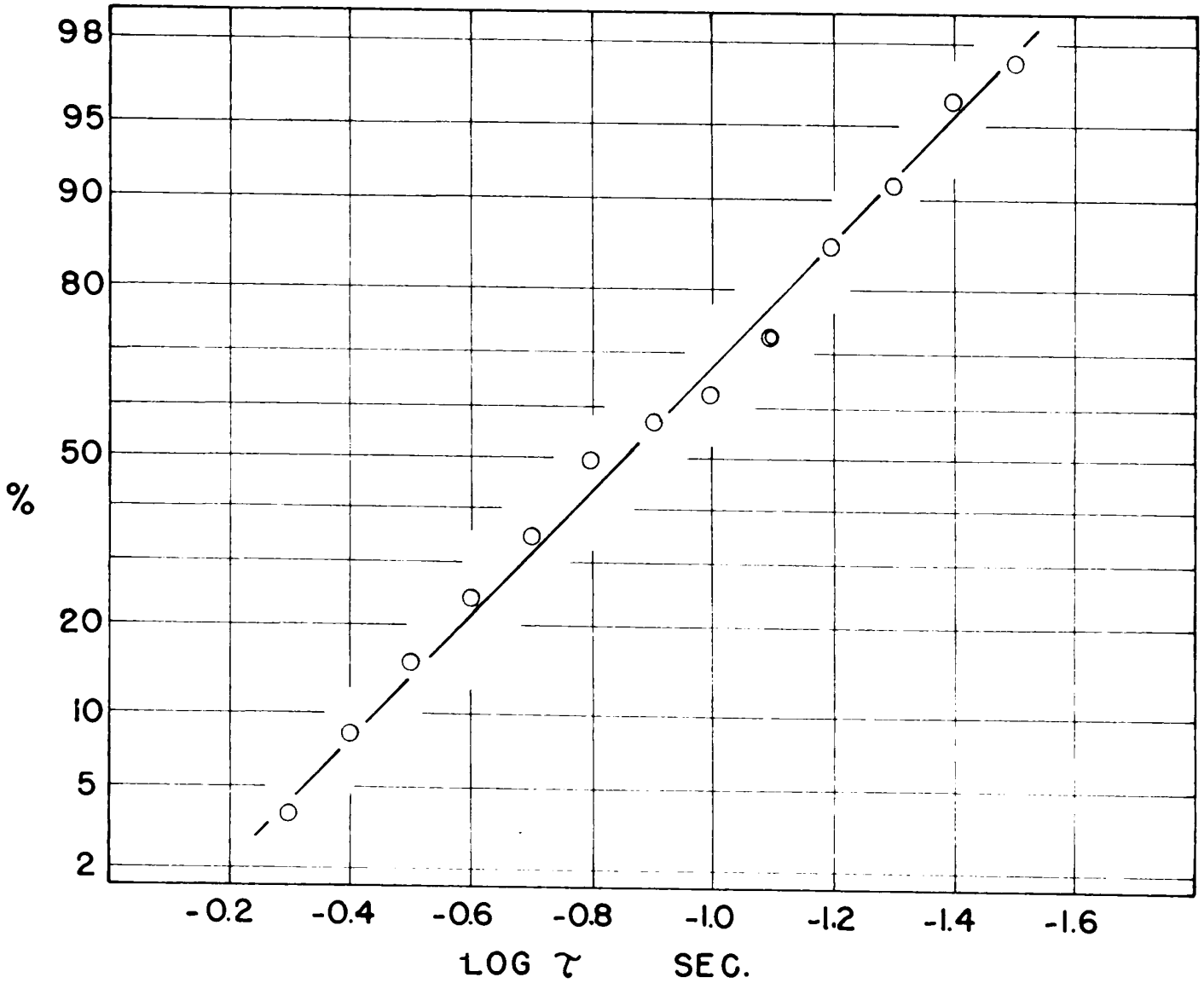

DISTRIBUTION OF DURATIONS OF METEOR SIGNALS RECORDED 1330 AUG. 10 TO 1800 MST AUG. 12, 1961

FIGURE 16

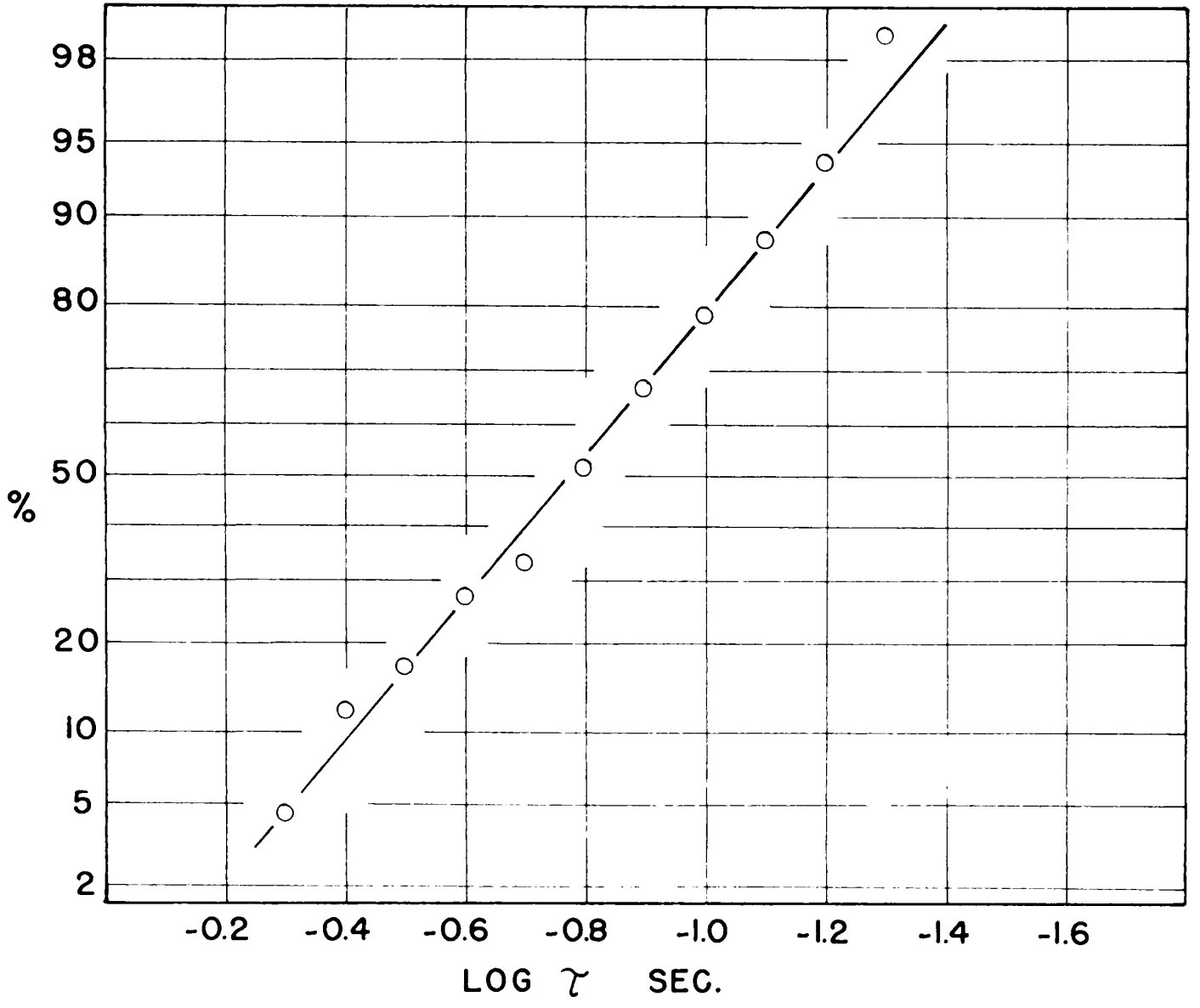

DISTRIBUTION OF DURATIONS OF METEOR SIGNALS RECORDED 2200 AUG. 1 TO 0600 MST AUG. 2, 1961

FIGURE 17

is a plot on a probability graph of these durations; this may be compared with the plot of Figure 18 which shows the distribution of those signals recorded during the same time of day on August 11 and 12, a total of 55. Evidently the distributions obtained during the Perseid shower is markedly non-Gaussian in the region Log τ = -1.1. This is further illustrated in Figure 19, where the frequency of occurrence of different duration groups is compared by means of a histogram for both groups of signals. Both have a peak near Log τ = -0.8, however the Perseid group has a second maximum near Log τ = -1.1. This second maximum may be attributed to the presence of short-duration signals from Perseid meteors.

A second measure of shower activity is the meteor rate, i.e. the number of meteors observed per unit time. The observability theory of Hines (1955) has been applied to the Perseid shower for the Ft. Smith - Saskatoon path. The result is shown in Figure 20, where it is compared with the observed meteor rate for a twenty-four hour period of the Perseid shower. The periods of peak activity agree quite well, however it must be concluded that there was a very strong background of sporadic meteor activity as well. It should be noted that the observed rate took into account only those meteor signals which had been previously selected as exhibiting exponential decays. The proportion of those selected varies with conditions; in particular a background of auroral enhancement tends to contaminate many otherwise good signals. An examination of a concurrent record, made with a chart speed of three inches per hour, showed that the auroral background, while present throughout much of this time, did not dominate the record at any time, and therefore, the observed meteor rate is believed to be valid throughout the period of observation.

Further evidence that many of the shorter-duration signals observed

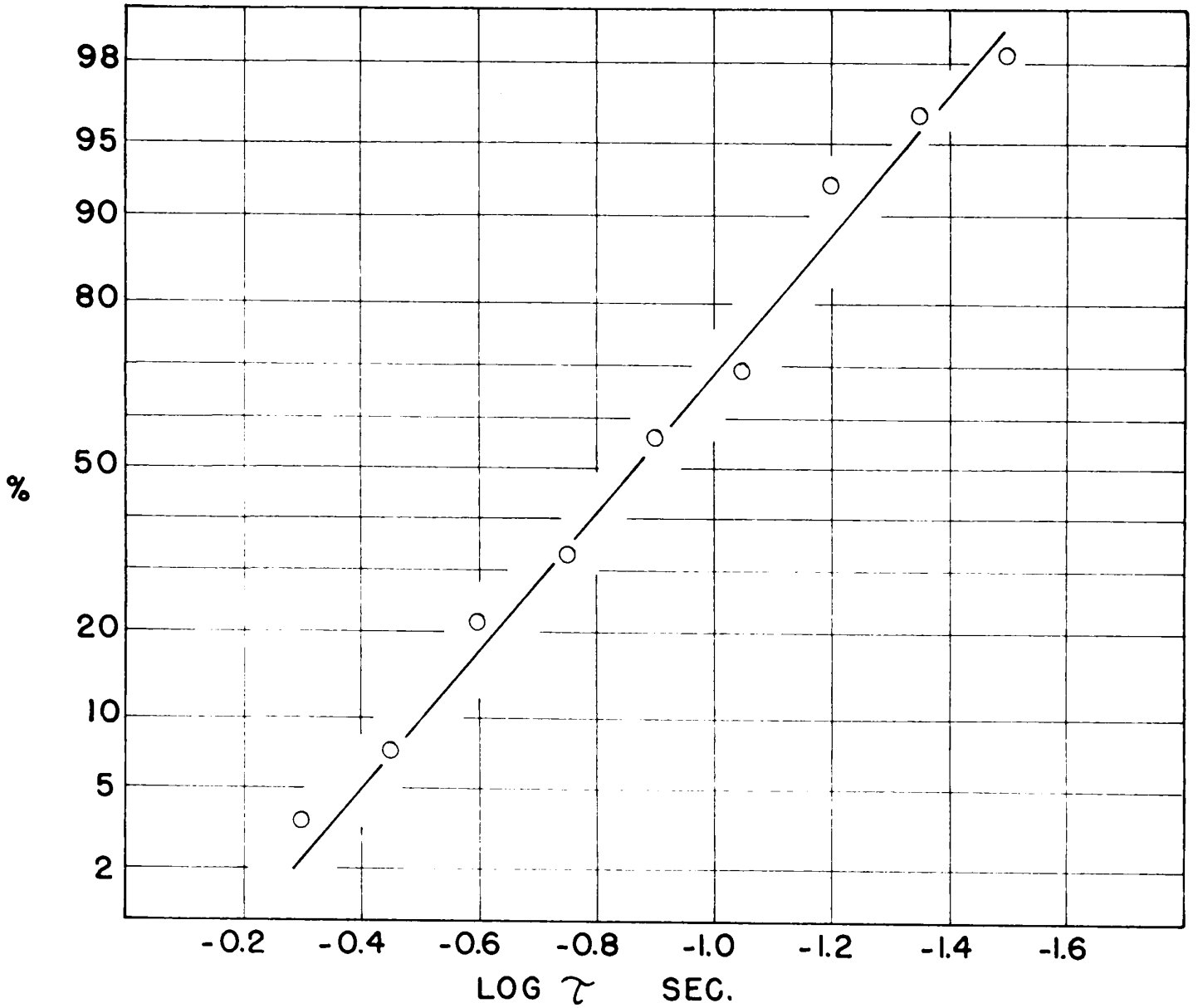

DISTRIBUTION OF DURATIONS OF METEOR SIGNALS RECORDED 2200 AUG.11 TO 0600 MST AUG. 12, 1961

FIGURE 18

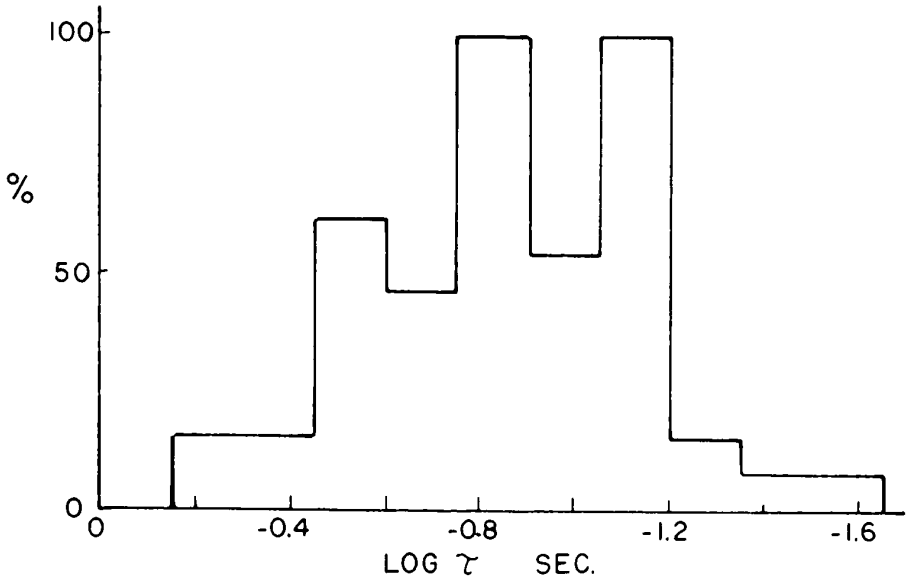

HISTOGRAM SHOWING
DISTRIBUTION OF DURATIONS OF METEOR SIGNALS
RECORDED 2200 AUG. 11 TO 0600 MST AUG. 12, 1961

FIGURE 19a

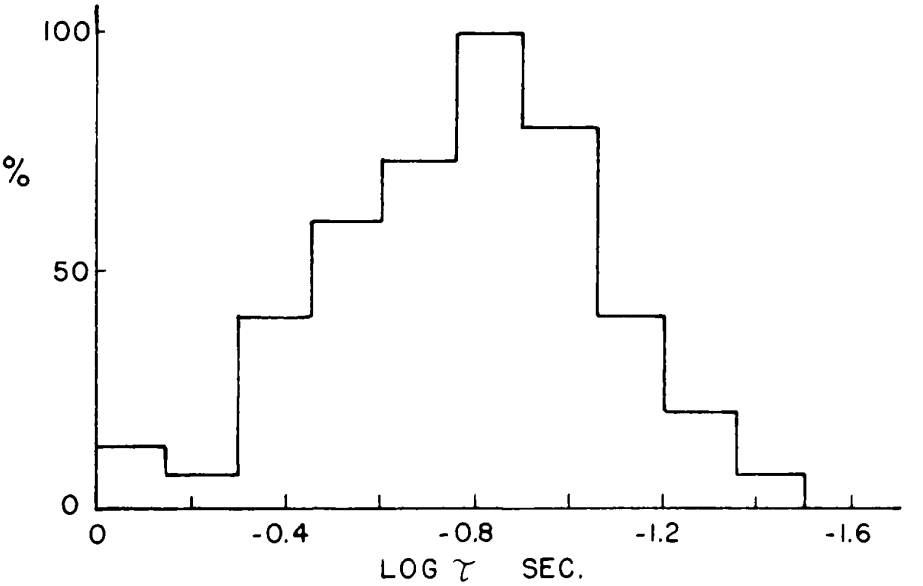

HISTOGRAM SHOWING
DISTRIBUTION OF DURATIONS OF METEOR SIGNALS
RECORDED 2200 AUG. 1 TO 0600 MST AUG. 2, 1961

FIGURE 19b

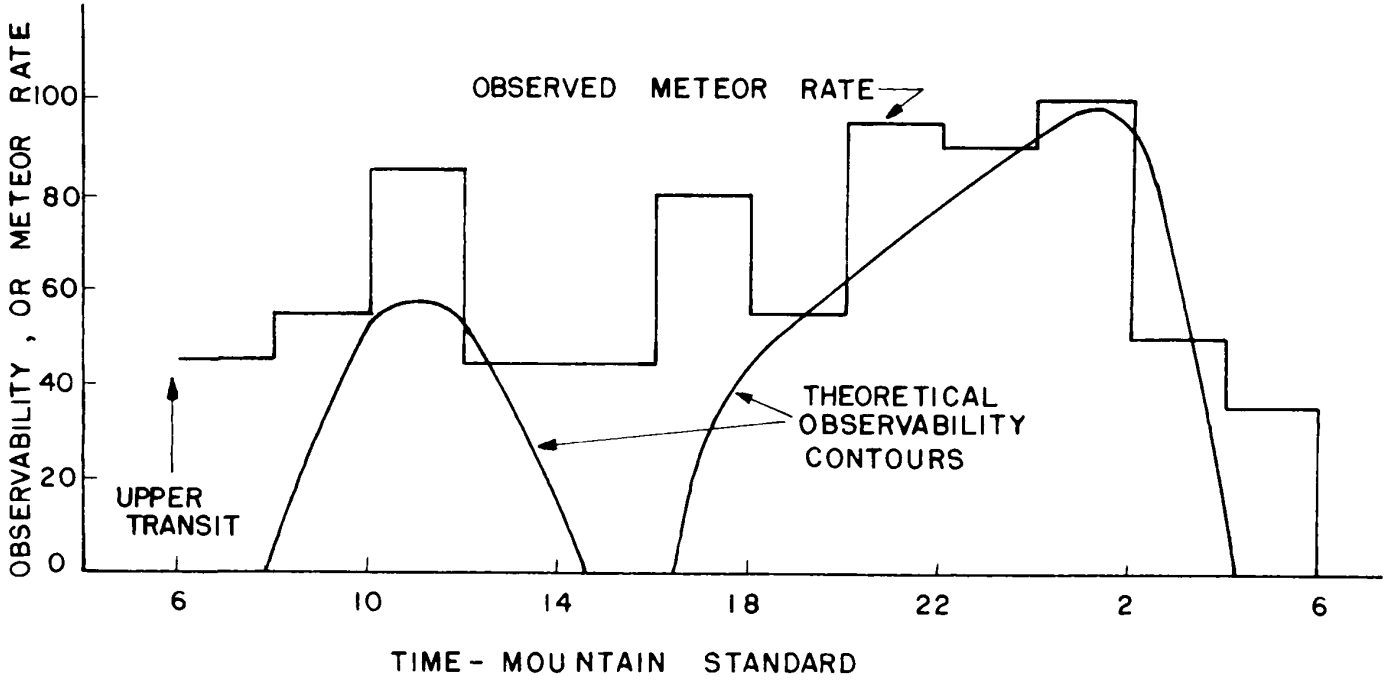

THEORETICAL OBSERVABILITY OF THE PERSEIDS SHOWER AND THE OBSERVED METEOR RATE

FIGURE 20

were from Perseid meteors may be cited. From an inspection of Figures 15 and 20 it may be seen that most of the short signals occurred at times when the observability of the shower was high, thus indicating that most of these signals actually were from Perseid meteors.

Although the presence of the Perseid shower is clearly shown in the observations, the problem remains of obtaining any useful information from the observations.

Since for shower meteors the average height of ionization, and hence the average height of reflection, is independent of time, the $\sec^2\phi$ variation in the expression for the forward-scattered signal duration should become significant. The solid curve of Figure 15 shows the expected variation of Log τ due to the $\sec^2\phi$ term. It was calculated assuming the reflection point to be in the mid-plane bisecting the TR axis, although the $\sec^2\phi$ variation parallel to the TR axis is small (see Figure 21), so that the conclusions are valid for all meteors near the mid-plane, in the region of greatest sensitivity. The expected $\sec^2\phi$ variation may be compared with the broken curve drawn through the points which are the averages over two hour periods of the individual values of Log τ. Evidently, the data is so contaminated with sporadic meteor activity that the regular variation sought, has been completely masked. The average Log duration does become smaller between 1800 and 0100, and this might be explained in that during this time the observability of the Perseid shower was high and therefore a larger percentage of the shorter-duration Perseids have been observed. Thus the mean Log τ is shorter than near 1500 and 0600, when only sporadic meteors were observed. However the average Log τ between 1800 and 0100 is smaller than that which would be expected for a reflection point height of 102 km. If the $\sec^2\phi$ law is assumed to hold, then the only other alternative is that

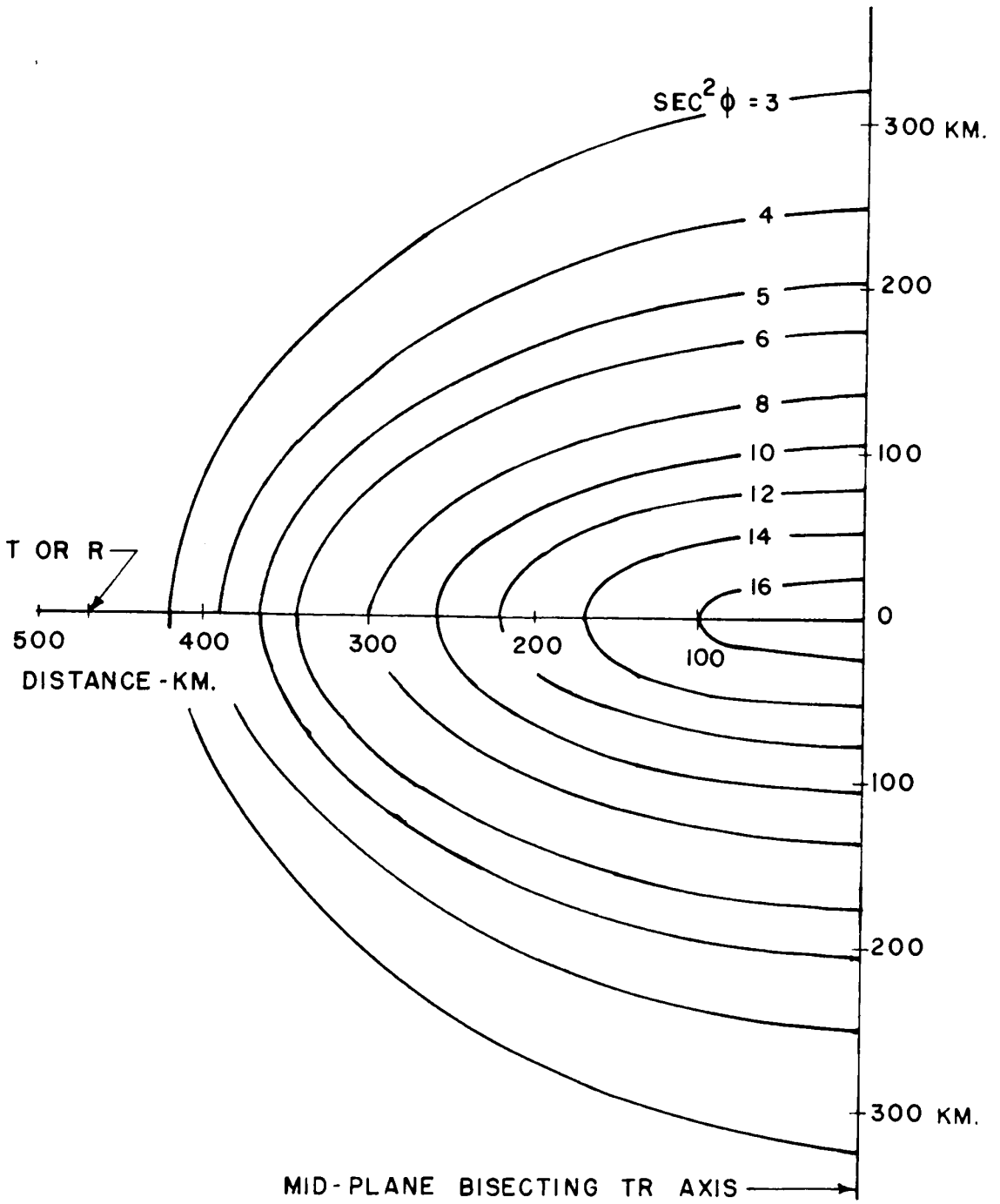

SEC² φ CONTOURS FOR 100 KM. LEVEL,

TR PATH LENGTH 940 KM.

FIGURE 21

the diffusion coefficient was that appropriate to a somewhat greater height than 102 km.

The effect of the earth's magnetic field, if present, would be to increase the durations of signals before upper transit, when the trails were nearly parallel to the magnetic field. Weiss (1955) has concluded that the probable maximum effect would be an increase in the duration by a factor of two. Since no such trend is discernible in Figure 15, it must be concluded that the hoped-for effect due to the magnetic field, if it occurs, has been completely masked by the scatter of the results.

CHAPTER VI - THREE FREQUENCY MEASUREMENTS

The extreme scatter found in the measurements of meteor signal durations, outlined in the previous two chapters, as well as the scatter found by other workers, seems to suggest that some unknown factor has been operative in all of these measurements. The theoretical relationship between the measured signal duration and the diffusion coefficient D is given by equations (4). There have been no conclusive measurements in the literature verifying the validity of the wavelength squared dependence of this relation, except to note that the general trend is correct for measurements on different frequencies. In view of this uncertainty, and of the persistent scatter in the present measurements, Forsyth (unpublished), has recently examined some three frequency forward-scatter records for the wavelength dependence of the durations. These records were obtained in 1955 for another purpose.

The results verify the statistical validity of equations (4), however there is still considerable scatter in the individual points. Since the scatter persists even for such three frequency measurements which pertain to the same meteor trail, it seems worthwhile to outline the work in some detail.

The three transmitters were located at Greenwood, Nova Scotia, and the receivers at Ottawa. The recordings were made on a moving chart recorder with a speed of ten millimeters per second, with a logarithmic amplitude response. From several hundred meteor signals, thirty were selected which appeared to be free from many of the defects listed in Chapter II. As well, the effect of the magnetic field is eliminated as a source of error because only measurements made on the same trail are

compared. For each signal the time for the amplitude to decay to $\frac{1}{e}$ of its initial value was determined as an average over the total usable amplitude of the signal. These times expressed in hundredths of a second were designated respectively as T_9 for a frequency of 32.22 Mc., T_8 for 39.22 Mc. and T_6 for 49.98 Mc. (The subscripts refer to the wavelengths). In order to remove the theoretical frequency dependence the decay times were each multiplied by a factor $16\pi^2/\lambda^2$ where λ is the appropriate wavelength. These reduced decay times were indicated by primes thus: T'_9, T'_8 T'_6. The logarithm of each of the three possible ratios of the reduced decay times for each signal is shown in Figure 22 plotted against the logarithm of T_9. From Figure 22 there seems to be no clear trend of the ratio with signal duration. This is in apparent disagreement with the results obtained by Forsyth and Vogan (1956), and by McKinley (1953), however in both of these earlier investigations, signal durations rather than decay rates were measured. As well, the signals were selected by means of much less stringent criteria.

In Figure 22 there is still a very substantial scatter in the ratios of the decay rates for each meteor. Clearly, this scatter can not be due to variations in atmospheric temperature and density. On the other hand, these measurements would seem to confirm the statistical validity of the theoretical frequency dependence. The mean value of the logarithm of each of the three possible ratios is listed in Table III together with its R.M.S. deviation. From Table III it seems that each group of thirty ratios is representative of a common parent group. Under these circumstances it is reasonable to combine the 90 measurements in order to see if they conform to the normal or gaussian distribution about the mean. This is done in Figure 23 where the cumulative (or ogive) distribution is plotted on a probability graph. The straight line represents a gaussian distribution

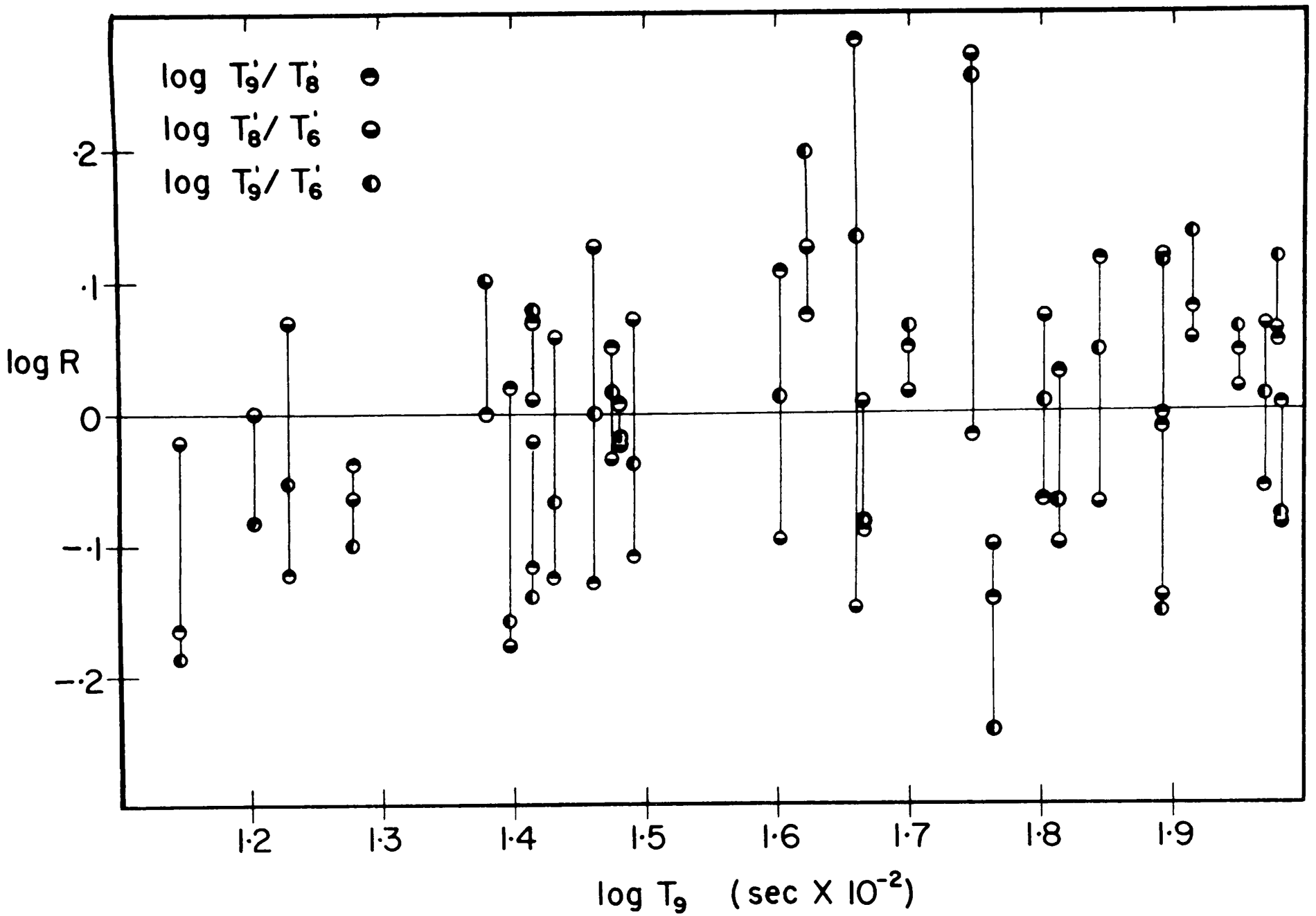

FIGURE 22 - THE VARIATION OF LOG R WITH SIGNAL DURATION

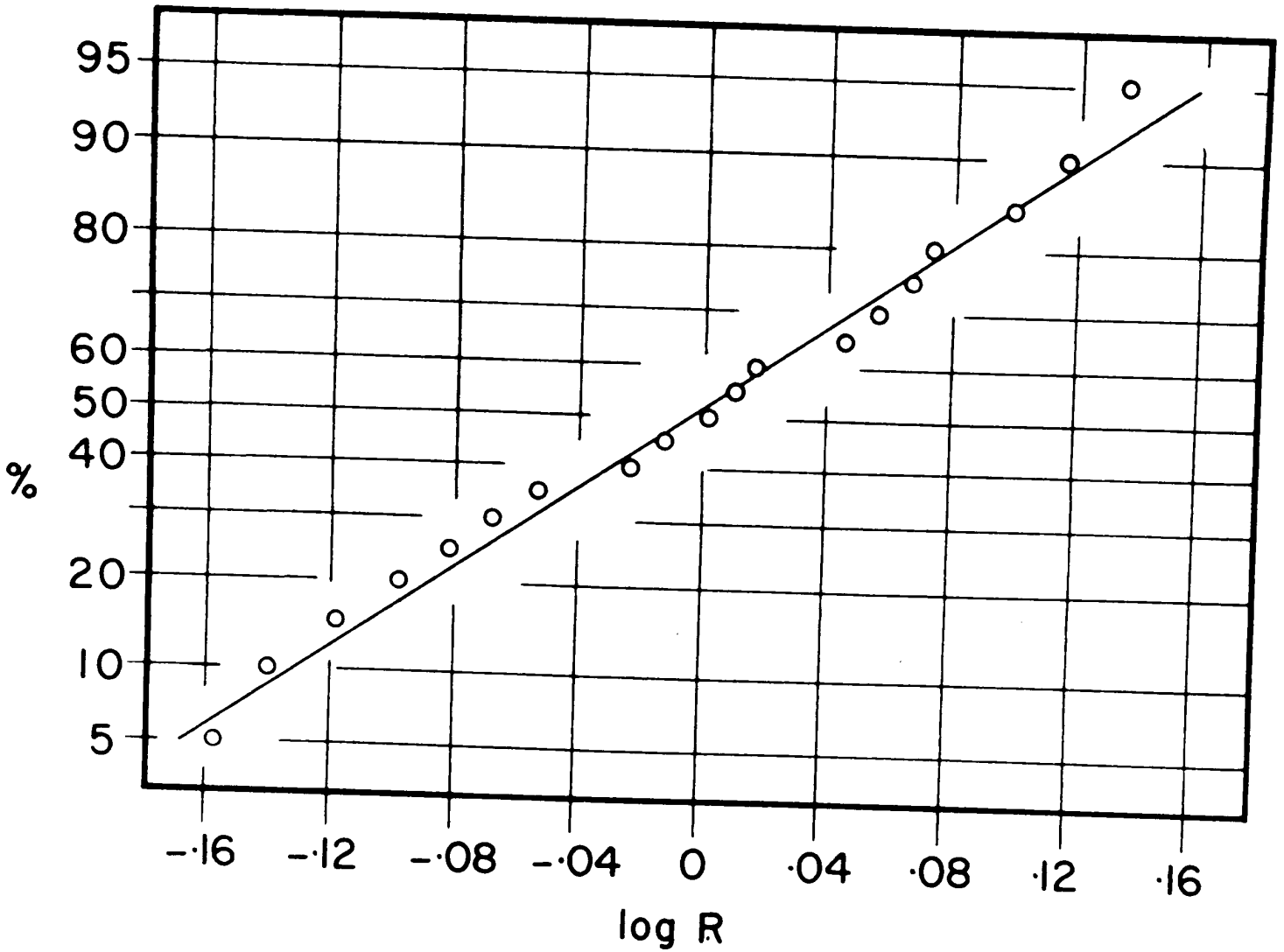

FIGURE 23 - DISTRIBUTION OF VALUES OF LOG R

having a mean value of -0.005 and an r.m.s. deviation of 0.10. Evidently the observations are well represented by such a distribution. It is worth noting that this R.M.S. deviation corresponds to a numerical value of the ratio of about 1.3 which is the magnitude of the estimated error for the back-scatter measurements made by Greenhow and Hall. Since the present measurements could not be affected by the other suggested sources of error, it seems likely that the observed scatter in decay rates is in fact due to imperfections in the meteor trails which prevent them from behaving as simple line scatterers.

TABLE III - SUMMARY OF THE THREE FREQUENCY MEASUREMENTS

	Mean	R.M.S. Deviation
$\log T_9'/T_8'$	-0.009	0.0955
$\log T_8'/T_6'$	+0.005	0.0964
$\log T_9'/T_6'$	-0.004	0.1154

CHAPTER VII - THE EFFECT OF TRAIL NON-UNIFORMITIES ON SIGNAL DECAY RATES

The dispersion found by various workers in measurements relating diffusion coefficient to height (Greenhow and Neufeld 1955, Murray 1959, Greenhow and Hall 1961), as well as the dispersion found in the measurements of Chapters V and VI, suggest strongly that the majority of meteor trails do not behave as simple line scatterers. A part of the difficulty may lie in the simplifying assumptions of the theory. In particular, in calculating the power reflected from a meteor trail, the trail is idealized as being uniform in line density, and infinite in extent. It is also implied that the trail diffuses uniformly over its length with a constant diffusion coefficient D. Since the reflected power is expressible in terms of Fresnel integrals, it is then assumed that the only important part of the trail, in calculating reflected power, is the principal Fresnel zone, centred about the specular reflection point. At VHF, the radius of the principal Fresnel zone is of the order of one or two kilometers, so that any measurements made must be appropriate to this narrow height range. With this simplified picture, the height uncertainty should at most be $\pm$ 1 km., provided the height finding apparatus is sufficiently accurate. In fact, experimental results indicate a much greater height error than this; Greenhow and Hall (1961) estimate their height error to be $\pm$ 4 km.

It is known that most trails have a vertical extent of about two scale heights, and that the ionization line density increases to a maximum and then decreases again to zero in this length (Greenhow and Neufeld 1957). Since the radio echo amplitude A_o is proportional to the line

signals. Since the important parameters, such as line density and the diffusion coefficient, vary with height rather than with distance along the trail, it is convenient to deal with the projection of the meteor trail into a vertical plane. For the case of forward-scatter, where the meteor trail is in the mid-plane bisecting the TR axis, the Fresnel zone length is given by the same expression as for backscatter, where the range R becomes the range from the transmitter (or receiver) to the meteor trail. For other orientations, the Fresnel zone length projected into the mid-plane remains the same, to a first approximation. In what follows, the vertical extent of a meteor trail is taken as its length. This is a convenience; the extension to other orientations may be made by projecting from the vertical plane to any given trail position.

A segmented trail may be considered an extreme case of irregular ionization. It is conceivable that such a trail with a regular variation in line density might be produced by a rotating particle. The reflected amplitude was calculated for a trail two scale heights in length, which was broken up into ten separated segments of uniform ionization, as in Figure 24.

From equation (3)

$$A = A_o \exp\left\{ - \frac{16\pi^2 Dt}{\lambda^2} \right\} \qquad \text{- - - - - - - - - - (3).}$$

Since D varies exponentially with height,

$$D = D_o \exp\left\{ \frac{h-h_o}{H} \right\} \qquad \text{- - - - - - - - - - - - - - (39)}$$

where H is the scale height. If A'_h is the amplitude reflected from a small segment of the trail at height h, then

$$A'_h (h,t) = A_h \exp\left\{ - \frac{t}{\gamma'_o} \exp \frac{h-h_o}{H} \right\} \qquad \text{- - - - - - - - (40)}$$

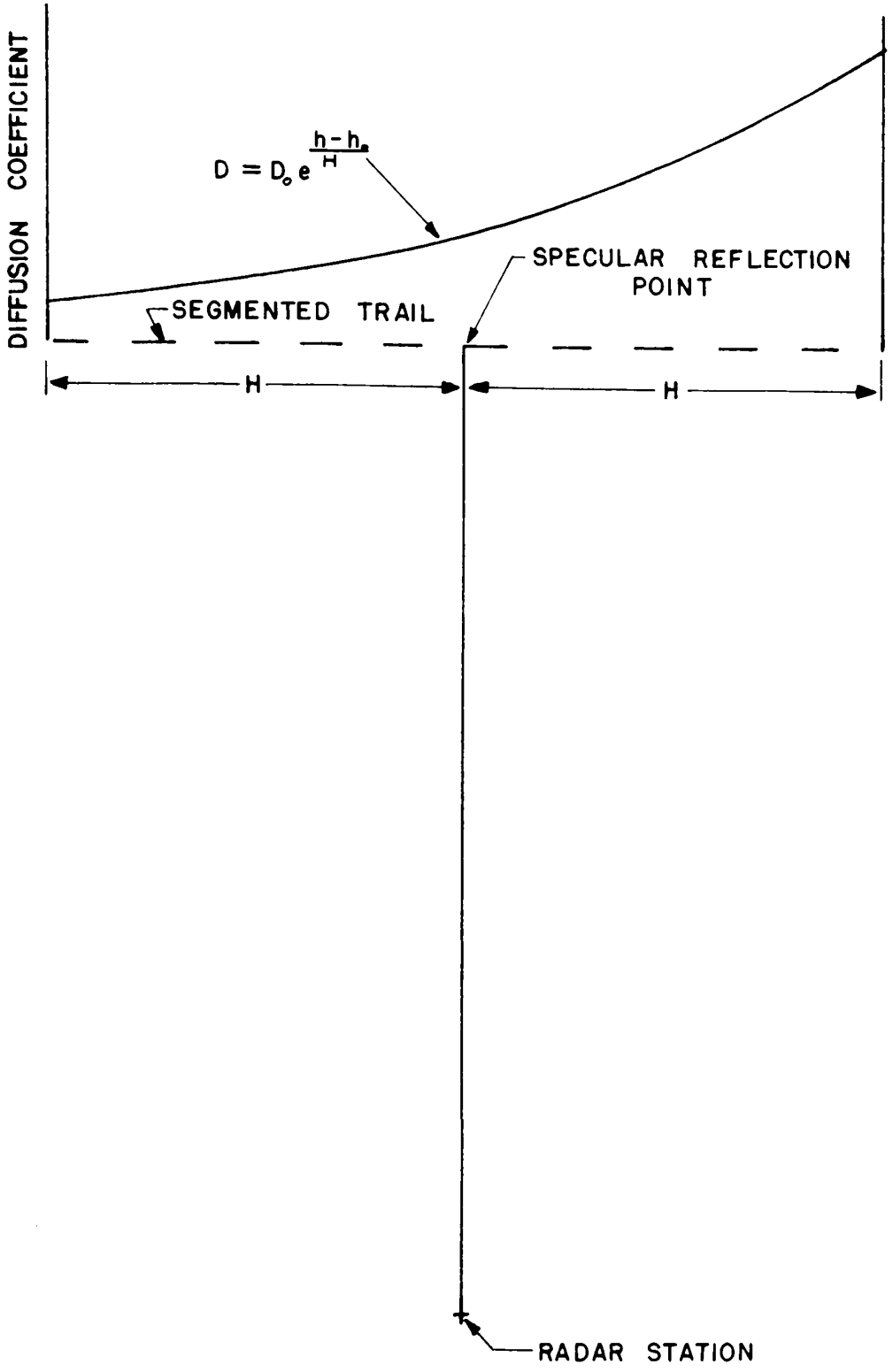

SEGMENTED METEOR TRAIL WITH VARIABLE DIFFUSION COEFFICIENT

FIGURE 24

where $\tau_o' = \frac{\lambda^2}{16\pi^2 D_o}$ - - - - - - - - - - - - (41),

and A_h is the initial amplitude reflected by the segment, given by the ordinary Fresnel theory. The amplitude from all of the segments of the trail is the sum of the A_h',

$$A'(t) = \sum_h A_h'(h,t) \quad - - - - - - - - - - - - - - - (42)$$

τ_o' is the time constant of decay for the trail at one end. The decay constant at the specular reflection point is

$$\tau_o = \frac{\tau_o'}{e} \quad - (43)$$

The reflected amplitude A_h of (40) for each segment was determined from tabulated values of the Fresnel integrals, the A_h's were then multiplied by the appropriate value of the exponential, for a series of suitable times. From these component $A_h'(h,t)$, the sum $A'(t)$ was formed, according to (42), and the results compared with the simpler theoretical model.

The procedure was carried out for two frequencies, as follows. From Fresnel diffraction theory, the radius of the principle Fresnel zone is

$$F = \sqrt{\frac{R\lambda}{2}} \quad - - - - - - - - - - - - - - - - - (44)$$

where R is the radar range to the specular reflection point, and λ is the radio wavelength. The Fresnel integrals are tabulated in terms of the parameter v, where

$$v = \frac{2s}{\sqrt{R\lambda}} \quad - - - - - - - - - - - - - - - - - (45)$$

and s is the distance along the trail from the specular reflection point. The segments were so chosen that, for the first wavelength λ_1, the length of a segment Δv_1 was

$$\Delta v_1 = \frac{1}{2} = \frac{2\Delta s}{\sqrt{R\lambda}} \quad - - - - - - - - - - - - - - - - - (46),$$

$$\text{or} \quad \Delta s = \frac{1}{2\sqrt{2}} \quad F \quad - - - - - - - - - - - - - - - - (47).$$

The second wavelength λ_2 was chosen so that

$$\frac{\Delta v_1}{\Delta v_2} = \left\{ \frac{\lambda_2}{\lambda_1} \right\}^{\frac{1}{2}} = \frac{5}{6} \qquad \text{- - - - - - - - - - - - - (48)}$$

This ratio corresponds approximately to the wavelengths used in Chapter VI.

The results for the segmented trail of Figure 24 are shown in Figure 26a, where the logarithm of the amplitude is plotted vs. the time in units of one decay constant, τ_o. The simple theory for a smooth trail gives an amplitude which decays to $\frac{1}{e}$ in amplitude in a time $t' = 1$, as given by the solid straight line. It may be seen that the departures from this, for the two frequencies, are quite marked after 3 decay times.

2 UNIFORM TRAIL, VARIABLE DIFFUSION COEFFICIENT

In order to illustrate the separate effects of the two corrections which were applied to obtain Figure 26a, the behavior has been calculated for a uniform trail, considering only the variation of D with height. The result is shown in Figure 26b. The departures from the ideal are not as severe, however the trend is still appreciable.

3 CONTINUOUS TRAIL, VARIABLE DIFFUSION COEFFICIENT AND LINE DENSITY

The third case for which calculations were made is illustrated in Figure 25. The diffusion coefficient D was taken to vary exponentially as before. The trail was considered smooth, but with a line density variation as given by the curve labelled q. The result for this situation is shown in Figure 26c. The difference between the decays for the two frequencies is negligible, and they depart from the simple exponential decay only after about three decay times. The effect of the assumed line density variation was to reduce the contributions to the reflected amplitude from the ends of the trail, and hence the more ideal behavior.

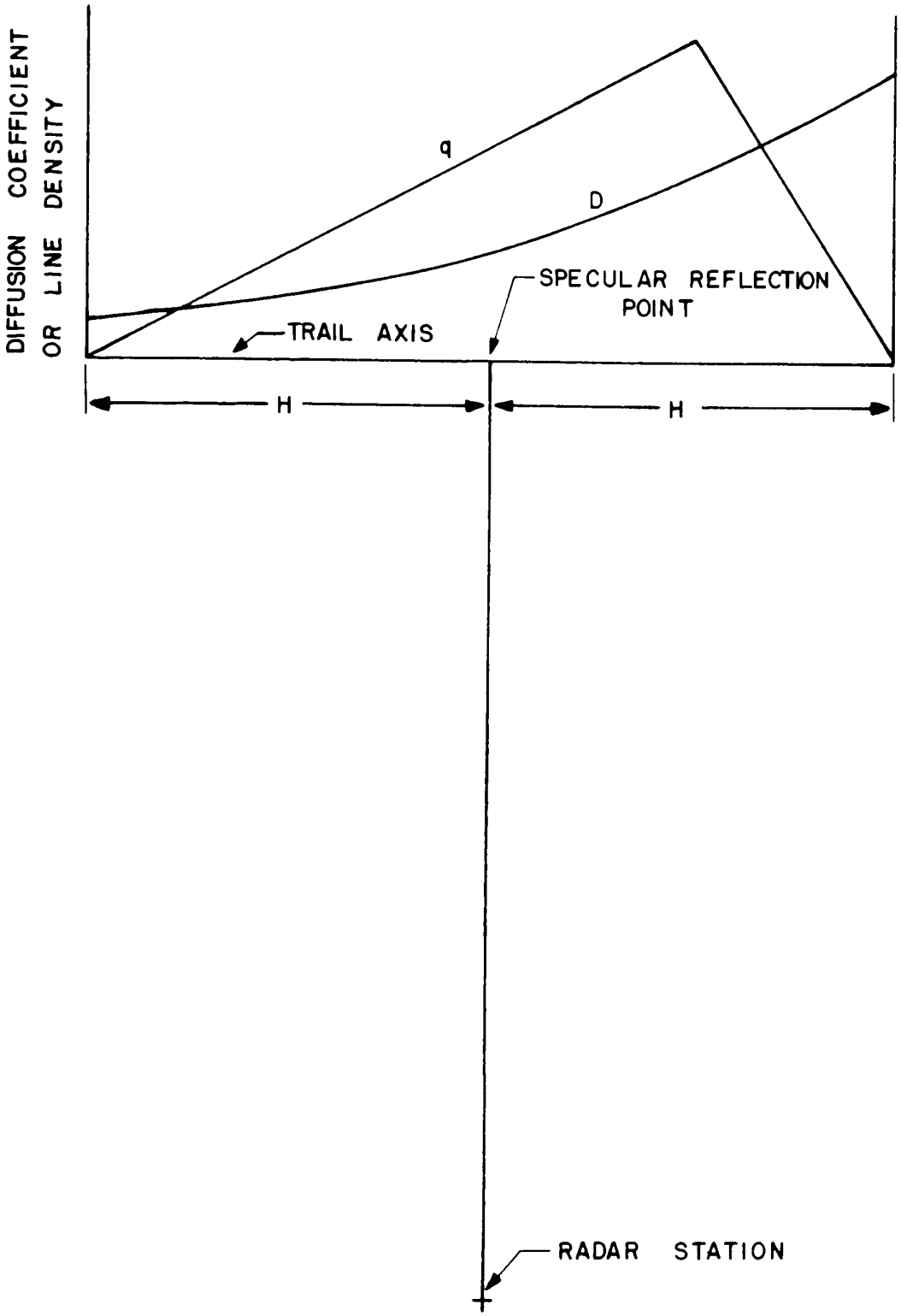

SMOOTH TRAIL, WITH VARIABLE DIFFUSION COEFFICIENT AND LINE DENSITY

FIGURE 25

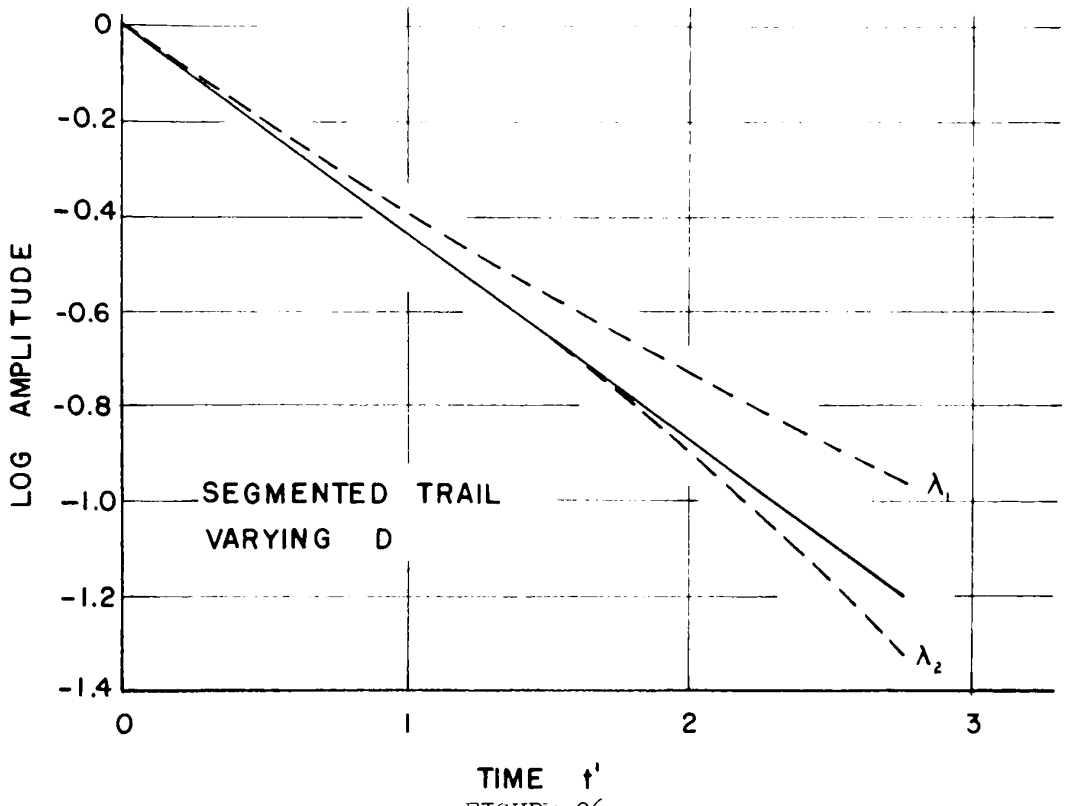

FIGURE 26a

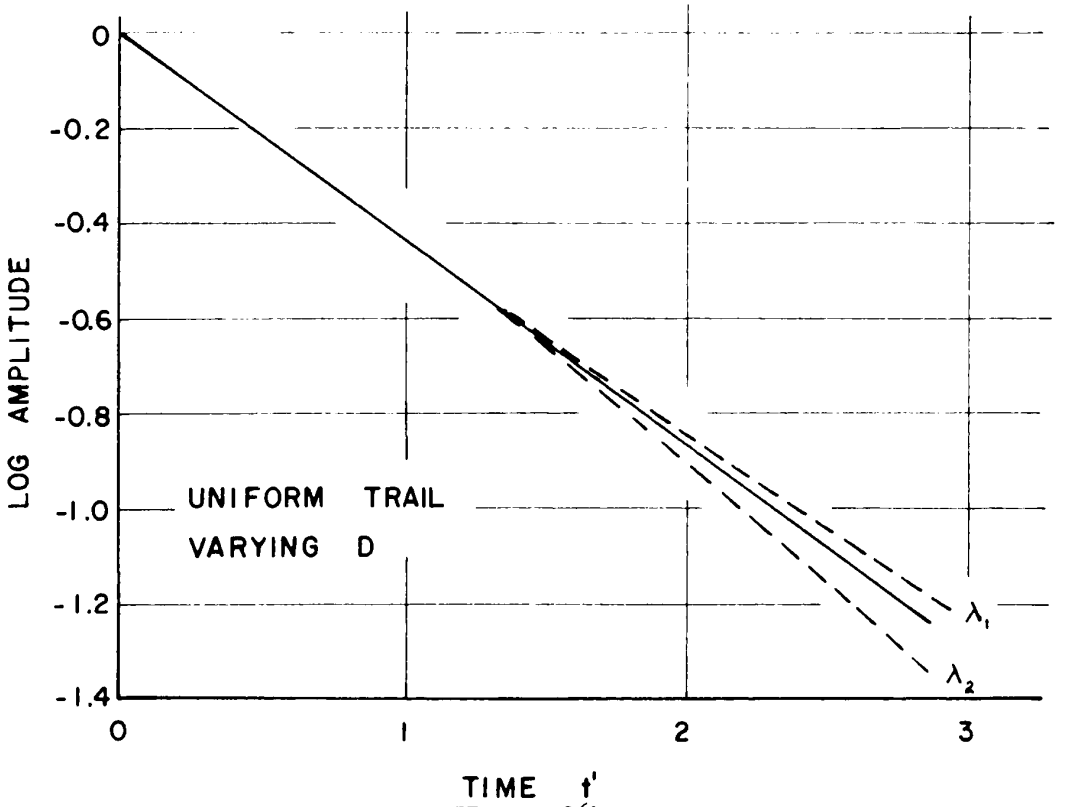

FIGURE 26b

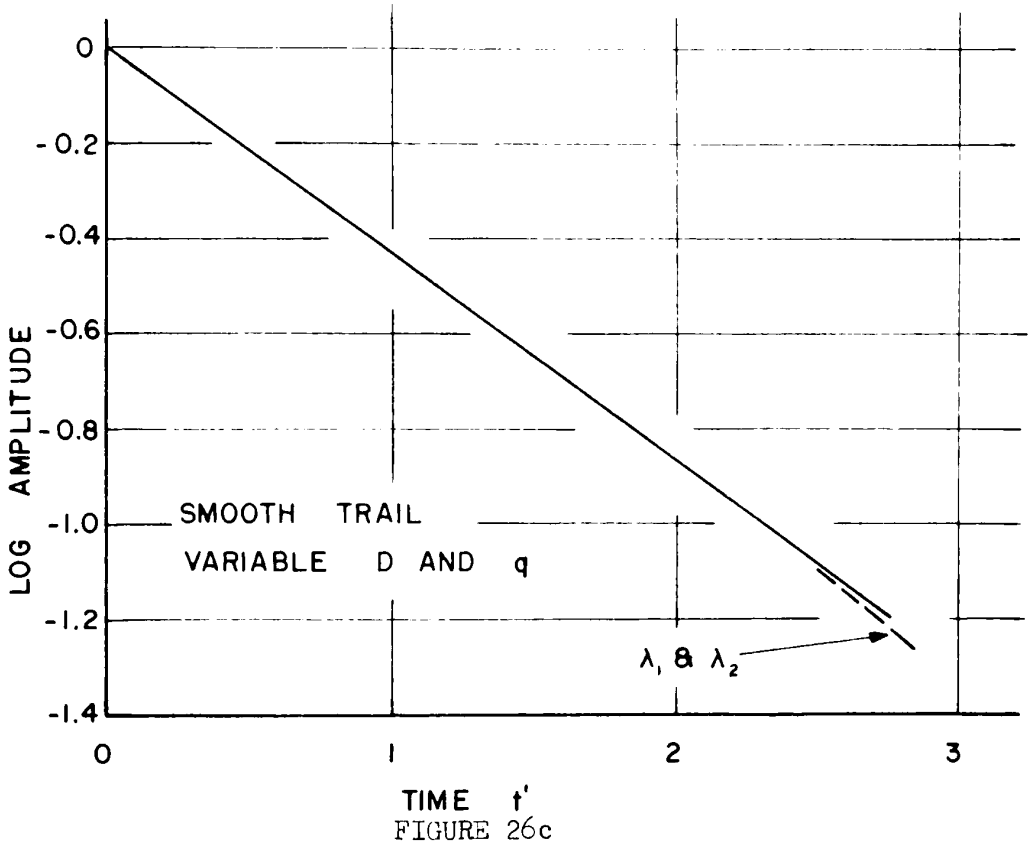

FIGURE 26c

TIME IN UNITS OF ONE DECAY CONSTANT τ_o

THE REFLECTED SIGNALS FROM NON-UNIFORM METEOR TRAILS

FIGURE 26

These calculations serve to illustrate a possible cause of dispersion in measurements of the decay times of meteor trails. The variation in D certainly does occur; this, coupled with an irregular variation of ionization density along the trail, appears sufficient to produce the observed dispersion.

CHAPTER VIII - CONCLUSIONS

Various geometries involving VHF forward-scatter and backscatter circuits, and UHF radar, have been investigated as to their potential usefulness in making measurements of the decay times of meteor trails. Of these, a forward-scatter circuit, in conjunction with a UHF radar, appears to be potentially the most useful.

Experimental work, involving coincident signal reflections from a single meteor trail, over two VHF forward-scatter paths, and over a single forward-scatter path together with a VHF backscatter system, has indicated that such two-path reflections occur only infrequently. In fact, the observed coincidence rate was so low that the derivation of useful information from this source appears unlikely.

When well-known meteor showers are observed over a forward-scatter path, the known radiant position of the shower can be used in conjunction with the geometry of forward-scattering to predict the positions of potentially useful meteors. The technique has been utilized in a study of the Perseid shower. While the presence of the shower and many of the shower characteristics may be studied, it appears that, in view of progress already made, in future more refined techniques will be required in order to solve many of the remaining, and more difficult, problems associated with the occurrence of meteor trails in the ionosphere.

A prominent characteristic of the measured decay times of signals from underdense meteor trails is the great dispersion in these measurements. While the diffusion coefficient is a rapidly varying function of height, measurements indicate that some other variable or variables must be present as well. In the past, studies of the variation of the

diffusion coefficient with height have involved backscatter systems. However, these have not resolved the uncertainty concerning the origin of the dispersion in these measurements, although there has been a tendency for some workers to attribute it entirely to experimental errors. It appears that this uncertainty could be resolved by the use of a forward-scatter system, because of the greater precision possible with such measurements. This greater precision arises from two factors: the first is that with forward-scatter systems it is possible to use continuous wave transmissions, with the attendant more precise control of transmitter power and frequency; the second is that forward-scattered signals persist for a longer time, permitting more accurate measurements of their decay rates. In order to utilize a forward-scatter system for this purpose, an auxiliary method of locating the trail in space is necessary. A UHF radar located near the forward-scatter path has been proposed as a reasonable solution.

Since it seems unlikely that the observed dispersion in meteor decay rate measurements is due entirely to errors of measurement, a tentative mechanism, based upon an irregularly ionized trail, has been proposed to explain the observations. A few preliminary calculations indicate that the proposed mechanism is adequate to account for the observed dispersion.

IX REFERENCES

Bates, D.R. (1950), Phys. Rev. 77, 718; 78, 592.

Eshleman, V.R., and Manning, L.A. (1954), Proc. Inst. Radio Engrs., 42, 530.

Flood W.A. (1957), J. Geophys. Res., 62, 79.

Forsyth, P.A. (1958), Can. J. Phys. 36, 1112.

Forsyth, P.A. and Rolfe, W. (1955) DRTE Report 12-1-8.

Forsyth, P.A. and Vogan, E.L. (1956), Can. J. Phys., 34, 535.

Greenhow, J.S. (1954), Phil. Mag., 45, 471.

Greenhow, J.S. and Hall, S.E. (1961), Planet Space Sci. 5, 109.

Greenhow, J.S. and Neufeld, E.L. (1957), Mon. Not. R. Astr. Soc. 117, 359.

Hines, C.O. (1955), Can. J. Phys. 33, 493.

Hines, C.O. and Forsyth, P.A. (1957), Can. J. Phys., 35, 1033.

Huxley, L.G.H. (1952), Aust. J. Sci. Res., 5, 10.

Kaiser, T.R. and Closs, R.L. (1952), Phil. Mag. 43, 1.

Kaiser, T.R. (1953), Adv. in Phys., 2, 495.

Lovell, A.C.B. (1947), Reports on Progress in Physics, 11, 415.

Lovell, A.C.B. and Clegg, J.A. (1948), Proc. Phys. Soc. A., 60, 491.

McKinley, D.W.R. (1953) Can. J. Phys. 31, 1121.

McKinley, D.W.R. and McNamara, A.G. (1956), Can. J. Phys., 34, 625.

McKinley, D.W.R. and Millman, P.M. (1953), Can. J. Phys., 31, 171.

McNamara, A.G. and McKinley, D.W.R. (1959), J. Atmos. Terr. Phys. 16, 156.

Manning, L.A. (1958), J. Geophys. Res., 63, 181.

Manning, L.A. (1959), J. Geophys. Res., 64, 1415.

Murray, E.L. (1959), Planet Space Sci. 1, 125.

Opik, J.E. (1958), Physics of Meteor Flight in the Atmosphere, Interscience Publishers, Inc. New York.

Pierce, J.A. (1938) Proc. Inst. Radio Engrs., 26, 892.

Rao, M.S. and Armstrong, R.L. (1958), Can. J. Phys. 36, 1601.

Rocket Panel (1952), Phys. Rev. 88, 1027.

Skellet, A.M. (1935), Proc. Inst. Radio Engrs., 23, 132.

Watson, F.G. (1941), Between the Planets, The Blakiston Co., Philadelphia, Pa.

Weiss, A.A. (1955), Aust. J. Phys., 8, 279.

APPENDIX A - DETAILS OF THE APPARATUS

The basic function of the apparatus to be described here, was to record on a fast chart recorder the short duration radio signals reflected from meteor trails. A signal burst or bursts from one or both of two radio receivers was made to trigger on a Sanborn chart recorder for a short time; meanwhile the signals from the two radio receivers were stored on a magnetic tape for about two seconds and subsequently played back and recorded on the Sanborn recorder. This technique permitted a high chart speed (25 mm. per sec.) without wasting large amounts of chart paper between signal bursts. Figure 1 is a block diagram of most of the apparatus. Each part is described in some detail below.

1 TRANSMITTERS, RECEIVERS, AND ANTENNAS

Two V.H.F. forward scatter paths were used. The transmitters were located at Forth Smith, North West Territories, and Churchill, Manitoba. Each was maintained at a transmitter power of 50 watts. The receivers were located at Saskatoon.

Five-element Yagi antennas were used at both ends of each forward scatter path. The antennas were so oriented that their patterns intersected at the 100 km level over the mid-point of the respective transmitter-receiver (TR) paths.

There was also a back-scatter transmitter located at Prince Albert, Saskatchewan. It had transmitter power of 50 watts, beamed from a five-element Yagi in the direction of magnetic north. The receiving antenna at Saskatoon was a similar Yagi, beamed in the same direction. The elevation angle of the main lobe of each of these antennas was $11\frac{1}{4}^{o}$, so

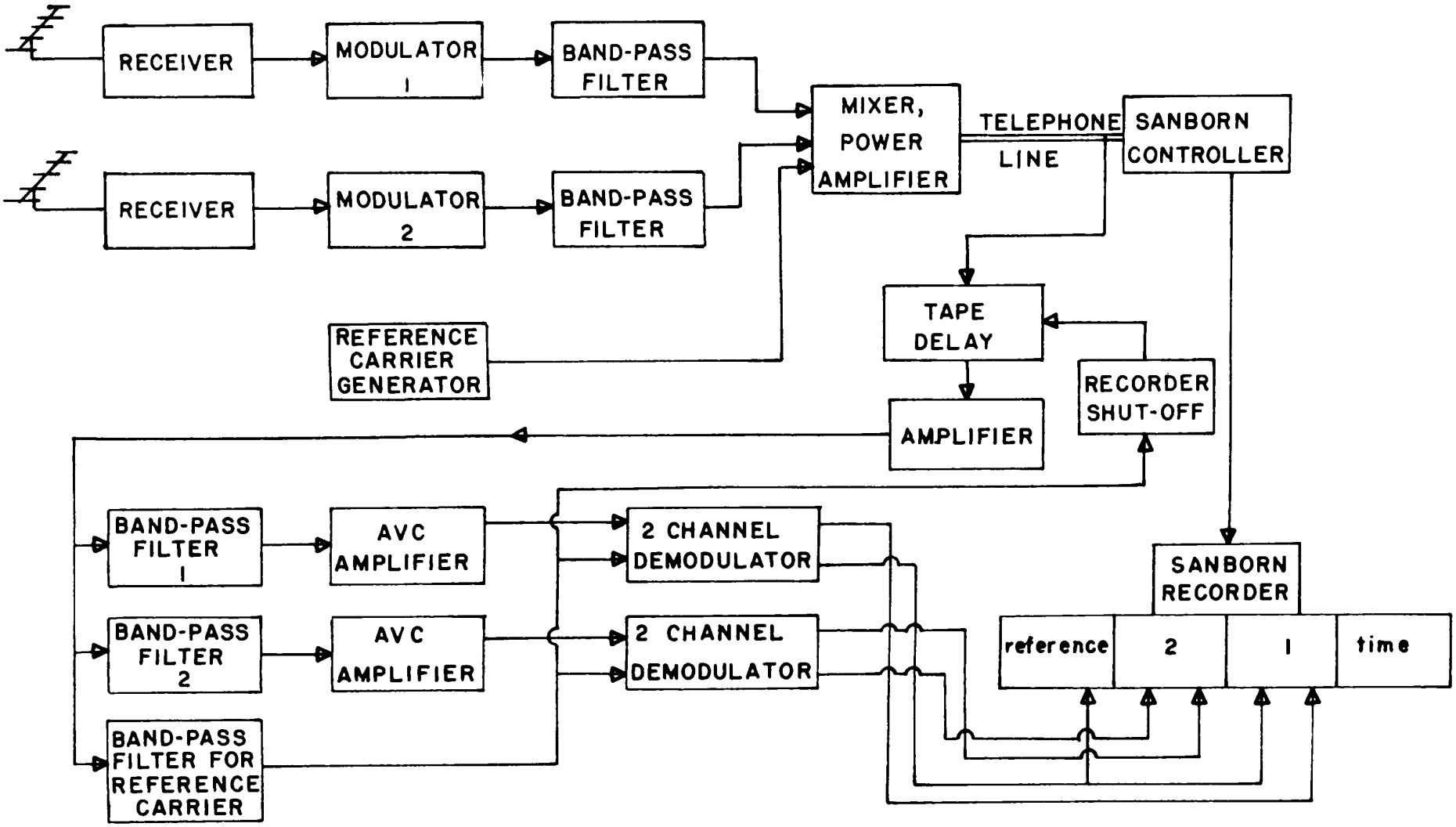

BLOCK DIAGRAM OF APPARATUS

FIGURE 1

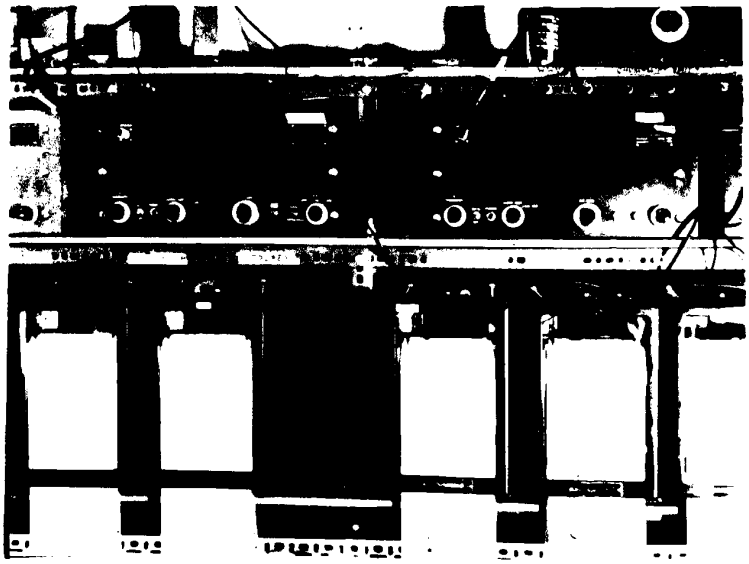

THE RECEIVERS

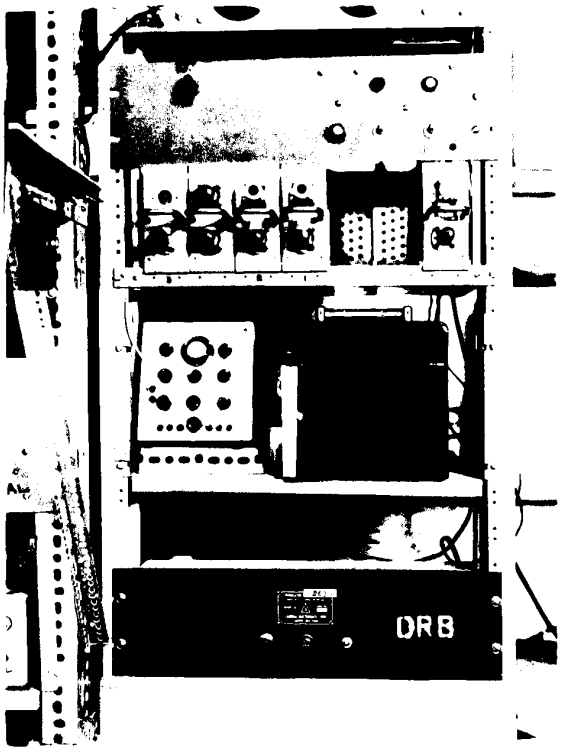

MODULATORS, POWER AMPLIFIER

FIGURE 2 - PHOTOGRAPHS OF THE APPARATUS

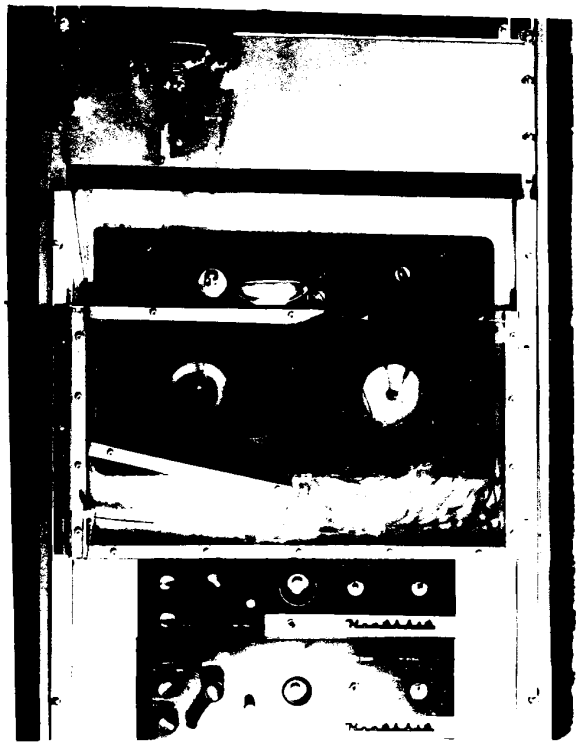

"LETTER-BOX" TAPE STORAGE SYSTEM

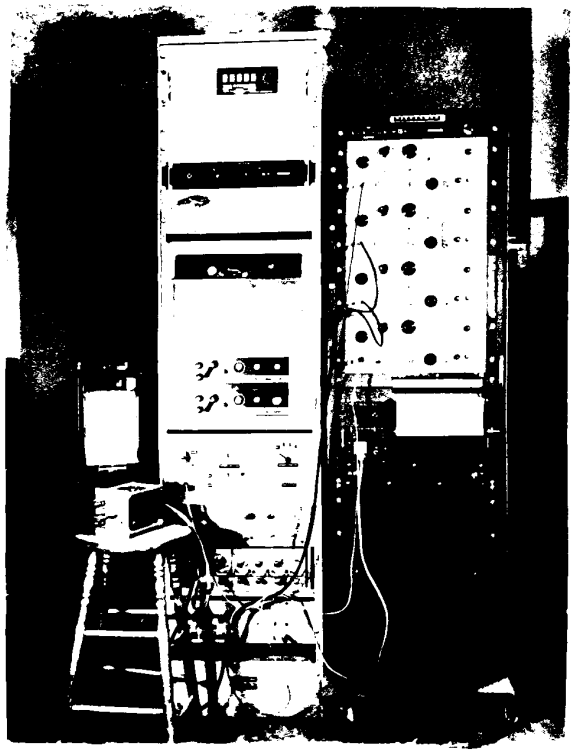

SIGNAL DELAY AND RECORDING EQUIPMENT

FIGURE 2 (Continued)

that the main lobe maximum intersected the 100 km level at a range of about 450 km.

The transmitted carriers were unmodulated. Keying breaks of about two minutes duration were made at intervals of fifteen minutes for identification purposes.

The three receivers were all similar, as follows:

make - Ferranti, type #155

frequencies

Fort Smith	40.49 Mc.
Churchill	40.51 Mc.
Back-scatter	42.00 Mc.

bandwidth - 3 kc.

The receivers were operated with automatic volume control (AVC), so that the receiver output was proportional to the logarithm of the input.

2 THE CHART RECORDER

Sanborn model 154-100B, four channel recorder

chart speeds used - 10 and 25 mm. per sec.

frequency response - d.c. to 100 cps.

The frequency response of the overall system was limited by the amplitude modulated carrier system of the tape delay, as explained under section 3.

3 THE MAGNETIC TAPE SIGNAL-STORAGE SYSTEM

The fluctuating voltage from the detector of each radio receiver was made to modulate an audio-frequency carrier; a diagram of the modulator is shown in Figure 3. A bandpass filter followed each modulator

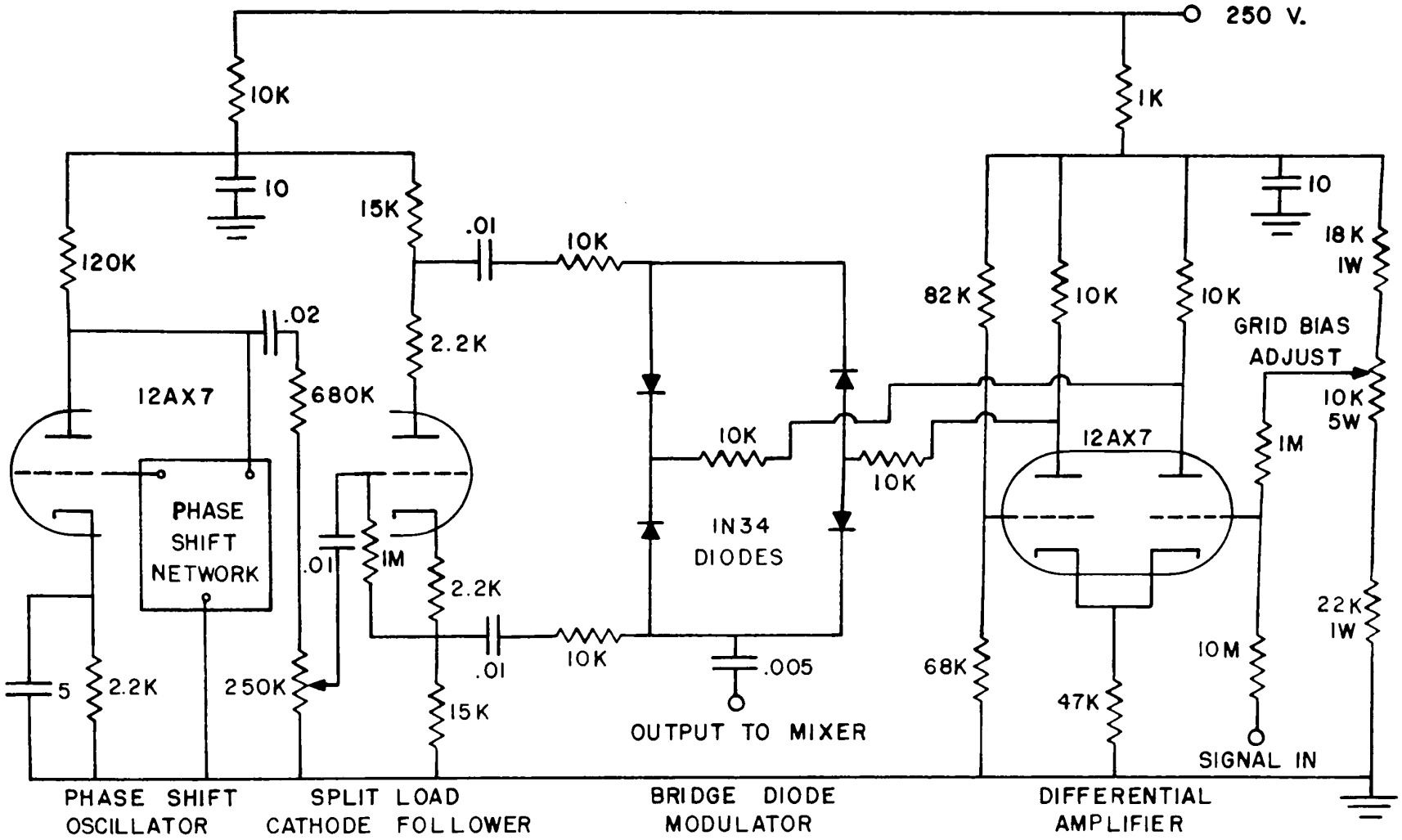

CARRIER GENERATOR AND MODULATOR

FIGURE 3

to limit the bandwidth of the modulation so that the two channels did not interfere when the carriers were linearly mixed and subsequently separated again. These bandpass filters were identical to the second stage of the filter shown in Figure 5. After modulation, the two "signal carriers" were mixed along with a third unmodulated carrier, in a resistive mixer, and the resultant amplified in a power amplifier for transmission via telephone line from the remote receiving site to the Physics Building on the University of Saskatchewan campus, where the remainder of the equipment was located. The function of the unmodulated carrier, designated the "reference carrier", will be described later. A diagram of the reference carrier oscillator, mixer, and power amplifier is shown in Figure 4.

The tape delay consisted of a Heathkit model #TRIAH half-track recorder mounted vertically in a rack, with a second record-playback head mounted on a separate $5\frac{1}{4}$" rack panel above the recorder. In operation the magnetic tape passed first over the remote head where the mixed carrier signal was recorded on the tape, then down to the second head where the signal was played back. The signal delay was about two seconds at the 7.5 ips. tape speed. The magnetic tape was made an endless loop by storing about sixty feet of the tape in a narrow "letter box" below the tape recorder. This "letter-box" is shown in the photograph of the apparatus, Figure 2. It consisted of one sheet of Plexiglass and one sheet of Perspex, each about 9 x 17 inches, separated by wooden spacers 5/16 inches thick. The two sides of the box were made of different materials in an effort to lessen the tendency of the tape to cling to one side of the box because of the static charge which accumulated. Plexiglass and Perspex tend to accumulate opposite charges. It appears that

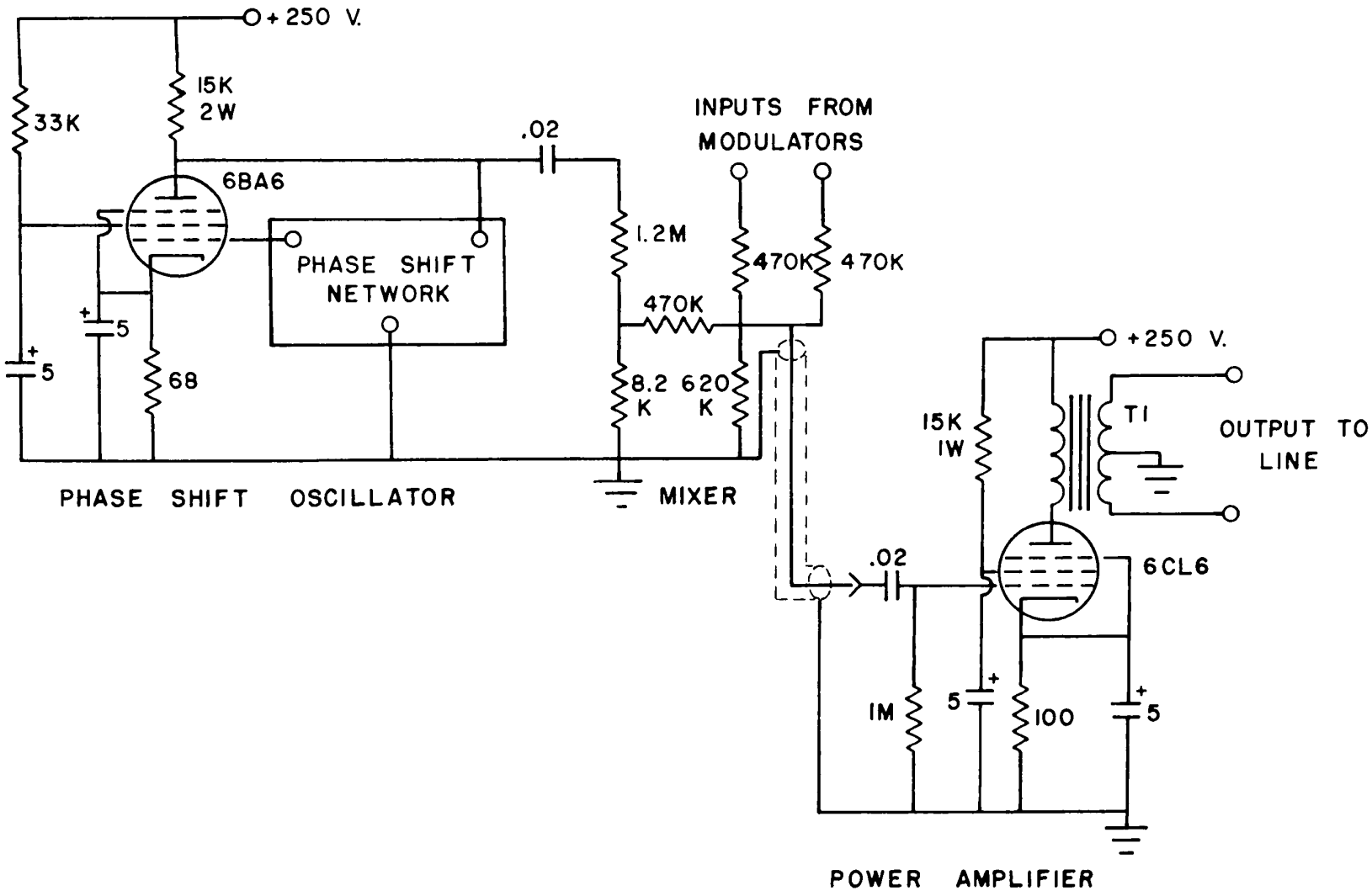

2600 CPS OSCILLATOR, MIXER AND POWER AMPLIFIER

FIGURE 4

the letter-box storage would hold more tape if it were made narrower and deeper, however the one shown worked well and was suited to the available space.

Following playback and amplification the three carriers were separated by bandpass filters, Figure 5. The first stage of each filter consisted of a UTC series BMI interstage bandpass filter. The second stage was a cascode amplifier with feedback through a twin T network. The bandpass filters were quite narrow and limited the frequency response of the system. The filter characteristics are shown in Figure 6. The frequency response of the overall system was measured and found to be flat within $\pm 2\%$ from d.c. to 2 cps., and down to one-half amplitude at 9 cps. In addition, the rise time of the system, defined as the time for a square pulse to rise from 10% to 90% of the final amplitude, was measured to be 0.066 seconds.

The radio receivers were operated with automatic volume control (AVC) which gave an approximately logarithmic output. In order to produce a more nearly logarithmic response for the whole system, adjustable AVC carrier amplifiers were provided between the bandpass filters and the detectors of the two signal channels. Figure 7 is a diagram of the AVC carrier amplifier. The 6BA6 pentode acted as a variable gain amplifier as in conventional radio AVC circuits. The output of the stage was detected and fed back as a negative bias to the control grid, reducing the stage gain. The AVC compression control varied the fraction of the detected voltage fed back to the grid; it was thus possible to obtain any one of a family of amplitude response curves for the amplifier between the two limiting curves shown in Figure 8. The two cathode followers served as impedance transformers: one was the output, the other drove

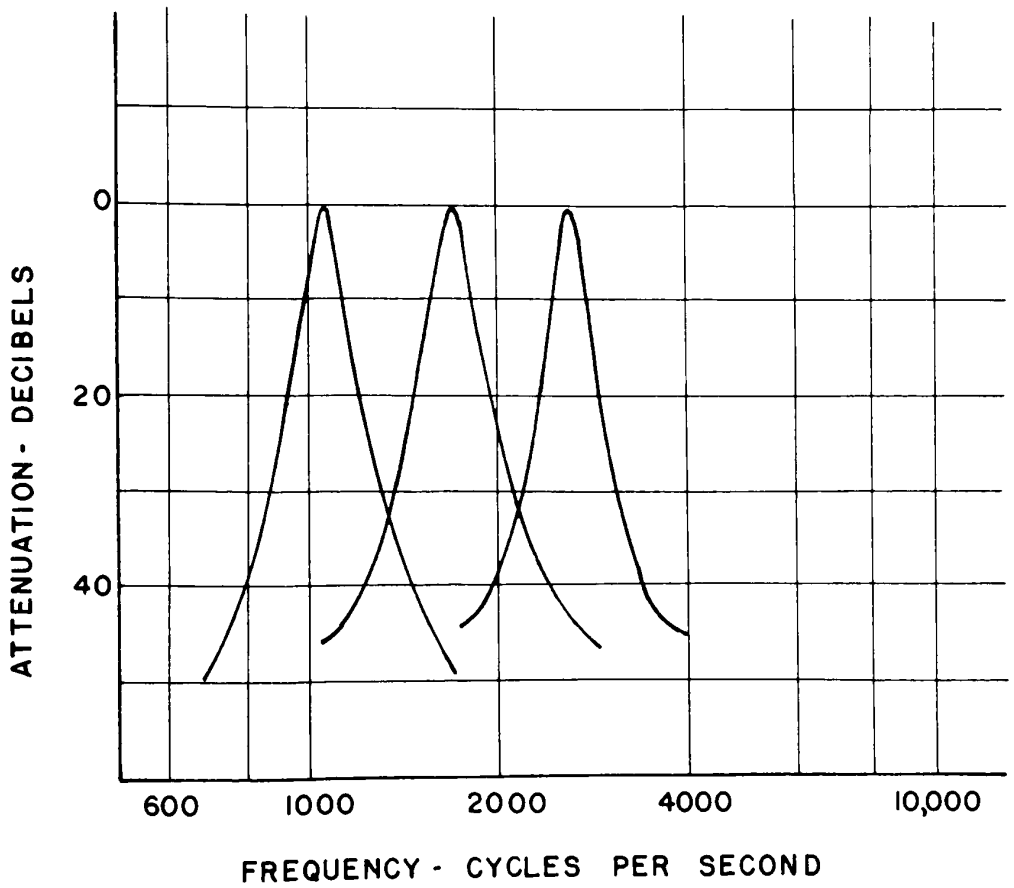

BAND-PASS FILTER CHARACTERISTICS

FIGURE 6

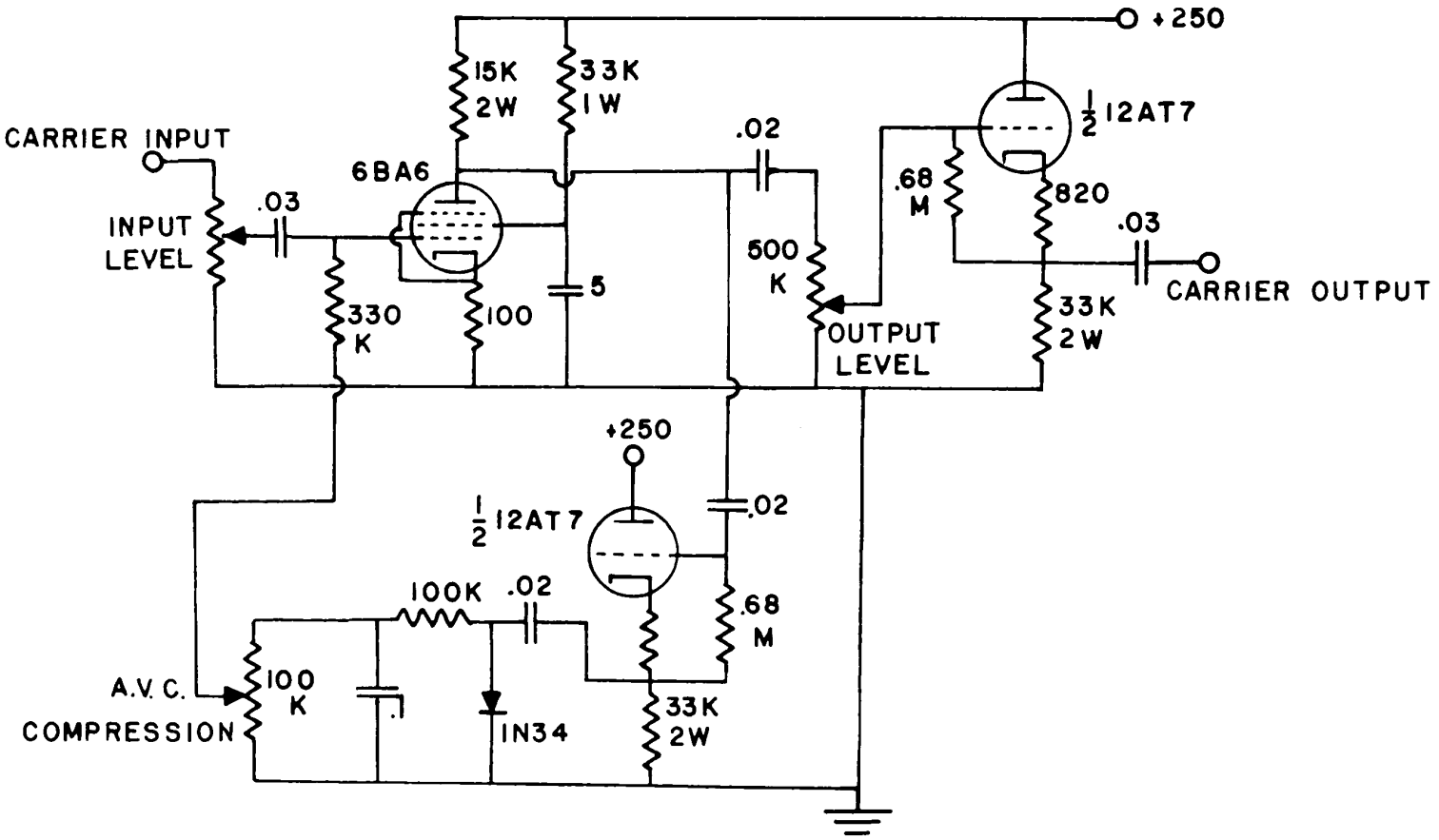

A.V.C. AMPLIFIER

FIGURE 7

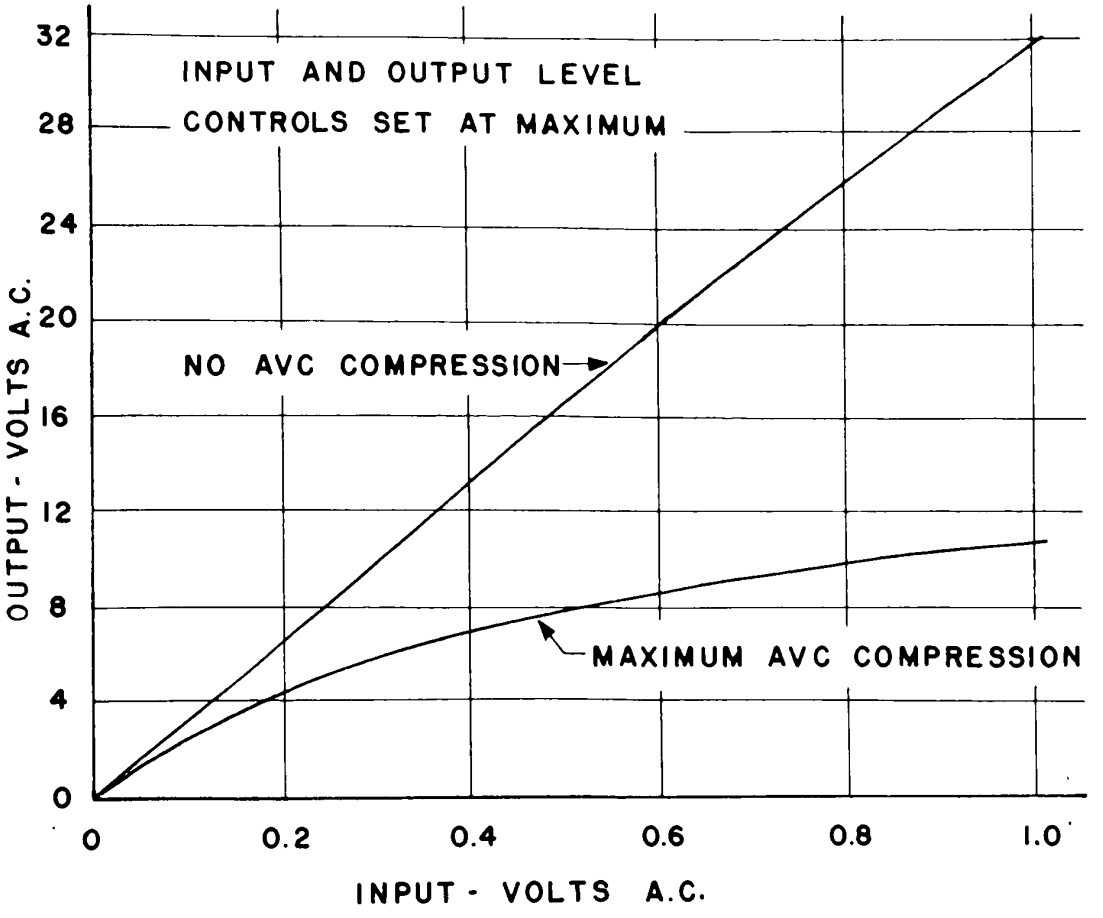

A.V.C. AMPLIFIER AMPLITUDE RESPONSE

FIGURE 8

the diode detector which furnished the AVC voltage.

The record-playback process involved in the two-second tape delay introduced noise into the system. This arose through fluctuations in total signal amplitude caused by varying contact of the magnetic tape with the record and playback heads. These amplitude fluctuations were detected from the various carriers along with the desired signal, and they therefore constituted unwanted noise. This noise was correlated on the separate carriers, however; so that a system of noise cancellation was possible. The noise introduced onto the reference carrier was detected and added out of phase to the two signals, thus reducing the noise in each output. A diagram of the two-channel demodulator is shown in Figure 9. One channel detected the signal plus noise from a signal carrier, the other channel detected the noise from the reference carrier. Two such two channel demodulators were used, one for each signal channel, so that the gain of the noise signal could be varied independently for each in order to obtain the most effective cancellation. There was some indication that the amplitude of the noise signal produced depended somewhat on the carrier frequency. The actual noise cancellation took place in the Sanborn recorder, which had a differential input.

A third channel of the Sanborn recorded the signal detected from the reference carrier alone. This served two purposes; first it indicated when the noise of the system became too high, secondly it provided a check on the gain setting of the tape delay. The output amplitude of the tape recorder tended to decrease slightly with time as the tape loop operated. If the tape was stopped and started again, the amplitude returned to its higher value and then decreased as before.

A safety device was provided to remove power from the tape recorder

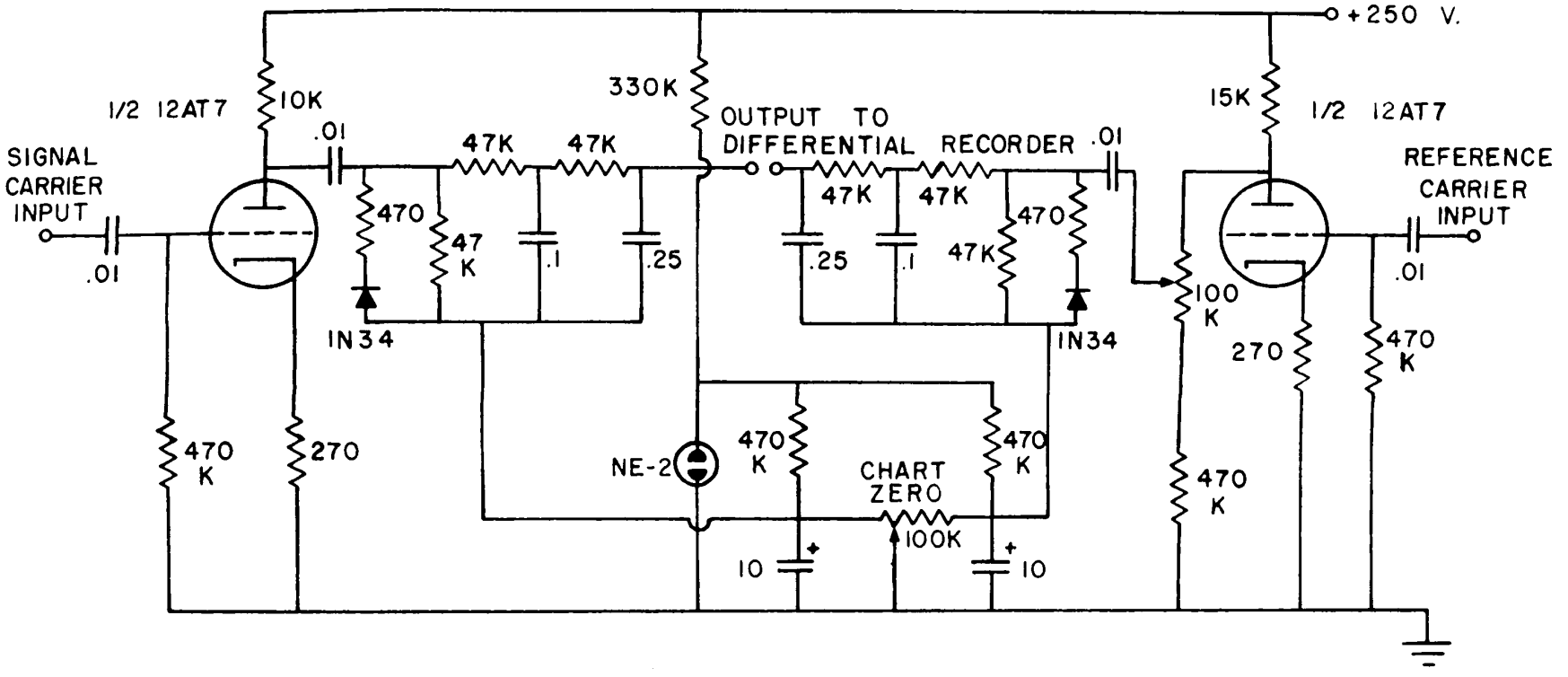

TWO CHANNEL DEMODULATOR

FIGURE 9

motor in the event that the tape loop became entangled; this is shown in Figure 10. The reference carrier was amplified and detected, and the resultant d.c. voltage applied to the grid of a Schmitt trigger. If the reference carrier disappeared, the voltage on the Schmitt trigger control grid rose, allowing the relay to open and thus removing power from the motor. The time constant of the detector was long enough that momentary drop-outs in the carrier did not cause the relay to open.

4 THE SANBORN CONTROLLER

The Sanborn controller, Figures 11, 12, and 13, was a trigger circuit used to turn the Sanborn recorder on whenever the signal level from one or both receivers exceeded a preset level. It could be set to turn on when a signal existed on only one of the two channels (OR operation), or it could be set to turn on only when signals existed on both channels simultaneously (AND operation).

The input to the circuit was from a balanced telephone line; the transformer T1 coupled from the line, through the input level control R1, to the grid of the cathode follower stage V1. The cathode follower drove the two bandpass filter stages V2 and V3, and provided an input signal for the tape recorder. The bandpass filters were cascode amplifiers as in Figure 5.

The bandpass amplifiers were followed by cathode followers V4A and V4B. These each drove two detectors, one with a short time constant, .04 seconds, the other with a longer time constant, 5 seconds. The two detectors were connected to the grids of a differential amplifier V5 (or V6). The voltage (positive going) on the short time-constant integrator tended to turn the circuit on, and this it normally did, for short duration signals. However, if the signal level remained high for a period of about 15 seconds, the

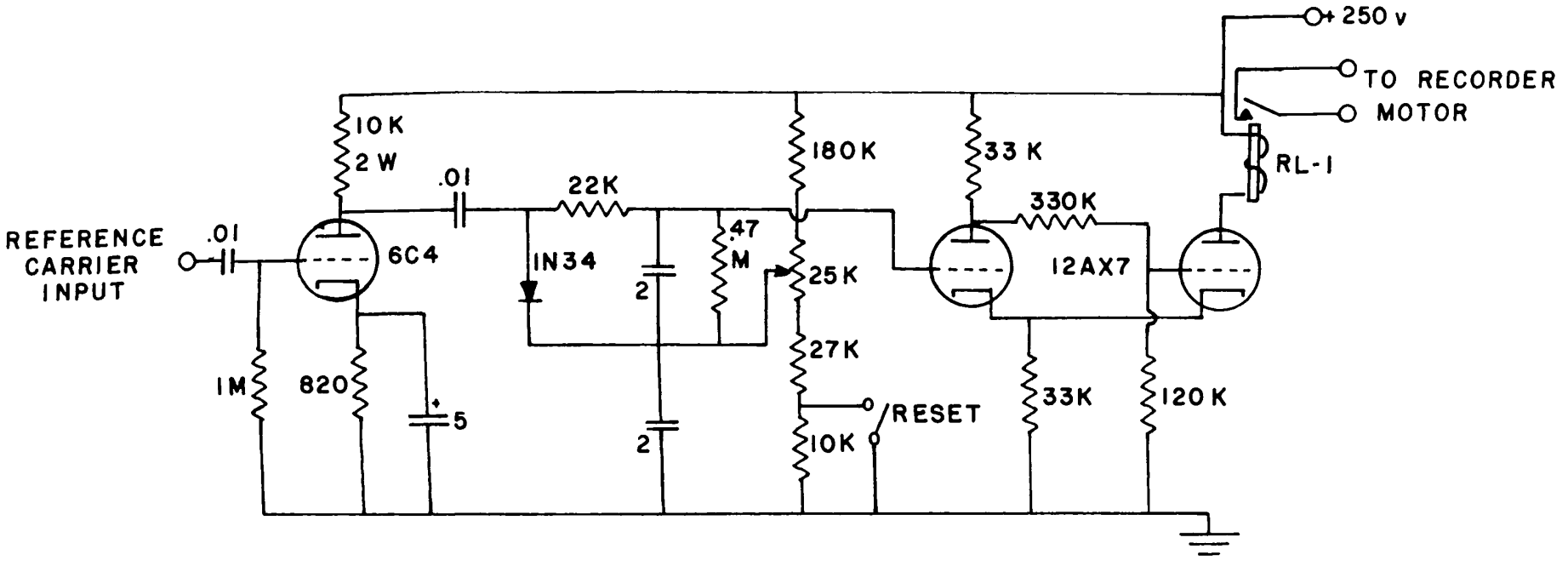

RL-1 SIGMA 8000 OHM RELAY

TAPE RECORDER SHUT-OFF

FIGURE 10

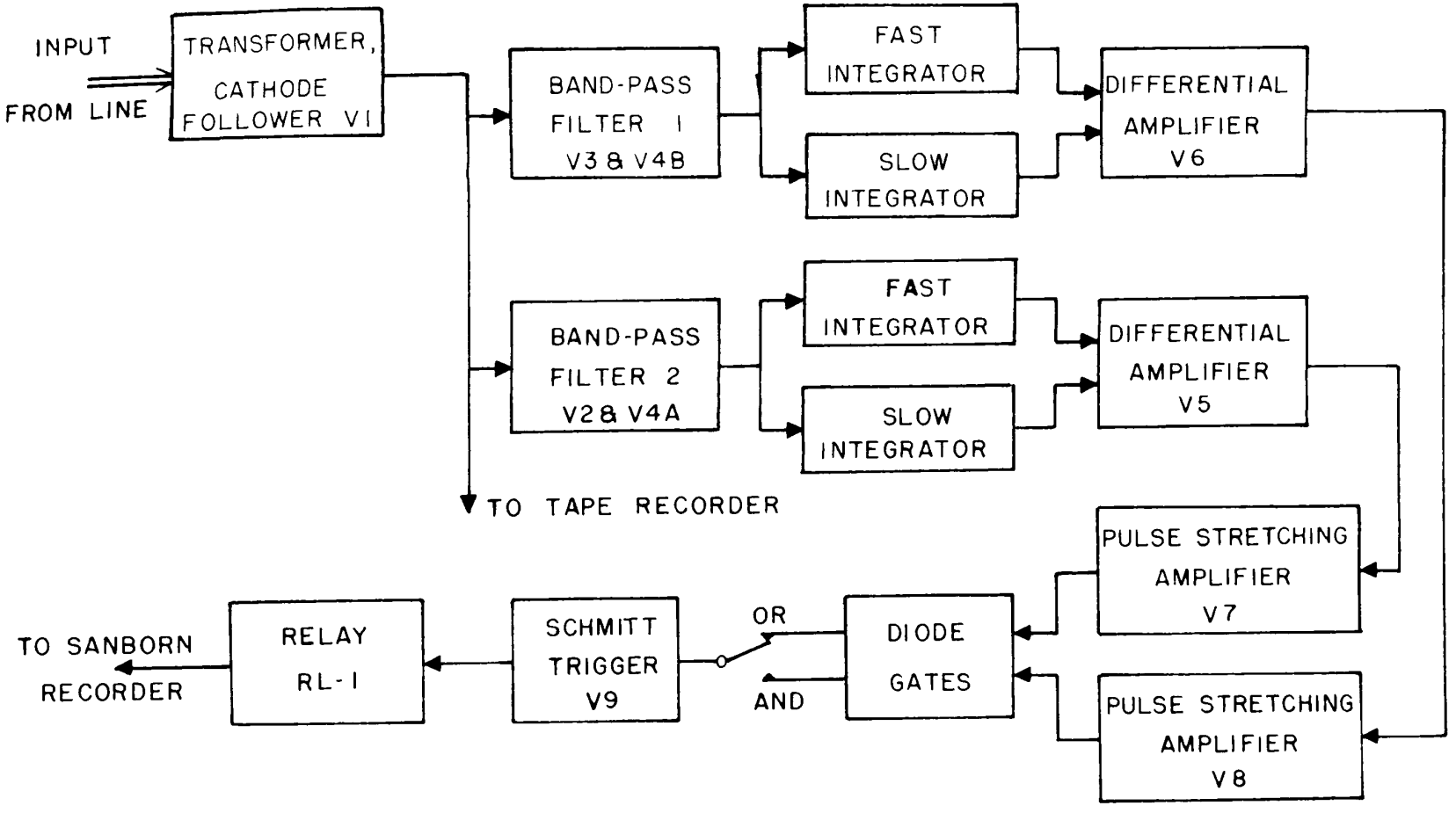

BLOCK DIAGRAM OF SANBORN CONTROLLER

FIGURE 11

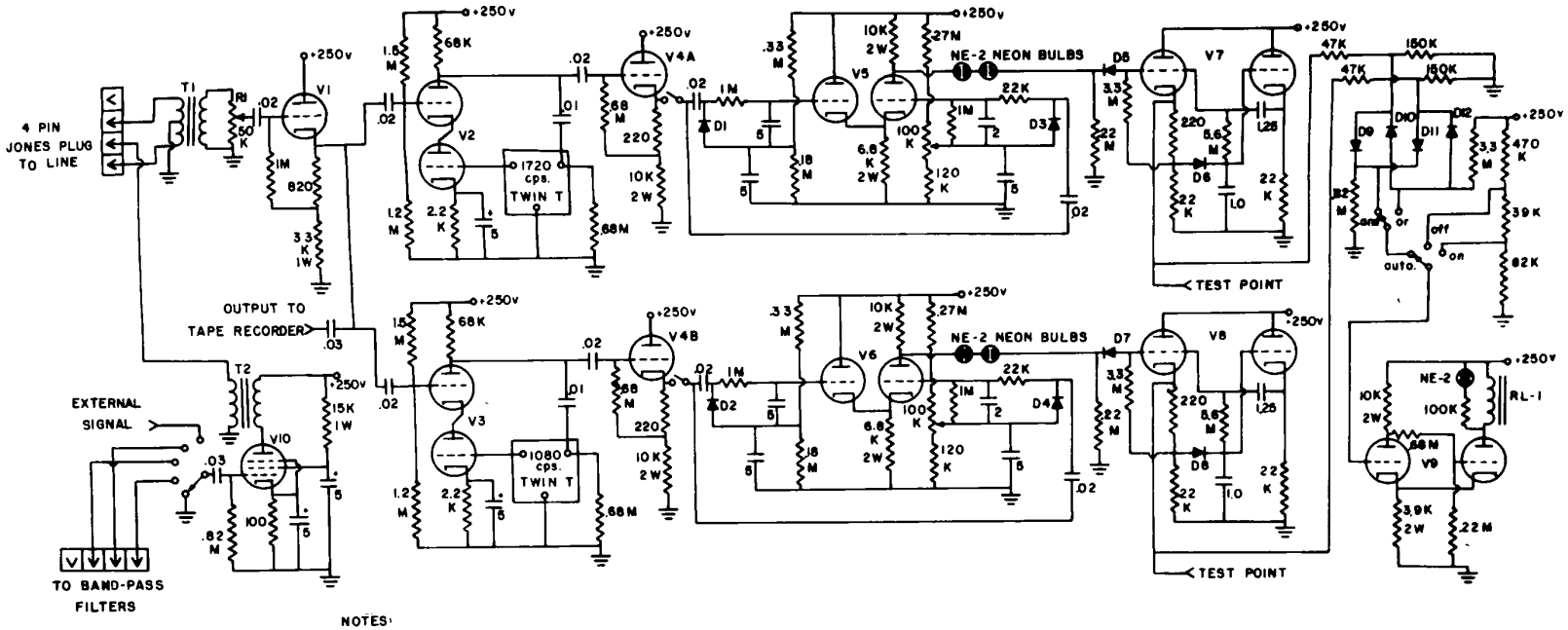

NOTES:

D1, D2, D9-D12: 1N34 DIODES D3-D8: 1N2069 DIODES

RL-1: C.P. CLARE & CO. SN41017 RELAY

T1: HAMMOND 132 TRANSFORMER T2: HAMMOND 139 TRANSFORMER

TUBES: V1-6C4 V2,V3-12AX7 V4,V7,V8-12AT7 V5,V6,V9-12AU7 V10-6CL6

SANBORN CONTROLLER

FIGURE 12

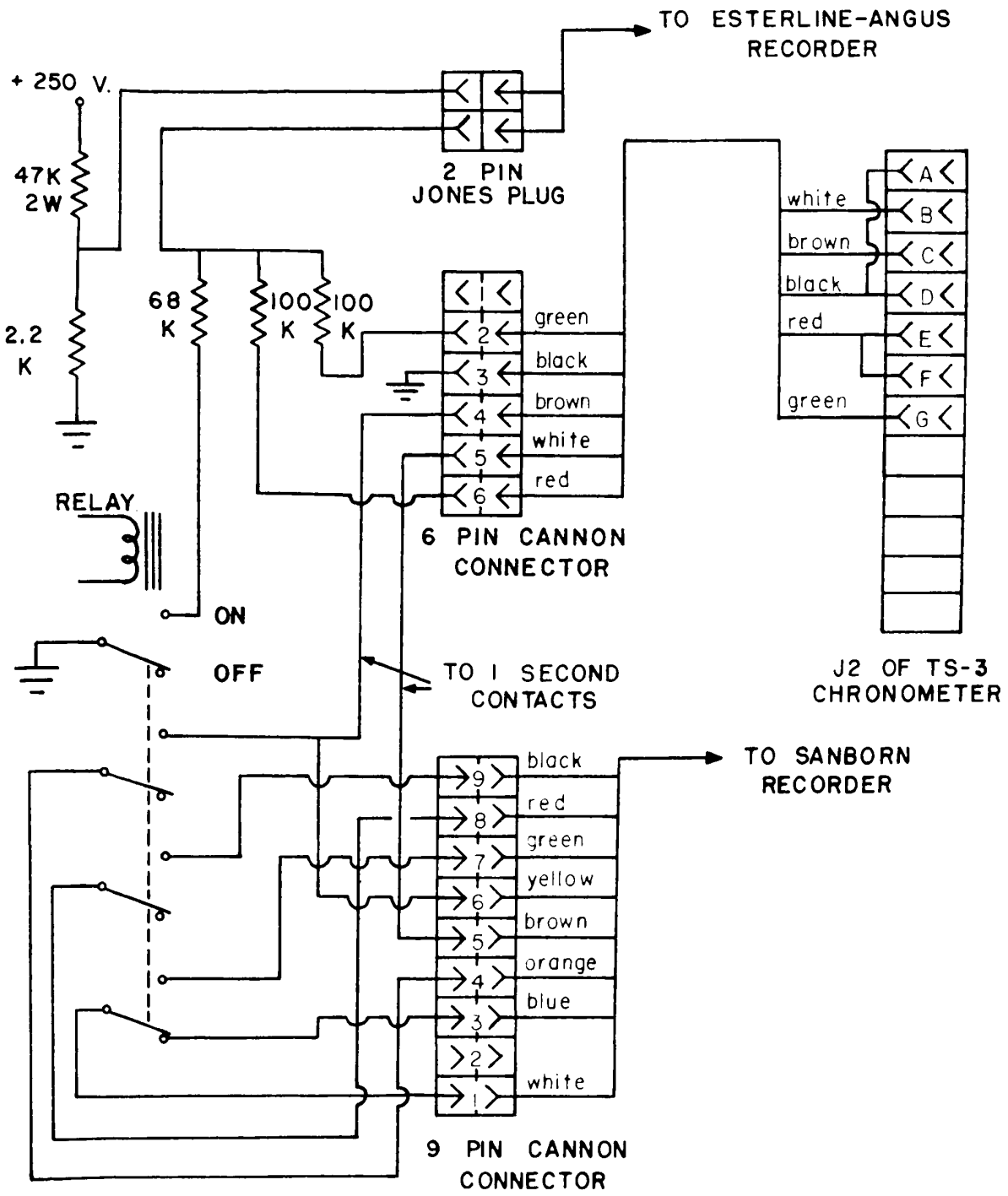

SANBORN CONTROLLER RELAY CIRCUIT

FIGURE 13

voltage on the second detector rose sufficiently to turn the circuit off. This prevented the Sanborn recorder from being held on for long periods during times of strong radio-auroral enhancements, which were of no interest in the present study.

The differential amplifiers were direct-coupled through two NE-2 neon bulbs in series, to pulse stretching circuits V7 and V8. These were essentially the same as those described by Forsyth and Rolfe (1955). The pulse stretchers here functioned to preserve the amplitude of negative going pulses for a fixed duration of 5 - 6 seconds. If the input to a pulse stretcher remained large (negative) for a period longer than 5 - 6 seconds, the output followed the input back to zero-input level on the first occasion the input returned to zero. The output of the pulse stretcher, like the input, was negative going.

The outputs of the pulse stretching amplifiers V7 and V8 were coupled through one of two switch-selected diode gates, to the control grid of a Schmitt trigger, V9. In the OR mode, the output of the diode gate was the "greatest of" the two inputs, thus the Schmitt trigger was turned on when either signal exceeded a specified level. In the AND mode, the output of the diode gate was the "least of" the two inputs, so that it was necessary for both to exceed a predetermined level in order to turn the Schmitt trigger on.

In the configuration used, the Schmitt trigger was called "on" when the right hand triode was conducting, thus closing the relay in its plate circuit. The NE-2 neon bulb across this relay served merely as an indicator. The relay controlled the Sanborn recorder motor, switched the heating current to the Sanborn pens, completed the circuit to the external one second marker, and closed a circuit to an Esterline-Angus recorder

thus placing a marker on the Esterline-Angus record each time the Sanborn recorder was triggered on. The Esterline-Angus record was part of a scheme to record the absolute time of each meteor-burst signal, as explained further in section 5.

Figure 13 is a diagram of the circuitry associated with the Sanborn controller relay, the Esterline-Angus operations recorder, and the chronometer time standard. Figure 14 is a diagram of a timer-marker plug-in unit which was built for remote control of the Sanborn recorder. It replaced the regular Timer-Marker Panel of the Sanborn recorder.

The power amplifier stage V10 on the Sanborn controller chassis was used for monitoring purposes at the remote site. A four position switch connected the grid of the stage to any one of the three band-pass filter outputs, or to an external signal source.

5 TIME MEASUREMENT

Absolute timing of each meteor burst was provided through use of a Times Facsimile Corporation Chronometer, which had a stability of 1 part in 10^7, or 3 seconds per year. It provided contacts which closed once per second, once per minute, and once per hour. The chronometer could be set to within about 2 milliseconds of the time signals broadcast by WWV, using an oscilloscope. The one second contacts were connected to the "remote marker" of the Sanborn recorder, so that the side pen placed on the record one second markers which were synchronized with the time standard. The one minute and one hour contacts were used to place markers on the Esterline-Angus operations recorder. Upon these time marks were superimposed the markers indicating each occasion the Sanborn recorder was switched on.

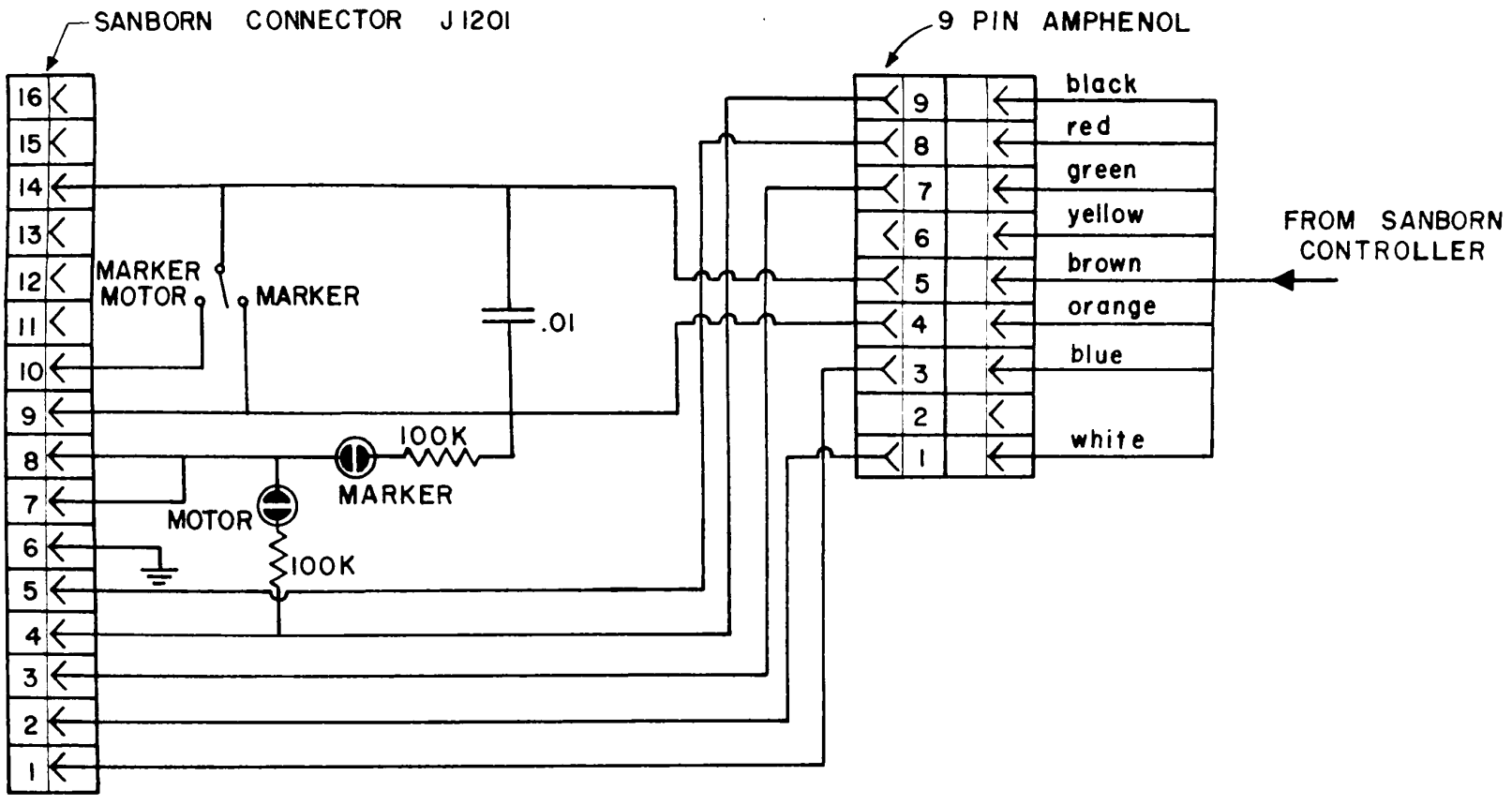

MODIFIED TIMER-MARKER PANEL

FIGURE 14

A further step was necessary to measure the absolute time of a particular signal. The Esterline-Angus record provided the time of an event only to the nearest minute. A continuously rotating potentiometer (Electro-Mec type #14BNR-G1), rotating at 1 r.p.m., was used to place a triangular wave on one channel of the Sanborn record. In the first 30 seconds of the minute, the signal increased uniformly to maximum; while in the last thirty seconds it decreased uniformly to zero. The phase of the triangular wave was made adjustable by providing for rotation of the body of the potentiometer during operation. It was possible to measure the amplitude of the waveform at any given instant to yield the time within one second, the slope of the line determining the half minute. By then measuring from the one second markers, it was possible to determine time on the record to within 1/10 second. (It was, of course, necessary to take the tape delay into account).

This accurate timing was planned so that work could be carried out in conjunction with the Prince Albert Radar Laboratory. When this work became impossible (due to a fire at the Laboratory), the accurate timing was not necessary, nor was it always used, due to mechanical difficulties with the chronometer. When the one second markers from the chronometer were not available, the internal one second marker generator of the Sanborn recorder was used. Since this generator was not synchronized with absolute time, it merely indicated chart speed. Without the chronometer, time was measurable with an accuracy of about ± 5 seconds. This was quite adequate for the work described here.

6 CALIBRATION AND ADJUSTMENT

A one cps. oscillator, Figure 15, was used to check the operation of

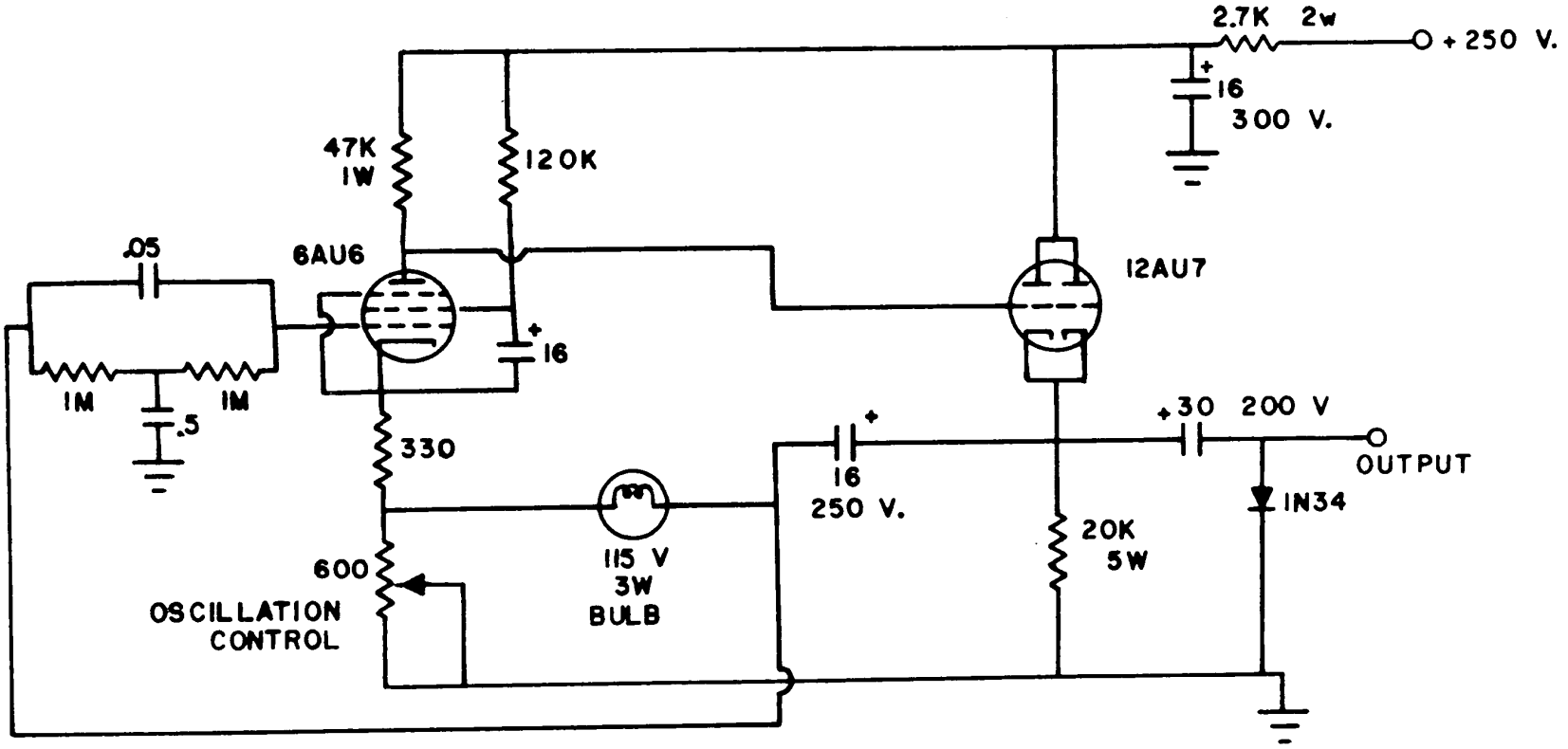

1 CPS. OSCILLATOR

FIGURE 15

the overall system. The oscillator circuit is similar to that of the Heathkit AG-9A Audio Generator. In use the receivers were disconnected and the oscillator connected to the inputs of the two modulators. The output of the oscillator was clamped to ground by a diode, producing a negative-going signal (the detector output of each receiver was negative-going). It was necessary to adjust the carrier level of the modulators daily, since they were subject to drift. With zero input to the modulators, the "grid bias adjust" control on each modulator was set for 0.10 volts r.m.s. carrier level.

The frequencies of the carrier oscillators were adjusted about once a week. It was originally intended that the oscillator frequencies be adjusted to the centre frequencies of their respective bandpass filters, by adjusting the frequencies for maximum output from the filters, using the power amplifier stage, V10 of Figure 12, to provide, at the receiving site, a monitor signal from each bandpass filter in turn. A somewnat more convenient procedure was adopted in which an operator adjusted the frequency of a commercial audio generator to the centre frequency of a bandpass filter. The audio generator output was then connected to the input of the power amplifier stage V10, and another operator at the receiving site adjusted the carrier frequency, by means of a Lissajous figure, to the frequency of the audio generator. The two operators maintained contact by telephone.

The amplitude response of the overall system was measured by connecting a Measurements Corporation Standard Signal Generator, model 80, to the input of each receiver, in place of the antenna. This signal generator had an output accuracy of ± 1 db. Calibration levels were recorded on the Sanborn record at intervals of 5 db over a range of 35 db.

APPENDIX B - A PHOTOGRAPHIC READ-OUT FOR THE PRINCE ALBERT RADAR

When the original plans were made for use of the facilities of the Prince Albert Radar Laboratory for meteor studies, the author undertook to build a photographic read-out unit which would record on 35 mm. film the information available from the radar. This information was supplied in binary form to a row of 91 neon bulbs, which were to be photographed. The switching circuits for the bulbs were available; it was then necessary to build a suitable array of bulbs together with an automatically controlled camera to photograph them.

In Figure 1 are two photographs of the camera, together with a light-proof plywood box with the neon bulbs arranged on the arc of a circle in front of the camera lens. The bulbs were designated model #RT2-27-1 and were obtained from the Signalite Corporation, Neptune, New Jersey. These were preferred to the NE-2 bulbs manufactured by General Electric, which they resembled in appearance, because the Signalite bulbs contained a small amount of radioactive substance which reduced their dark firing voltage. The bulbs were mounted in one-quarter inch holes drilled in a 1 x 1 inch brass bar which had been bent to a radius of about twenty-one inches. Individual 82K series resistors for each bulb were mounted on a bakelite strip, adjacent to the bulbs. The bulbs were viewed from their sides through one eighth inch holes in the brass bar. These holes were plugged with short pieces of polystyrene rod which had been carefully polished at each end.

The camera was one which had been built by the Defence Research Board, and was designated model #LG-17. It had no shutter, and the film advanced continuously. It was modified so that the film advance could be

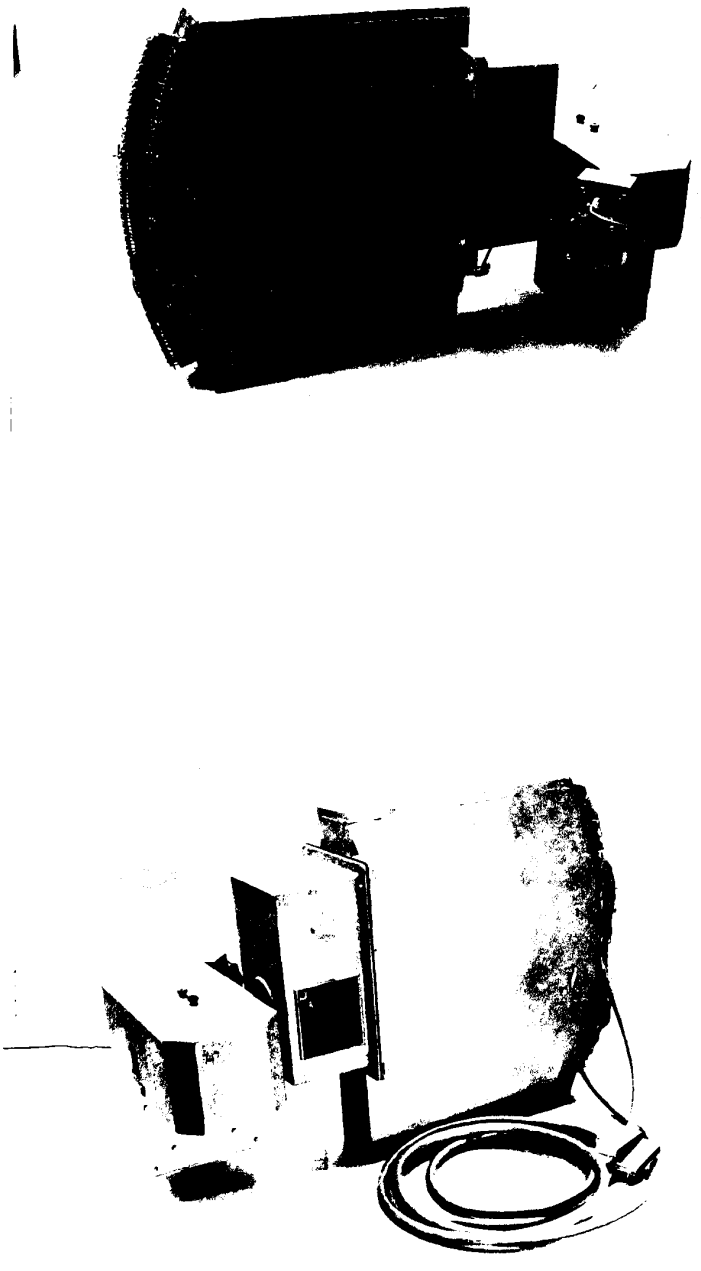

FIGURE 1 - CAMERA AND NEON BULB READ-OUT

controlled automatically. This was done by using a second electric motor, connected through a magnetic clutch to the film advance sprocket, thus permitting the film to be advanced by supplying power to the magnetic clutch. The original camera motor continued to operate the film take-up spool. After the modifications, the film advance speed was 36 inches per minute.

A transistorized trigger circuit, Figure 2, was built to control the magnetic clutch of the camera. It operated in such a manner that the film advanced only when a radar signal was received from a target. "Hit-mark" pulses (indicating a radar target) triggered the monostable multivibrator T1 and T2. The square-wave output of the multivibrator was integrated, and the resultant voltage applied to the base of the power transistor T5, which had as its collector load the windings of the magnetic clutch. The two emitter followers T3 and T4 in series were necessary in order to present a high load impedance to the integrator. The action of the circuit was such that the clutch was energized on the first hit-mark pulse, and it did not de-energize until about 100 milliseconds after the last pulse.

The trigger circuit was destroyed in the fire at the Radar Laboratory; the camera and associated equipment shown in Figure 1 were not at Prince Albert at that time.

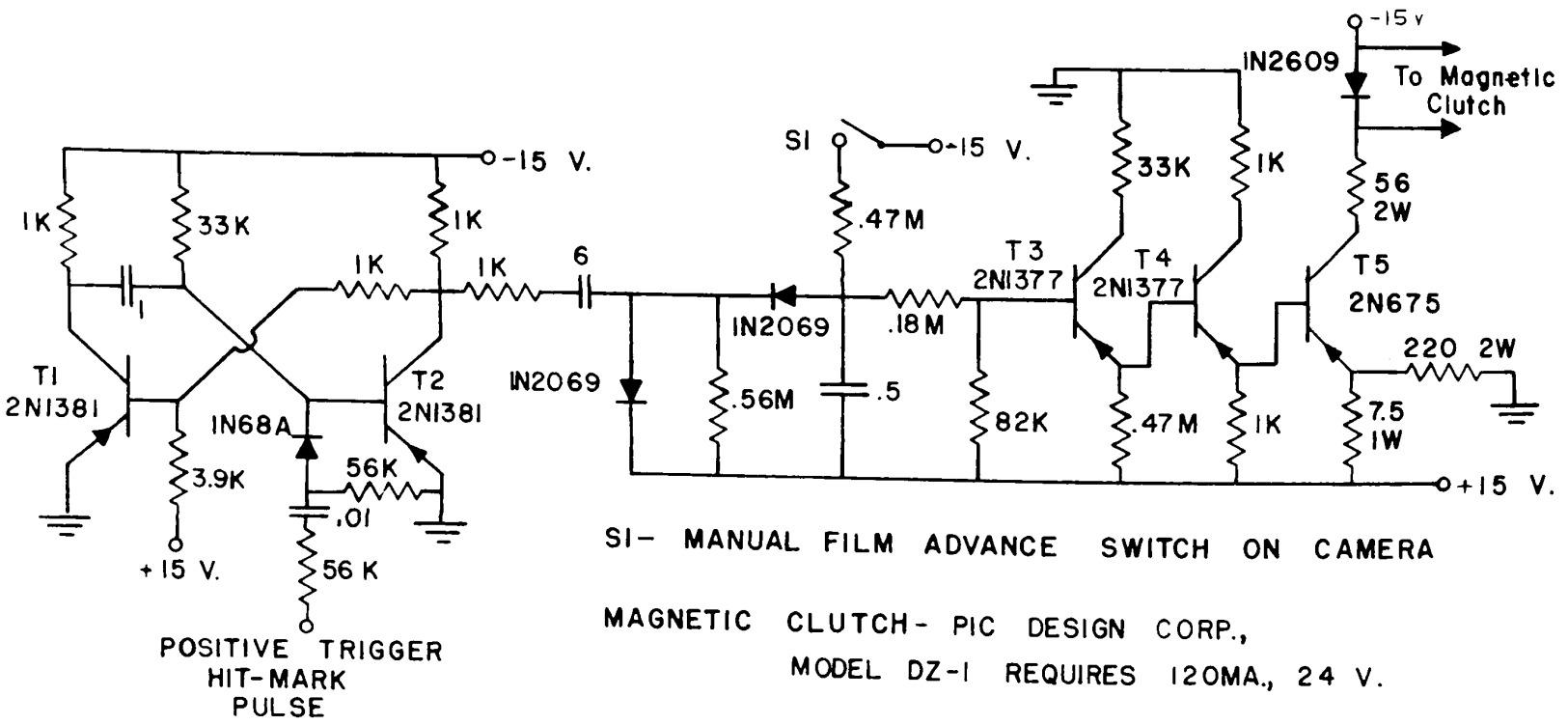

S1- MANUAL FILM ADVANCE SWITCH ON CAMERA

MAGNETIC CLUTCH- PIC DESIGN CORP.,
MODEL DZ-1 REQUIRES 120MA., 24 V.

ALL CAPACITANCES IN MFD.

HIT-MARK PULSES 33 MSEC. APART

15 V. × 5 μSEC. WIDE

CAMERA CONTROL CIRCUIT

FIGURE 2